NAZARBAYEV UNIVERSITY

DEVELOPMENT OF INTEGRATED MEMBRANE BIOREACTOR AND CHEMICAL PROCESSES FOR ADVANCED WASTEWATER TREATMENT

by

Yerkanat Kanafin

Submitted in partial fulfilment of the requirements for the degree of Doctor of Philosophy in Science, Engineering and Technology

15.10.2023

DEVELOPMENT OF INTEGRATED MEMBRANE BIOREACTOR AND CHEMICAL PROCESSES FOR ADVANCED WASTEWATER TREATMENT

by

Yerkanat Kanafin

Submitted in partial fulfilment of the requirements for the degree of Doctor of Philosophy in Science, Engineering and Technology

School of Engineering and Digital Sciences

Nazarbayev University

Supervised by

Dr. Stavros G. Poulopoulos

Dr. Elizabeth Arkhangelsky

Dr. Vassilis J. Inglezakis

October 2023

DECLARATION

I declare that the research contained in this thesis, unless otherwise formally indicated within the text, is the original work of the author. The thesis has not been previously submitted to this or any other university for a degree and does not incorporate any material already submitted for a degree.

Signed:

Dated: 15.10.2023

ABSTRACT

The global rise in population and rapid industrialization and urbanization have resulted in a significant increase in wastewater production, putting a strain on existing treatment facilities. This has led to the release of certain pollutants into the aquatic environment, including emerging contaminants such as pharmaceuticals, pesticides, hygiene products, endocrine-disrupting agents, surfactants, and industrial chemicals. These pollutants are found in wastewater, groundwater, rivers and lakes and pose a potential threat to human health and cause various illnesses such as reproductive disorders, cardiovascular disorders, cancer, immune deficiency, nervous system syndrome, brain development delay, and memory disruption. The secondary treatment (biological processes) in a typical treatment plant is the most crucial step as it removes approximately 80-90% of pollutants. However, conventional treatment methods are not effective in completely removing emerging contaminants, and advanced treatment techniques must be utilized. In this work, different types of wastewaters containing emerging pollutants were treated using conventional activated sludge process, membrane filtration, and advanced oxidation processes.

The following emerging pollutants were used as targets: caffeine, ibuprofen, metronidazole, naproxen, sulfamethoxazole, bisphenol A, and carbamazepine.

The implementation of a sequencing batch reactor (SBR) led to the elimination of a significant amount (78-86%) of total organic carbon (TOC), with only small reductions (11%, 45%, and 6%) observed for naproxen, bisphenol A, and sulfamethoxazole, respectively. The SBR effluents then were treated with membrane filtration and chemical oxidation processes. Track-etch membranes (TEMs) and phase inversion membrane (PIM) were employed. It should be emphasized that TEMs were employed in wastewater treatment for the first time. TOC removal efficiency ranged from 1% to 6% for each of the four membranes evaluated. 10 nm TEM demonstrated almost complete removal of bisphenol A (93%) and insignificant removals for naproxen (11%) and sulfamethoxazole (14%). The elimination mechanism of bisphenol A employing membranes was probably connected to size exclusion and sorption. Ultimately, the effluents from SBR and membrane filtration were treated with sulfate-radical-based advanced oxidation processes (AOPs). Remarkably, full removal of emerging contaminants and TOC were obtained after 30 minutes for the effluents after membrane filtration using 10 mM of $K_2S_2O_8$ and 25 mg/L of zero-valent iron (ZVI) under UV, demonstrating the great potential of combining membrane filtration and AOPs.

Pharmaceuticals commonly found in wastewater, such as caffeine, metronidazole, and ibuprofen, were investigated for removal using a combination of continuous flow-activated

sludge process and advanced oxidation processes. The study found that ibuprofen and caffeine were completely degraded, while metronidazole was only partially degraded. However, the presence of ibuprofen and caffeine hindered the nitrification process, while metronidazole suppressed the activity of denitrifying microorganisms. Biological treatment resulted in complete degradation of ibuprofen and caffeine but only 56% degradation of metronidazole. Advanced oxidation processes using hydroxyl and sulfate radicals were then used to eliminate the remaining metronidazole. The study demonstrated the effectiveness of AOPs in treating effluents from biological treatment processes.

Moreover, AOPs were used to treat actual slaughterhouse wastewater. TiO_2 photocatalysis resulted in a 44% decrease in TOC after 60 min, while UV/98 mM H_2O_2 led to a 74% reduction in TOC after 150 minutes. Adjusting the pH to 3 and introducing Fe^{2+} into the system increased TOC removal to 82.5% after 150 minutes. Combining 15 mM $K_2S_2O_8$ and UV led to a TOC reduction of 85%. Persulfate oxidation was also applied for the first time to treat wastewater from a slaughterhouse. The study shows that UV/$K_2S_2O_8$ may be used as an additional post-treatment technique after biological treatment for water discharge criteria fulfillment and wastewater reuse.

Additional experiments were carried out using sulfate radical-based AOPs. Real municipal wastewater was treated using the UV/$K_2S_2O_8$/Fe^{2+} process. Response surface methodology (RSM) was utilized to improve the treatment process by investigating the impacts of four independent parameters on TOC, TC, and TN removal. RSM precisely established the most suitable parameters for complete TOC removal, leading to total TOC mineralization at pH of 7.7, 30 mM $K_2S_2O_8$, and $K_2S_2O_8$ to Fe^{2+} ratio of 7.5 after 106 min. Attempts to use statistical models to determine optimum conditions for complete TC and TN elimination were, however, unproductive.

In addition, for the first time, a continuous flow UV/$K_2S_2O_8$/ZVI system was put into operation for wastewater treatment. The RSM was used to study the impacts of the following process factors on TOC reduction: space time, the concentration of $K_2S_2O_8$, and the $K_2S_2O_8$/ZVI molar ratio. Carbamazepine was spiked into both synthetic and actual municipal wastewater to investigate its fate during persulfate oxidation. In the case of synthetic wastewater, 71% TOC reduction and full elimination of carbamazepine were accomplished. In the case of real wastewater, 60% TOC removal and full carbamazepine elimination have been achieved. The complexity of real wastewater and the presence of radical-reducing agents may explain the difference in TOC removal with synthetic wastewater.

Finally, the UV/$K_2S_2O_8$/Goethite process was tested using landfill leachate, a highly contaminated effluent. Sulfamethoxazole was injected into both synthetic (SLL) and real

landfill leachate (RLL) and used to evaluate the best treatment parameters for TOC and sulfamethoxazole removal using RSM. After 4.7 h of using the UV/$K_2S_2O_8$/Goethite system, 87% TOC and 100% sulfamethoxazole were removed from the RLL. In addition, air stripping at pH 11 for 3 hours was utilized to eliminate ammonia from the RLL. For the first time, our studies indicate the efficiency of the UV/$K_2S_2O_8$/Goethite system in eliminating organic materials from landfill leachate.

To summarize, it was discovered that at certain concentrations, emerging pollutants block the activity of microorganisms, hence affecting the effectiveness of the activated sludge process. AOPs based on sulfate radicals are an efficient post-treatment process for the removal of emerging pollutants and TOC following the conventional biological treatment or membrane filtration. Different chemical species such as Fe^{2+}, zero-valent iron, and goethite were used to activate persulfate or hydrogen peroxide under UV. The materials used were characterized using state-of-the-art characterization techniques. Overall, the integrated use of track-etch membrane bioreactor and advanced oxidation processes demonstrated significant efficiency in the elimination of emerging pollutants in wastewater treatment.

ACKNOWLEDGEMENTS

My four years of PhD studies were filled with excitement, adventurous exploration, and personal growth. Throughout my graduate school experience, I had the privilege of interacting with many amazing individuals in both professional and social settings, who helped me overcome challenging tasks. Therefore, I would like to express my gratitude to all the people who made this journey possible.

First and foremost, I would like to wholeheartedly thank my supervisor, Prof. Stavros Poulopoulos, for his unwavering support, valuable advice, understanding, and belief in me. I feel incredibly fortunate to have had the opportunity to work with such a brilliant scientist. Despite managing a department and a large research cluster, he remains open-minded and approachable. I am also deeply appreciative of my other academic supervisors, Prof. Vassilis Inglezakis and Prof. Elizabeth Arkhangelsky, for their continuous support throughout my PhD journey. I am honored to have had the chance to learn from their expertise in biological processes and membrane technologies.

I would like to express my gratitude to the faculty of the School of Engineering and Digital Sciences, especially, Prof. Luis R. Rojas-Solorzano and Prof. Konstantinos Kostas for their encouragement and valuable comments throughout my research. I am also grateful to our research team and colleagues from Nazarbayev University and abroad who collaborated with me at various stages of my research. My friends from the doctoral classes deserve a special mention for the brainstorming sessions and enjoyable conversations.

Although most of my closest friends live in different cities, I want to thank them all for their support and friendship over the years.

Lastly, I dedicate this final paragraph to the most important people in my life. I want to express my endless love and gratitude to my father, Nurmukhambet Kanafin, and mother, Bibigul Aldazharova, for their unconditional love, support, and encouragement. You have sacrificed so much to provide my siblings and me with a decent upbringing and education. I also want to thank my brothers, Nurkanat and Becktas, and my sister, Aida, for always believing in me. And finally, I want to thank my wife, Dinara, and my wonderful son, Issatay, for their unwavering support and motivation, and for bringing joy to my life throughout these years.

Sincerely,

Yerkanat Kanafin

TABLE OF CONTENTS

LIST OF TABLES

Table 8.5. Optimum experimental conditions derived from the RSM model.

LIST OF FIGURES

Fig. 8.4. Surface plots for TOC removal model: (a) time and PS content, (b) PS content and goethite dosage, and (c) time and goethite dosage.

Fig. 8.5. The optimum area for the synthetic landfill leachate treatment.

Fig. 8.6. A possible mechanism for the PS activation by goethite and UV during the remediation of landfill leachate.

Fig. 8.7. The elimination of ammonium nitrogen from of the actual landfill leachate after the UV/PS/Goethite treatment using air stripping at pH 11 for 3 h.

LIST OF ABBREVIATIONS

h_{vb}^{+} - the valence band holes

e_{cb}^{-} - the conduction band electrons

$^{\bullet}OH$ – hydroxyl radical

AOPs – advanced oxidation processes

BBD - Box-Behnken design

BOD - biological oxygen demand

BPA - bisphenol A

CAF - caffeine

CAS – conventional activated sludge process

CBZ – carbamazepine

COD - chemical oxygen demand

CSTR - continuous stirred tank reactor

DOC - dissolved organic carbon

EEO - electrical energy per order

EPs - emerging pollutants

FTIR - Fourier-transform infrared spectroscopy

Hcp - Henry solubility

HPLC - high-performance liquid chromatography

HR-AOPs – hydroxyl-radical based AOPs

HRT - hydraulic retention time

IBU – ibuprofen

IC - ion chromatography

MBR - membrane bioreactor

MNZ – metronidazole

NPX – naproxen

$O_2^{\bullet-}$ - superoxide anion radical

PBD - Plackett-Burman design

PIM - phase inversion membrane

PIMBR - the phase inversion-MBR

PMS - peroxymonosulfate

PS - persulfate

RAS - recycled activated sludge

RLL - real landfill leachate

RSM - response surface methodology

S_{BET} - BET surface area

SBR - sequencing batch reactor

SEM-EDS – scanning electron microscopy with energy dispersive spectroscopy

SLL - synthetic landfill leachate

SMX – sulfamethoxazole

$SO_4^{\bullet-}$ - sulfate radicals

SR-AOPs – sulfate-radical based AOPs

SRT - solid retention time

TC – total carbon

TEM - track-etch membranes

TEMBR - track-etch MBR

TIC – total inorganic carbon

TMS - trace metal solution

TN – total nitrogen

TOC - total organic carbon

TP - total phosphorus

TSS - total suspended solids

US – ultrasonication

UV – ultraviolet light

VSS - volatile suspended solids

XRD – X-ray diffraction

ZVI - zero-valent iron

CHAPTER 1: INTRODUCTION

1.1. Background

The study into wastewater treatment systems is motivated by environmental and health concerns generated by the profusion of newly discovered pollutants in the aquatic environment. The current increase in wastewater generation worldwide is being caused by the expansion of the world's population as well as the speedy pace of industrialization and urbanization [1]. Wastewater treatment facilities primarily utilize the activated sludge process for treating wastewater. The activated sludge process relies on microorganisms to break down both organic and inorganic pollutants found in wastewater, but this method may not effectively remove certain pollutants [2]. As a result, these pollutants can enter the aquatic environment if they are not completely eliminated during the treatment process [2]. Therefore, to avoid environmental risk, there is a need for additional water treatment technologies such as membrane filtration and advanced oxidation processes.

Emerging pollutants are the least studied of the many groups of water contaminants. Pharmaceuticals, agrochemicals, personal hygiene items, endocrine-disrupting substances, surfactants, and industrial chemicals are examples of pollutants (Fig. 1.1.) [3].

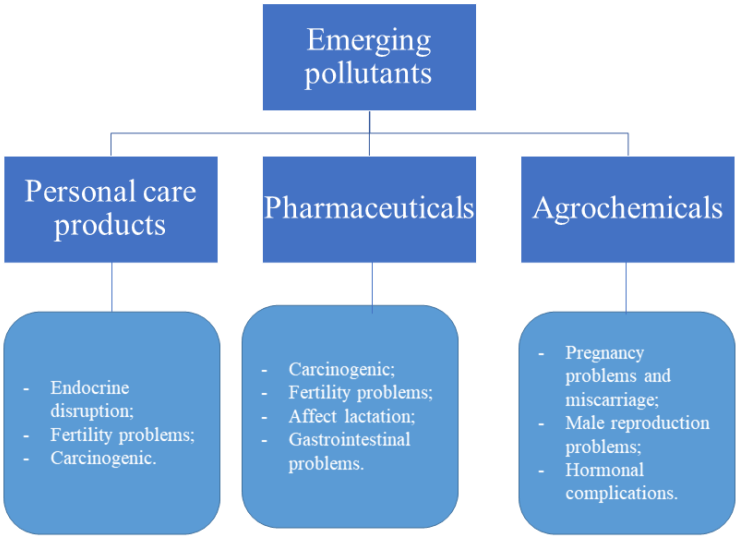

Fig.1.1. Major impacts on human health of commonly detected pollutants of emerging concern. Adapted from [3].

Wastewater treatment technologies are applied to treat wastewater before its release into the environment, involving biological, physical, and chemical processes. In a typical wastewater treatment plant, the secondary treatment (biological processes) constitutes the heart of the process, since approximately 80-90% of all pollutants are removed [4]. Despite the widespread use of the activated sludge process, it is not always effective in completely

eliminating harmful organic compounds from wastewater. This is particularly true for emerging contaminants and requires the implementation of more advanced treatment methods [5].

Advanced oxidation processes (AOPs) are highly effective methods for treating wastewater, utilizing hydroxyl ($^{\bullet}OH$) or sulfate ($SO_4^{\bullet-}$) radicals as powerful oxidizing agents [6]. These radicals have been proven to effectively degrade organic contaminants and have similar oxidation potentials (2.5-3.1V for $SO_4^{\bullet-}$ and 2.8V for $^{\bullet}OH$) [7,8].]. However, unlike hydroxyl radicals, sulfate radicals can be used in a wider pH range (2-8) [7,8]. Various methods such as UV irradiation, ultrasound, heat, transition metals, carbon-based materials, and heterogeneous catalysts can activate hydrogen peroxide and persulfate [9,10]. Combining these methods can produce a synergistic effect [9]. Another promising AOP technique is heterogeneous photocatalysis [11], which utilizes semiconductors as photocatalysts. These materials absorb light energy and convert it into chemical energy through the formation of electron-hole pairs [12]. Redox reactions then produce the necessary oxidants to break down organic pollutants, and the addition of H_2O_2 can accelerate the reaction. TiO_2-based materials, particularly P25 nanopowder, are widely used for this purpose due to their availability and effectiveness under UV irradiation [12,13]. However, high-energy UV irradiation can be costly, and but not many photocatalysts work in the visible light spectrum ($\lambda > 310$ nm), making the use of artificial visible light or solar light problematic [14]. Most research on AOPs has focused on treating singsingle-pollutanter solutions, and the impact of other macropollutants present in real wastewater has not been thoroughly investigated [15].

Another promising method for water purification is a membrane bioreactor (MBR) technology [16]. Today, MBR is a well-known and effective technique that is applied globally. MBR is a hybrid system that uses membrane filtration for physical liquid-solid separation along with biological treatment [17]. This technology offers several advantages, such as smaller plant size, higher loading rates, shorter retention times, lower sludge production, and the ability to simultaneously nitrify and denitrify over longer periods [18,19]. The removal efficiency relies on the membrane’s type, sludge age, aerobic/anaerobic/anoxic conditions, pH, temperature, conductivity, and other parameters [18]. The current challenges in MBR include membrane fouling and cost-effectiveness [17]. In this work, track-etch membranes instead of conventional phase inversion membranes were utilized in MBRs. Unlike phase inversion membranes, which have limited control over pore size, geometry, density, and distribution, track-etch membranes are produced by irradiating a polymer film with high-energy ions and then subjecting it to physical and

chemical treatments (i.e. etching) [20]. Previous work of NU professors showed that the country is ppossesses the required tools to produce high quality and cheap symmetric /asymmetric track etch membranes, i.e. 20 USD per m^2 of the membrane [20]. Currently, there are no earlier data on the efficiency of TEMBR in the contaminants of emerging concern removal.

This research is focused on the development of advanced wastewater treatment technology by integrating bio- and membrane-based processes with advanced oxidation processes. Synthetic or real wastewater, containing toxic and/or emerging pollutants, was obtained and characterized by various parameters (pH, TC/TIC/TOC, TN, chemical oxygen demand (COD), concentration of ions, and target compounds). Initially, biological treatment methods in batch and continuous flow mode were deployed to look at how emerging contaminants affect biological removal. Then, effluents of the biological process were further treated with membrane filtration to test the efficiency of the track-etched membranes. The removal efficiencies of different AOPs such as photolysis with H_2O_2, photo-Fenton processes, persulfate-mediated oxidation, and photocatalysis under UV irradiation were compared based on the removal efficiency of TOC and target compound and energy consumption. The efficiency of landfill leachate treatment experiments were optimized by RSM [21]. The use of statistical design allows us to investigate and propose the most beneficial operating conditions of photochemical and membrane treatment to purify efficiently complex wastewater with a focus on the removal of emerging pollutants [22].

1.2. Thesis hypotheses and statements

The thesis hypotheses and statements were determined based on the literature review of conventional and current methods of wastewater treatment.

Thesis hypotheses:

- Pollutants of emerging concern inhibit the activity of microorganisms and, therefore, affect the efficiency of the activated sludge process;
- Advanced oxidation processes could be an efficient post-treatment technique to remove emerging pollutants after biological wastewater treatment;
- Taking into account that track-etch membranes have better properties than conventional membranes, they could be an efficient replacement in MBR technology for the removal of emerging pollutants;
- Oxidative radical sources such as persulfate could be activated using inexpensive Fe-based materials.

Thesis statements:

- To conduct an extensive literature review on the current situation and advances of activated sludge process, membrane bioreactor, and advanced oxidation processes;
- To assess the impact of emerging pollutants on the activated sludge process in terms of removal of organic carbon and nitrogen;
- To further treat effluents after the activated sludge process with membrane filtration using track etch membranes;
- To test advanced oxidation processes for the treatment of real and synthetic wastewater as well as the effluents after the activated sludge process;
- To test Fe-based materials for persulfate activation under different concentrations and conditions using response surface methodology;
- To study persulfate activating materials using state-of-the-art characterization techniques (SEM-EDS, XRD, FTIR, nitrogen porosimetry, etc.);
- To extend the application of AOPs from synthetic wastewater to real wastewater of different origin;
- To study the removal of organic pollutants and evaluate electrical energy per order (EEO) and compare with existing literature.

1.3. The aims and objectives of the research

The aim of this thesis is to integrate biological, physical and chemical processes for advanced wastewater treatment. The secondary aim includes the assessment of advanced oxidation processes using real wastewaters.

The objectives of this thesis are following:

- To evaluate the impact of emerging pollutants on the conventional wastewater treatment process using batch and continuous flow biological reactors;
- To treat the activated sludge process effluents using membrane filtration and advanced oxidation processes;
- To apply sulfate radical-driven advanced oxidation processes with the real wastewater of different origin.

1.4. The novelty of the research

Based on the existing literature, the novelty of the research is:

- Sulfate radical-based advanced oxidation processes were applied for the treatment of real wastewater of different origin;

- The application and comparison of Fe-based materials for activation of persulfate for the treatment of real wastewater of different origin;
- The use of the response surface methodology for assessing the efficiency of the photo-Fenton-like processes for the treatment of real municipal wastewater;
- Track-etch membranes were applied for wastewater treatment purposes for the first time;
- Evaluation of the electrical energy per order of the AOPs using real wastewater and comparison with the literature.

1.5. Research contributions

Six (6) published research papers and one (1) review article:

1) Y.N. Kanafin, Y. Kakimov, A. Adamov, A. Makhatova, A. Yeshmuratov, S.G. Poulopoulos, V.J. Inglezakis, E. Arkhangelsky. The effect of caffeine, metronidazole and ibuprofen on continuous flow activated sludge process. *Journal of Chemical Technology & Biotechnology*, Volume 96, 2021, 1370 – 2380. https://doi.org/10.1002/jctb.6658

2) Y.N. Kanafin, A. Makhatova, V. Zarikas, E. Arkhangelsky, S.G. Poulopoulos. Photo-Fenton-like Treatment of Municipal Wastewater. *Catalysts*, Volume 11(10), 2021, 1206. https://doi.org/10.3390/catal11101206

3) Y.N. Kanafin, D. Kanafina, S. Malamis, E. Katsou, V.J. Inglezakis, S.G. Poulopoulos, E. Arkhangelsky. Anaerobic membrane bioreactors for municipal wastewater treatment: a literature review. *Membranes*, Volume 11(12), 2021, 967. https://doi.org/10.3390/membranes11120967

4) Y.N. Kanafin, A. Makhatova, K. Meiramkulova, S.G. Poulopoulos. Treatment of a poultry slaughterhouse wastewater using advanced oxidation processes. *Journal of Water Process Engineering*, Volume 47, 2022, 102694. https://doi.org/10.1016/j.jwpe.2022.102694

5) Y.N. Kanafin, P. Abdirova, E. Arkhangelsky, D.D. Dionysiou, S.G. Poulopoulos. UVA and goethite activated persulfate oxidation of landfill leachate. *Chemical Engineering Journal Advances*, Volume 14, 2023, 100452

6) Y.N. Kanafin, P. Abdirova, D. Kanafina, E. Arkhangelsky, G.Z. Kyzas, S.G. Poulopoulos. UV and zero-valent iron (ZVI) activated continuous flow persulfate oxidation of municipal wastewater. *Catalysts*, 2023, 13(1), 25. https://doi.org/10.3390/catal13010025

7) Y.N. Kanafin, A. Satayeva, P. Abdirova, V.J. Inglezakis, E. Arkhangelsky, S.G. Poulopoulos. Membrane bioreactor and advanced oxidation processes for combined treatment of the synthetic wastewater containing naproxen, bisphenol A, and sulfamethoxazole. *Journal of Water Process Engineering*, Volume 55, 2023, 104250. https://doi.org/10.1016/j.jwpe.2023.104250

Three (3) published conference papers:

1) Y.N. Kanafin, A. Satayeva, E. Arkhangelsky, S.G. Poulopoulos. Treatment of a biological effluent containing metronidazole. *Chemical Engineering Transactions*. Volume 86, 2021, 595 - 600, https://doi.org/10.3303/CET2186100

2) Y.N. Kanafin, A. Makhatova, E. Arkhangelsky, S.G. Poulopoulos. Photochemical treatment of an actual municipal wastewater by means of UV, potassium persulfate and iron. *IOP Conference Series: Earth and Environmental Science*. Volume 899, 2021, 012067, doi:10.1088/1755-1315/899/1/012067

3) Y.N. Kanafin, P. Abdirova, A. Baltabek, E. Arkhangelsky, S.G. Poulopoulos. Study of the effects of the sulfate-radical sources for wastewater treatment using response surface methodology. *Chemical Engineering Transactions*. Volume 95, 2022, 345 - 350, https://doi.org/10.3303/CET2186100

Two (2) presentations at international conferences:

1) Y.N. Kanafin, A. Satayeva, E. Arkhangelsky, S.G. Poulopoulos. Treatment of a biological effluent containing metronidazole. *15th International conference on chemical and process engineering*, May 23-26, 2021, Naples, Italy (oral presentation).

2) Y.N. Kanafin, A. Makhatova, E. Arkhangelsky, S.G. Poulopoulos. Photochemical treatment of an actual municipal wastewater by means of UV, potassium persulfate and iron. *2nd International Conference on Environmental Design*, October 23-24, 2021, Athens, Greece (oral presentation).

1.6. Thesis overview

This Ph.D. thesis is divided into nine chapters, which are as follows:

Chapter 1 serves as an introduction, presenting a general outline of the research, the thesis hypotheses and statements, as well as the novelty and significant contributions of the study.

Chapter 2 provides an in-depth examination of the relevant research presented in the thesis through a comprehensive literature review. The first section delves into topics such as wastewater generation and composition, as well as the contamination of water resources with

emerging pollutants and their impact on human health and the environment. The second section focuses on conventional wastewater treatment methods, specifically the use of activated sludge process and sequencing batch reactor. The third section introduces the concept of membrane bioreactors, discussing their configuration, operation, and effectiveness in treating wastewater. Moving on, the fourth section explores various advanced oxidation processes and their potential for removing emerging pollutants. The literature review concludes by summarizing the findings and identifying gaps in the existing literature. Furthermore, the research contributions based on this literature review have been published in *Membranes* under the title "Anaerobic membrane bioreactors for municipal wastewater treatment: a literature review".

Chapter 3 provides a detailed overview of the materials, physical and chemical methods utilized in the research, as well as descriptions of the characterization techniques employed. Additionally, this chapter outlines the experimental procedures for both batch and continuous flow bio- and photoreactors, including their respective layouts.

In Chapter 4, the research results of experiments on the treatment of synthetic wastewater containing ibuprofen, metronidazole, and caffeine using a combination of continuous flow biological treatment and photochemical treatment are presented. These findings were published in *Journal of Chemical Technology and Biotechnology* with a research paper titled "The effect of caffeine, metronidazole and ibuprofen on continuous flow activated sludge process" and in *Chemical Engineering Transactions* with a paper titled "Treatment of a biological effluent containing metronidazole".

In Chapter 5, the research outcomes of experiments on the treatment of synthetic wastewater containing naproxen, bisphenol A, and sulfamethoxazole using a combination of membrane bioreactor and photochemical treatment are discussed. These results were published in *Journal of Water Process Engineering* with a research paper titled "Membrane bioreactor and advanced oxidation processes for combined treatment of the synthetic wastewater containing naproxen, bisphenol A, and sulfamethoxazole".

In Chapter 6, the effectiveness of various advanced oxidation processes in treating wastewater from poultry slaughterhouses is examined and the electrical energy per order is compared with existing literature. The research findings from these investigations are published in the *Journal of Water Process Engineering* under the title "Treatment of a poultry slaughterhouse wastewater using advanced oxidation processes".

The results of experiments using AOPs based on sulfate radicals for treating synthetic and actual municipal wastewater are discussed in Chapter 7. These research' findings were published in *Catalysts* in publications titled “Photo-Fenton-like treatment of municipal wastewater” and “UV and zero-valent iron (ZVI) activated continuous flow persulfate oxidation of municipal wastewater”.

Chapter 8 investigates the possibility of using sulfate radical-based advanced oxidation techniques to treat extremely polluted landfill leachate. The study's findings were reported in *Chemical Engineering Journal Advances* in a paper titled “UVA and goethite activated persulfate oxidation of landfill leachate”.

Chapter 9 summarizes the thesis by outlining potential future research that could be conducted in order to expand and improve on the preceding work.

CHAPTER 2: LITERATURE REVIEW

2.1. Wastewater generation and common pollutants

2.1.1 Wastewater generation and composition

Worldwide water supplies are becoming increasingly scarce due to rapid population increase and climate change [1]. To achieve sustainable development, protect human lives, and preserve ecosystem health, clean water is of highest importance [23]. The supply of water in an adequate and suitable quality at the location of intended usage is a prerequisite for all significant human activities, such as agriculture, social infrastructure, manufacturing, chemical industry, energy production, and household [24]. Clean water and sanitation are the emphasis of Sustainable Development Goal (SDG) 6, where the statuses 6.3.1 and 6.3.2 take wastewater and water quality into account [25]. According to the UN Environment Programme's 2020 report, the quality of 72% of the world's monitored water bodies is considered to be acceptable [26]. It should be noted that the data were gathered regionally, therefore, different safety and quality regulations have been applied [25].

The annual production of wastewater worldwide is currently estimated to be 359.4×10^9 m^3 [24]. Today, 52% of the wastewater produced is purified, and each year, 40.7×10^9 m^3 of wastewater are reused [24]. According to a recent survey, high-income nations treat 70% of the wastewater that is produced [27]. Contrarily, for middle-income and low-income countries, the proportion of treated wastewater was in the range of 38% and 8%, respectively [27]. Despite the fact that wastewater treatment systems are an essential process in developed countries, many developing countries continue to directly dump untreated municipal wastewater into natural water systems [23]. For instance, 87 municipal wastewater treatment facilities were registered in Kazakhstan in 2015, and it was confirmed that 33 of them had unacceptable technical conditions [28].

Due to water shortages and growing populations, the issues related to wastewater generation and treatment will get worse in the future. Implementing effective wastewater treatment procedures and recycling the treated wastewater for industrial and agricultural uses is the urgent issue for addressing the water shortage [27]. The presence of untreated wastewater can be harmful to human and aquatic life due to the potential presence of pathogens such as viruses, bacteria, protozoa, and fungi that can cause water-borne diseases [2]. To address this issue and increase the amount of treated wastewater, there is a need for more wastewater treatment facilities, particularly in low-income countries with large populations.

Understanding the chemical characteristics of wastewater is crucial because it facilitates knowledge of reactions and interactions with organic and inorganic components in wastewater [29]. Typically, the content of wastewater might differ from place to place due

to domestic practices and industrial operations. However, the general wastewater matrix can be classified into the following groups: dissolved minerals, inorganic pollutants (nitrates, total phosphorus (TP), heavy metals, etc.), pathogens, and organic matter (dissolved organic carbon (DOC), proteins, carbohydrates and micropollutants) [29,30]. The frequently detected concentrations of the pollutants can be seen in Fig. 2.1 [31].

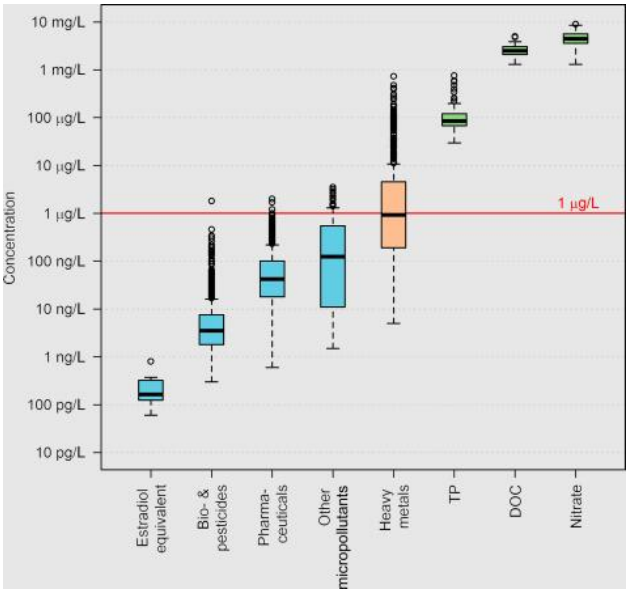

Fig. 2.1. The ranges of wastewater pollutant concentrations recorded at the 24 locations [Reprinted with permission from [31]. Copyright 2022, Elsevier]

As can be seen from Fig. 2.1, nitrates, dissolved organic carbon (DOC) and phosphorus are considered as macropollutants, while the heavy metals have concentrations which are typical for both macro- and micropollutants. The abundance of nitrates and phosphorus compounds in water may lead to river eutrophication and deterioration of water quality [29,32]. DOC is comprised of fragmented cells and organic macromolecules [29] and serve as a carbon source for microbial growth in activated sludge process [33,34].

Even though emerging contaminants account for only a small portion of the dissolved organic matter content, these substances are designed to have highly targeted (biological) effects [31]. These include healing a sickness, preventing weed development and giving a calorie-free alternative to sugar and etc. In short, emerging contaminants have biological activity orders of magnitude more than normal dissolved organic matter. Their mode of action is frequently highly particular and may affect certain groups of organisms (for example, only bacteria, only bugs, etc.). Therefore, emerging contaminants vary fundamentally from nutrients, which are required by all organisms. Heavy metals are commonly detected in trace amounts in wastewater, however, they are dangerous and tend accumulate in human body causing risk for human health [35]. Finally, micropollutants also

include organic contaminants of emerging concern or so-called emerging pollutants which will be discussed in the next section.

2.1.2 Emerging pollutants

Emerging pollutants have been identified in all types of surface waters starting from the drinking water and in the outflows from wastewater treatment facilities. Pharmaceuticals, endocrine disruptors, agrochemicals, and cosmetics are some of the organic pollutants of emerging concern that pose a risk to the environment [31]. Even with the construction of wastewater treatment facilities, which are mainly based on the biological treatment, the environment is still not protected against the spread of newly emerging pollutants and their subsequent effects. Some of these chemicals escape activated sludge-based wastewater treatment facilities because of their stable structure, and they are then released into the aquatic environment [36]. The organic molecules' biodegradability is additionally aided by the compounds' branching structure and large molecular weight [16]. Degradations of 60% or more have been observed for compounds having MW greater than 300 [37]. The more chemicals there are, the more complicated the wastewater matrix is, which increases the complexity of the wastewater treatment [36]. Consequently, it is necessary to create complementary techniques of wastewater treatment. Emerging pollutants may enter the aquatic environment either directly or indirectly as a result of anthropogenic activities like wastewater discharge, farming practices, agriculture, and landfill leachate (Fig. 2.2) [38].

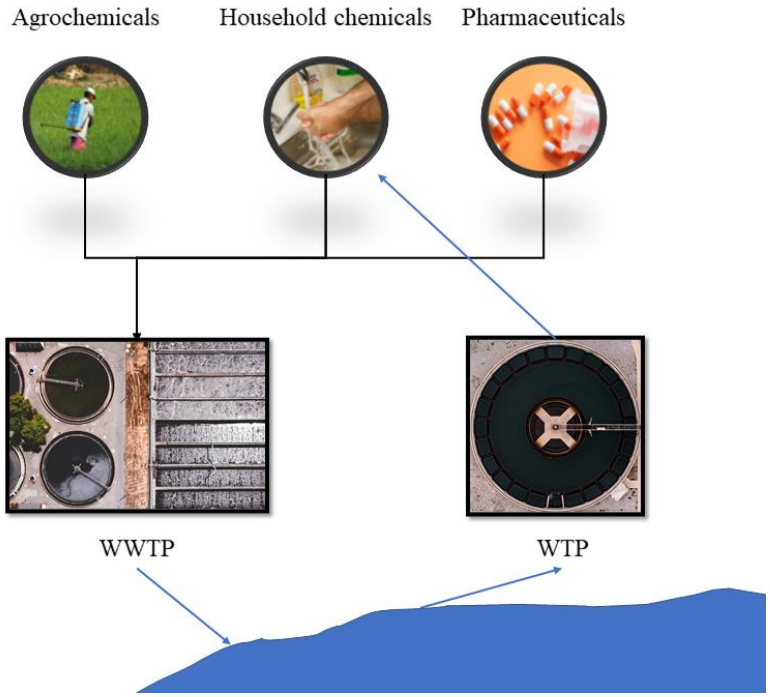

Fig. 2.2. The source and environmental pathway of emerging pollutants (EPs). Adapted from [38].

Few emerging pollutants are regularly monitored in the environment due to inadequate information of their toxicity, effects, and behaviors, while many are still unregulated [39]. Pharmaceuticals are a type of growing environmental contaminant that is widely and increasingly employed worldwide. Antibiotics, analgesics, neurostimulants, anti-inflammatory medications, anticonvulsants, beta-blockers, and other potentially hazardous compounds are included in the list [40]. Currently, a wide variety of emerging pollutants have been found in aquatic systems at detectable quantities. The reported concentrations of emerging pollutants are presented in Table 2.1.

Table 2.1 Concentrations of selected emerging pollutants detected in drinking water, groundwater, surface waters and wastewater.

Pollutant	Concentration, ng/L	Type of water	Location	Ref.
Caffeine	51.2 – 3060	River	Jiulong River, China	[41]
	16600	River	Taiwan	[42]
	34.3 - 95.5	Drinking water	Seoul, Korea	[43]
	1250 – 1720	Wastewater	Bangkok, Thailand	[44]
	213 – 96600	Wastewater	Arta, Greece	[45]
	170 – 200	Groundwater	Kabwe, Zambia	[46]
	4920 – 12400	Wastewater	Guanajuato, Mexico	[47]
Ibuprofen	92	Groundwater	Serbia	[48]
	34	River	River Mississippi, USA	[49]
	414	River	River Mankyung, South Korea	[50]
	2200	Wastewater	Taiwan	[51]
	10	Groundwater	An experimental agricultural field in Ottawa, Canada	[52]
Metronidazole	136.2	River	Gościcina river, Poland	[53]
	5900	Hospital wastewater	Almeria, Spain	[54]
	3600 – 101000	Hospital wastewater	Kalmar, Sweden	[55]
	< 1.5	River	River Taff, Wales UK	[56]
	< 1.5	River	River Warta, Poland	[56]
Sulfamethoxazole	46	Groundwater	Baix Llobregat, Barcelona, Spain	[57]
	50.6	River	Tiber River, Italy	[58]
	1720	Wastewater	Hanoi, Vietnam	[59]
	802	Wastewater	Manila, Philippines	[59]
	538	Wastewater	Kolkata, India	[59]
	76	Wastewater	Kuala Lumpur, Malaysia	[59]
	282	Wastewater	Jakarta, Indonesia	[59]
Bisphenol A	5	Drinking water	Nevada, USA	[60]
	1	Drinking water	Lake Maggiore, Italy	[61]
	70 – 1680	Wastewater	Quebec, Canada	[62]
	2830 – 4950	Wastewater	Slovenia	[63]
	1.2	Drinking water	Songhua River basin	[64]
Naproxen	27.6	Groundwater	Serbia	[48]
	447	River	Fyris River, Sweden	[65]
	11400 – 32000	River	Malir River, Pakistan	[65]
	9580	Wastewater	Reghaïa, Algeria	[66]
	40 – 210	Lake	Lake Haapajarvi, Finland	[67]
	145	Groundwater	Baix Llobregat, Barcelona, Spain	[57]

Carbamazepine	3.4	Groundwater	Serbia	[48]
	33 – 137	Wastewater	Canada	[68]
	290 – 960	Wastewater	Tainan, Taiwan	[69]
	<0.5 – 120	River	Lao-Jie River and Zen-Wen River, Taiwan	[69]
	136	Groundwater	Barcelona, Spain	[70]

Table 2.1 shows that the emerging pollutants were detected at levels ranging from 1 ng/L to 101 μg/L. However, even at these the emerging pollutants can have significant effect on public health [38].

2.1.3 Adverse effects of emerging pollutants

Governments find it difficult to regulate the use of emerging pollutants as a result of the lack of pertinent data on the effects, fate, and concentration levels of organic pollutants [38]. Emerging organic pollutants have been linked to severe ecological damage, toxicity, and dangers to both major and minor health in aquatic habitats [71]. As it has been presented in Table 2.1, a significant amount of organic pollutants have been detected in the environment. The vast majority of emerging pollutants have uncertain or challenging to determine long-term consequences, which is still a worry considering the lack of awareness among individuals about the potential harm their actions may cause to the environment [72]. The most serious negative impacts to date include cancer-causing, endocrine-disrupting effects, and an increase in resistant infections, which pose a serious danger to living things' immune systems [73]. The reported negative consequences of selected emerging contaminants on the ecosystem are summarized in Table 2.2.

Table 2.2. Reported environmental and health effects of emerging pollutants.

Pollutant	Adverse effects	Ref.
Caffeine (stimulant drug)	Endocrine disruption in goldfish (*Carassiusauratus*)	[38]
	Mortality, the generation of oxidative stress, changes in the reproduction and growth of aquatic and terrestrial insect species.	[74]
Ibuprofen (nonsteroidal anti-inflammatory drug)	Immune system impairment, changes in the growth of the reproductive and endocrine systems, the induction of antioxidative stress in fish and daphnia.	[75]
Metronidazole (antibiotic)	Causes mutations in some bacteria, fungus, and rodents. Carcinogenic effect in animals.	[76]
	Surface water contamination may promote the growth of resistant bacteria.	[77]
Sulfamethoxazole (antibiotic)	Toxic effects on the zebrafish (*Danio rerio*), striped marsh frog (*Limnodynastes peronii*), crustacean (*Daphnia magna*) and green algae (*Selenastrum capricornutum* and *Chlorella vulgaris*) and carcinogenic effect in algae (*Scenedesmus obliquus*).	[78]
Bisphenol A (industrial chemical)	Studies have shown that this chemical compound has the ability to mimic estrogen in rats and can lead to hormonal changes that elevate the probability of breast cancer. It has also been linked to anti-androgen properties, which can cause feminizing effects in men.	[79]
Naproxen (nonsteroidal anti-inflammatory drug)	Genotoxic effect, accumulation and the suppression of the metabolizing enzyme activity in aquatic organisms, gastrointestinal and renal effects in zebrafish, growth inhibition in algae and amphibians.	[80]
Carbamazepine (anticonvulsant drug)	Oxidation stress of rainbow trout (Oncorhynchusmykiss)	[38]
	At 100 ng/L concentration harmed specific phases of chick embryonic development, which modeled human embryonic development.	[81]

As it has been summarized in Table 2.2, emerging pollutants have a negative impact on human societies, wildlife, and both land and aquatic ecosystems. Numerous sexual and reproductive disorders in both wildlife and people are brought on by endocrine disrupting

substances. Exposure to these substances during fetal and postnatal development may impede endocrine system development and signaling. The consequences of development are long-lasting and occasionally irreversible [38]. The environmental consequences of emerging pollutants, however, differ from those seen in laboratory settings. When environmental pollutants are present, a variety of parameters, including pH, soil type, and water matix, may affect the fate of the chemicals [82].

The UN SDG 6 places a strong emphasis on the urgency of the issue, and by 2030, it aims to achieve the wise recycling and safe reusing of water throughout the world, as well as to seize pollution and eliminate the release of emerging pollutants into aquatic environment [25]. This motivates the scientific community to create solutions to eliminate the danger of organic contaminants that are affordable, ecologically acceptable, useful, and implementable on a broad scale.

2.2 Conventional wastewater treatment

2.2.1 Activated sludge process

Biological treatment has been extensively utilized for the treatment of wastewater, mostly using the biodegradation mechanism. Large-molecular-weight contaminants are broken down into smaller organic and inorganic molecules during the biodegradation process, which involves bacteria, algae, and fungi [83]. Microorganisms in the typical biodegradation process utilize organic substances as primary sources for cellular proliferation [83]. Certain pollutants are hazardous and refractory to bacterial activity, preventing biodegradation; in this scenario, an additional carbon source is necessary to keep microbial activity for biological degradation, a process is termed as co-metabolism [84]. Traditionally, biodegradation technologies have been utilized to eliminate various contaminants of organic origin. They are divided into aerobic, anoxic and anaerobic processes. Activated sludge and sequence batch reactors are examples of aerobic uses. Anaerobic sludge and biofilm reactors are two examples of anaerobic techniques. The features of the wastewater are critical in the choosing of biological treatments [84].

Generally, in the activated sludge process, biomass is created in wastewater by microbial growth in bioreactor in aerobic and anoxic conditions. Using air and a biological floc, this process is used to remove organic content from sewage and industrial wastewaters with mainly bacteria and protozoa [85]. These microorganisms are capable of decomposing organic materials into CO_2, water, and other inorganic chemicals [85]. The removal of nitrogen species such as ammonium, nitrites and nitrates is realized through denitrification and nitrification processes [86].

Oxidation of ammonium nitrogen and its conversion into nitrite nitrogen and ultimately to nitrates is known as biological nitrification. Two energy-producing biological processes occur during nitrification. Ammonium ion oxidation generates more energy than nitrite ion oxidation (Eqs. 2.1 and 2.2):

$$2NH_4^+ + 3O_2 \rightarrow 2NO_2^- + 4H^+ + 2H_2O, \quad (2.1)$$

$$2NO_2^- + O_2 \rightarrow 2NO_3^-. \quad (2.2)$$

Nitrifying bacteria of the genera *Nitrosocystis*, *Nitrosococcus*, *Nitrosospira*, *Nitrosolobus*, and *Nitrosomonas* oxidize ammonium ions to nitrites, whereas *Nitrobacter*, *Nitrococcus*, and *Nitrospira* convert nitrites to nitrates [86,87].

Biological denitrification is the breakdown of organic compounds by denitrifying bacteria (facultative anaerobes) using nitrite ions or nitrate ions. *Alcaligenes*, *Bacillus*, and *Pseudomonas* genera include the great majority of denitrifying bacteria [86]. The reduction of nitrite and nitrate nitrogen to nitrogen molecule takes place during the sequential denitrification process, which takes place inside the bacterial cell. The complete degrading process may be summarized into two reactions (Eq. 2.3 and 2.4) [86]:

$$NO_3^- + \text{organic carbon} \rightarrow NO_2^- + CO_2 + H_2O \quad (2.3)$$

$$NO_2^- + \text{organic carbon} \rightarrow N_2 + CO_2 + H_2O \quad (2.4)$$

The energy obtained from the anoxic respiration is smaller than that of aerobic respiration [86]. Therefore, the concentration of dissolved oxygen of less than 1 mg/L should be kept in the reactor vessel in order to maintain anoxic conditions as the aforementioned microorganisms can switch to aerobic respiration.

2.2.2 Sequencing batch reactor

Because of the advantageous features of SBR over a continuous flow reactor arrangement, there has been considerable interest in their application [88]. A sequential batch reactor is based on the batch process, as the name implies. The distinction with an SBR is that the control scheme and accompanying operations are designed to continuously repeat the batch process, resulting in very minimal reactor downtime. One of the significant benefits of the SBR over a continuous flow reactor type is that a secondary clarifier is not required to collect sludge that has flowed out of the bioreactor as part of the outflow. Because SBRs feature a settling phase within the reactor, the effluent of SBRs contains very little total suspended solid (TSS), requiring a reduced secondary clarifier, if any at all [88]. This saves money on both the initial investment in a WWTP and the running costs of the clarification tank and return sludge systems. Aside from the lower construction cost, maintaining sludge in the

reactor offers a few of other advantages [88,89]. Fig. 2.3 depicts the different operating modes of an SBR [89].

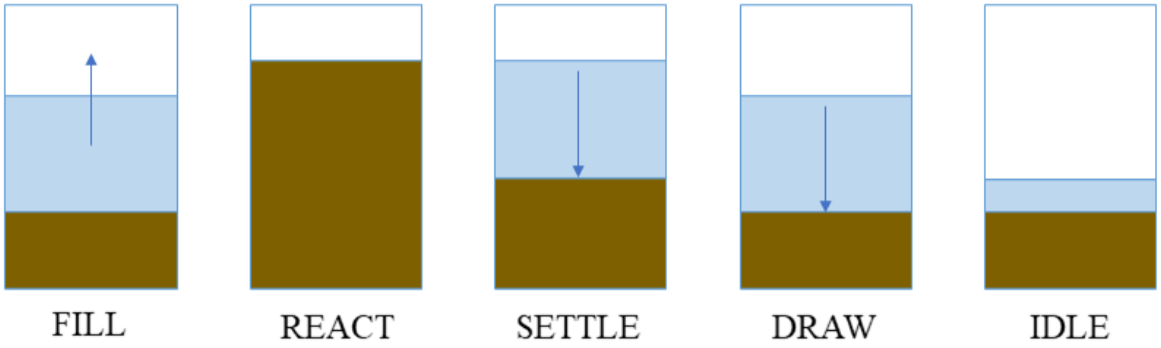

Fig. 2.3. Various stages of the SBR operating cycle. Adapted from [89,90].

The SBR system, as well as its variations, may require one or more tanks, depending on the size of the operation [89,90]. During the FILL phase, the tank collects raw wastewater that has come into touch with the active biomass that remained inside the tank after the previous cycle had completed. The REACT phase is meant to complete the biological processes that are principally responsible for organic breakdown. Then, the whole reactor tank operates as a batch clarifier during the SETTLE phase, with no input or outflow. Following the settling of the sludge formed by the REACT phase, the DRAW phase decants the treated supernatant using a decanter, either static or floating. The IDLE phase occurs between the DRAW and FILL stages. Depending on the operational plan, mixing the sludge and discarding superfluous sludge may be undertaken during this step [89,90]. Overall, the SBR process is an appealing option for removing emerging contaminants from wastewater because of its ability to produce anaerobic/anoxic/aerobic conditions applying the same reactor [89]. The efficiency of SBR against some common emerging pollutants are discussed in the next section.

2.2.3 The application of activated sludge process for the removal of emerging pollutants

Conventional wastewater treatment plants are primarily effective at eliminating organic contaminants that can be broken down by microorganisms, using activated sludge process. However, certain pharmaceuticals are not easily broken down and may possess resistant properties [91]. The elimination of specific emerging pollutants using the conventional activated sludge process (CAS) and sequencing batch reactor can be seen in Table 2.3.

Table 2.3. Removal of selected emerging pollutants by different biological treatment technologies.

EPs	Method	$C_{influent}$	Removal, %	Ref.
Caffeine	CAS	45 ng/L	68.6	[92]
	CAS	670 μg/L	100	[93]
	SBR	26 μg/L	≥99	[94]
	CAS	26 μg/L	≥99	[94]
	CAS	6679 ng/L	96	[95]
Ibuprofen	CAS	1 mg/L	99	[96]
	CAS	10 mg/L	99	[97]
	CAS	27 ng/L	99.5	[92]
	SBR	20 μg/L	99	[98]
	CAS	45 μg/L	100	[93]
Metronidazole	CAS	28 ng/L	34	[99]
	CAS	100 mg/L	22	[100]
	CAS	100 mg/L	<20	[101]
	CAS	5-100 mg/L	<5	[102]
Sulfamethoxazole	CAS	145 ng/L	65.5	[103]
	SBR	50 mg/L	≥99	[104]
	CAS	93 ng/L	73.8	[105]
	CAS	3.06 g/d	55.6	[106]
	CAS	21.1 μg/L	22	[107]
Bisphenol A	SBR	5 mg/L	32.2	[108]
	CAS	50 mg/L	80.2	[109]
	CAS	25-310 ng/L	59	[110]
	CAS	400 ng/L	1-77	[111]
	CAS	2880 ng/L	25.5	[112]
Naproxen	CAS	542 ng/L	96.8	[95]
	CAS	463 ng/L	71.8	[105]
	CAS	37 g/d	85.1	[106]
	CAS	9.5 μg/L	86	[107]
	CAS	50 mg/L	80	[113]
Carbamazepine	CAS	1012 ng/L	46.3	[95]
	CAS	19 μg/L	6	[107]
	CAS	156 ng/L	<10	[105]
	CAS	5.21 g/d	<10	[106]
	CAS	1850 ng/L	13.8	[103]

As can be seen from Table 2.3, CAS and SBR were capable to completely remove caffeine and ibuprofen in most cases. In case of sulfamethoxazole, bisphenol A and naproxen partial

removal has been observed, while removal of metronidazole and carbamazepine were not higher than 10-20 % predominantly, which demonstrates poor biodegradability of these compounds. Bon et al. studied the fate of bisphenol A in Hong Kong sewage treatment and reported that bisphenol A escape the process [112]. The average concentration of bisphenol A was 2880 ng/L in the influent wastewater, while the average removal the compound was 25.5%. Aboudalle et al. used CAS for the treatment of synthetic wastewater containing 100 mg/L of metronidazole and achieved only 22% removal of the target pollutant after 9 days [100]. In another research, Suarez et al. investigated the removal performance of lab scale activated sludge reactor against 16 emerging pollutants, including pharmaceuticals and hygiene products, and achieved 6% removal of carbamazepine and 22% removal of sulfamethoxazole [107]. Radjenovic et al. found 130-670 ng/L of naproxen in the primary influent wastewater of the full-scale activated sludge process and reported about 71.8 % elimination of naproxen and 73.8% removal of sulfamethoxazole [105]. As can be seen from the literature, certain emerging pollutants escape CAS and, therefore, effective post-treatment methods, such as advanced oxidation processes and membrane filtration, must be utilized to completely remove emerging pollutants from wastewaters [92].

2.3 Membrane bioreactor

2.3.1 Membrane bioreactor configurations and effects of operating conditions on membrane bioreactor

MBR technology bridges the gap between activated sludge process and membrane filtration. It has become more widespread, and is capable of treating a wide range of wastewaters, including industrial liquids and household effluents [114]. In contrast, the traditional activated sludge process cannot manage changes in effluent composition or variations in wastewater flow rate. MBR technology is also employed when the demand for effluent quality exceeds the capacity of the activated sludge process [115]. MBR is an excellent separation technology that is becoming increasingly cost-effective and superior to traditional water treatment with proven performance [105]. Normally, three types of MBR configurations are recorded: external (sidestream) MBR, externally submerged MBR and submerged MBR (Fig. 2.4) [115].

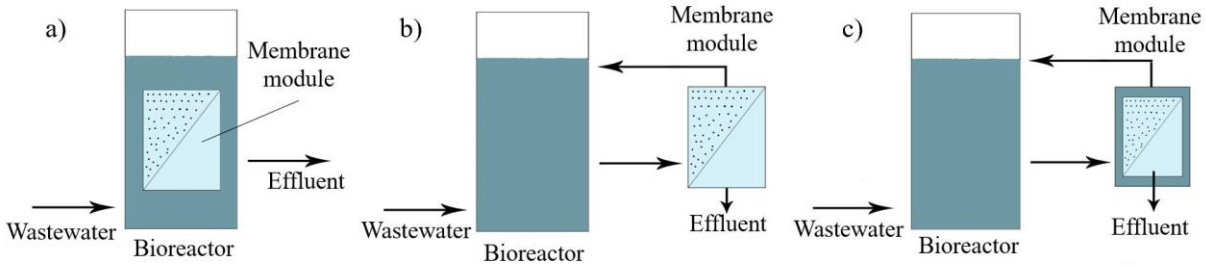

Fig. 2.4. Main configurations of membrane bioreactor. a) bioreactor with submerged membrane module; b) membrane unit connected to the bioreactor externally and c) submerged membrane unit connected to the bioreactor externally. Adapted from [115].

The membrane in a sidestream or external MBR exists outside, whereas the membrane in a submerged MBR is immersed in the aerated tank. Because the inclusion of a recycling pump in the sidestream, the cost of sidestream MBR is considerable [16]. Although modern membrane technology with submerged MBR improves performance, it also causes cake development, which reduces MBR performance [116]. To eliminate the cake from the membranes physical cleaning and chemical cleaning with acid are used and to decrease fouling in the entire process, membrane filtration process is followed by nanofiltration or reverse osmosis unit [117].

Solid retention time (SRT) and hydraulic retention time (HRT) are important parameters in the pollutant removal in MBRs [118]. SRT denotes the length of time that the solid fraction of wastewater remains in the bioreactor. The average time length for which a soluble chemical is present in the bioreactor is reflected by HRT [115]. It is determined by dividing the volume of the reactor) by the feed solution flow rate. It represents the length of time that wastewater treatment is conducted in the bioreactor.

It is proposed that in traditional bioreactors, SRT and HRT are identical, however in retaining biomass reactors, SRT is greater than HRT. The membrane bioreactor has been examined with various SRT and HRT, and it has been discovered that controlling these parameters is critical for achieving optimal bioreactor output. Different results were observed when pharmaceutical waste was removed from wastewater using MBR [117,119].

The sorption process is also affected by pH. The industrial discharge can acidify the wastewater, and a low pH has been observed to improve the hydrophobicity of the chemicals as well as the adsorption of solid compounds. This promotes rapid biodegradation and elimination [120]. Due to strong lipophilicity of some compounds, many studies demonstrate a high removal rate in MBR at low pH [121]. Some research have revealed that ketoprofen, diclofenac, and ibuprofen molecules are pH-dependent (ionizable) [119].

The elimination of micropollutants increases as the temperature rises [122]. It is thought that low temperature slows the treatment process and high temperature speeds it up, however extremely high temperatures may limit the microbial activity and slow down the process. Researchers studied the elimination of erythromycin and sulfamethoxazole at various temperatures and discovered that increasing the temperature from 14–18 °C to 18–23 °C enhances elimination by up to 30% [107].

The laboratory-scale study gives information regarding micropollutant removal under MBR work settings since laboratory conditions match real conditions. As it has been noticed through the removal of micropollutants by MBR on a pilot or industrial scale, the laboratory-scale investigation provides insight into scaling up the treatment process for future applications [115,123]. The pilot-scale study also takes risk events like power outages, chemical shocks, and treatment process aeration failure into account [124].

There are three types of conditions: anaerobic (no oxygen), aerobic (with oxygen), and anoxic (oxygen in bound form e.g. nitrates) [16]. The activity, variety, and enzymatic spectrum of microbes are all determined by redox conditions [118]. Some chemicals, such as tonalide and estrogen, degrade under both aerobic and anoxic environments [118,125]. Naproxen and ibuprofen are removed under aerobic conditions [16], but sulfamethoxazole and carbamazepine undergo minimal aerobic degradation [118]. Similarly, anoxic conditions are encountered in wastewater treatment, with modest removal of galaxolide and trimethoprim. More research is needed on microbial metabolism under varied redox settings, as well as the proper micropollutant transformation [115].

2.3.2 Performance of membrane bioreactor in wastewater treatment

Emerging pollutants found in sewage have piqued the interest of academics and the general public in recent years. Pharmaceuticals, endocrine disruptors, and personal care chemicals are among the most intensively studied emerging contaminants [105,126,127]. Table 2.4 displays data illustrating MBR treatment efficacy in eliminating common emerging contaminants.

Table 2.4. Removal of selected emerging pollutants by MBR.

EPs	Method	$C_{influent}$	Removal, %	Ref.
Caffeine	Flat-sheet MBR	7.92–26.05 µg/L	99.6	[128]
	Hollow-fiber MBR	7.92–26.05 µg/L	99.7	[128]
	MBR	1900 ng/L	49.6	[37]
	Anaerobic MBR	1.625 µg/L	76.9	[129]
	Anoxic MBR	1 mg/L	97	[126]
Ibuprofen	MBR	1480 ng/L	98.5	[103]
	Flat-sheet MBR	21700 ng/L	99.2	[105]
	Hollow-fiber MBR	21700 ng/L	99.5	[105]
	MBR	56.3 g/d	99.8	[106]
	MBR	6725 µg/m^3d	92	[130]
Metronidazole	MBR	0.486 µg/L	95	[131]
	MBR	290 ng/L	>90	[132]
	MBR	5 µg/L	40	[133]
	MBR	5 µg/L	36	[127]
Sulfamethoxazole	MBR	145 ng/L	61.4	[103]
	Flat-sheet MBR	93 ng/L	80.8	[105]
	Hollow-fiber MBR	93 ng/L	78.3	[105]
	MBR	3.06 g/d	60.5	[106]
	MBR	1 mg/L	97.2	[134]
Bisphenol A	MBR	90.16 ng/L	93	[135]
	Flat-sheet MBR	0.51–1.50 µg/L	96.0	[128]
	Hollow-fiber MBR	0.51–1.50 µg/L	96.7	[128]
	MBR	1800 ng/L	90.4	[37]
	MBR	20 µg/L	97	[136]
Naproxen	Flat-sheet MBR	463 ng/L	90.7	[105]
	Hollow-fiber MBR	463 ng/L	91.6	[105]
	MBR	37 g/d	99.3	[106]
	MBR	50 µg/L	89	[123]
	MBR	1700 ng/L	40.1	[37]
Carbamazepine	MBR	1287 µg/m^3d	13	[130]
	MBR	1850 ng/L	12.5	[103]
	Flat-sheet MBR	156 ng/L	<10	[105]
	Hollow-fiber MBR	156 ng/L	<10	[105]
	MBR	5.21 g/d	<10	[106]

Caffeine, ibuprofen, naproxen and bisphenol A were removed at a high rate of >90% in most cases in the literature, whereas sulfamethoxazole and metronidazole were removed at the rate of >36%. Furthermore, carbamazepine had a poor elimination efficiency of less

than 15%. Based on the data from Tables 2.3 and 2.4, the removal efficiencies of CAS and MBR were compared in Fig.2.5.

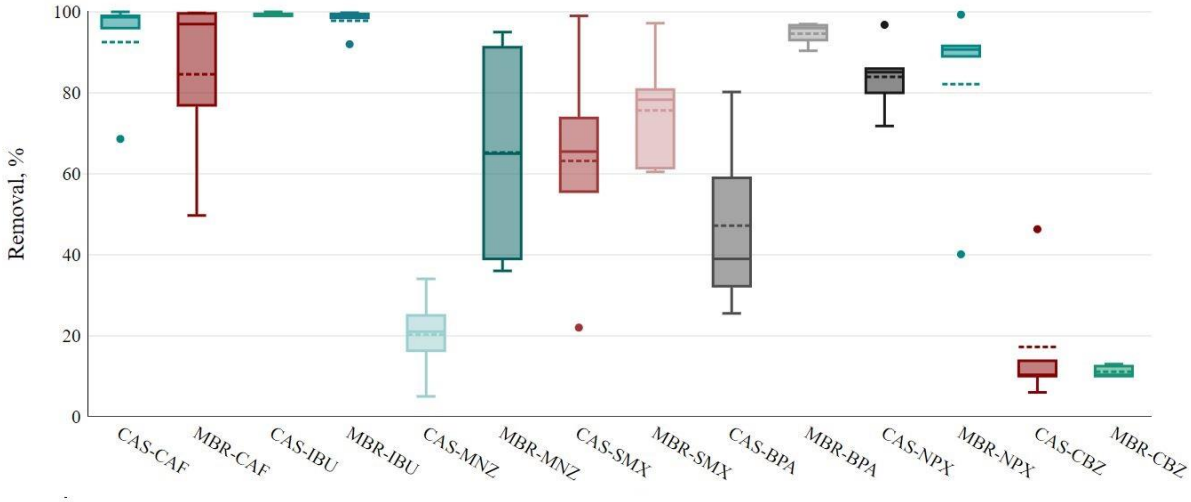

Fig.2.5. Comparison of the average removal efficiencies of CAS and MBR towards selected emerging pollutants.

The removal of caffeine, ibuprofen, sulfamethoxazole and naproxen were not significantly different for both methods and ranged between 63% and 99% (Fig. 2.5). However, MBR demonstrated efficient removal of metronidazole (65%) and bisphenol A (95%), while CAS clearly struggled to remove them from the system (20% for metronidazole and 47% for bisphenol A). In case of carbamazepine both methods were equally inefficient (less than 20% removal). MBR-based systems were usually observed to have superior treatment performance for specific types of emerging contaminants when compared to traditional activated sludge processes without tertiary treatment due to full retention of suspended particles and greater sludge concentration at longer SRT [105,117,119]. According to a recent study, the chemical characteristics of emerging contaminants were directly related to their ability to be removed during the biological treatment (either by biodegradation or hydrophobic binding) [137]. Previous research has demonstrated that the inclusion of nitriles, aromatic alcohols and esters can enhance biodegradability [138].

2.4 Advanced oxidation processes

2.4.1 Overview

AOPs are a broad category of chemical oxidation techniques that produce $^{\bullet}OH$ or $SO_4^{-\bullet}$ to breakdown contaminants in water [139]. Because of their superior effectiveness, capacity to mineralize recalcitrant contaminants as well as the enhancement of the biodegradability index, AOPs have attracted many research recently [140]. Techniques for producing

oxidative radicals vary greatly, and AOPs can be classed as based on O_3, UV, Fenton reaction, photocatalysis, electrochemical or physical processes (Table 2.5).

Table 2.5. Commonly utilized AOPs.

O_3-based	Fenton-based	UV-based	Photocatalytic	Physical	Electrochemical
O_3	Fe^{2+}/H_2O_2	UV/H_2O_2	UV/Cat.	Electron	Anodic oxidation
O_3/H_2O_2	$Fe^{3+}/H_2O_2/UV$	$UV/S_2O_8^{2-}$	$UV/Cat./H_2O_2$	beam	$Fe^{3+}/H_2O_2/(e-)$
O_3/Cat.	$Fe^{2+}/S_2O_8^{2-}/UV$	UV/Cl_2	$UV/Cat./ S_2O_8^{2-}$	US	UV/Cat./(e-)
O_3/UV	$Fe^{2+}/H_2O_2/US$			Plasma	$UV/Fe^{3+}/H_2O_2/(e-)$
				Microwave	$US/Fe^{3+}/H_2O_2/(e-)$

The principal oxidants responsible for AOPs' better efficacy in compared to traditional treatment procedures are hydroxyl and sulfate radicals [141]. In addition, AOPs can be classified depending on the oxidants produced. Hydroxyl radical AOPs (HR-AOPs) use hydroxyl radical with potential of 2.8 V, whereas sulfate radical AOPs (SR-AOPs) utilize sulfate radicals with oxidation potential of 2.5-3.1V [7,8]. Persulfate or peroxymonosulfate are significantly safer and easier to use, store, and transport than hydrogen peroxide, which is often employed as a hydroxyl radical source [142].

AOPs are typically composed of two stages: the radical generation and the oxidation of the targeted contaminants. There are a number of process variables that affect the radical production mechanism, including the presence of species (inorganic ions and natural organic matter) in wastewater composition that scavenge radicals [143]. In the next subsections, principles and suggested mechanisms of HR-AOPs and SR-AOPs, as well as heterogeneous photocatalysis.

2.4.2 Hydroxyl- and sulfate-radical based AOPs

Several AOPs based on sulfate and hydroxyl radical the formation via photochemical, electrochemical, sonochemical, and physicochemical processes are feasible [6,139]. The primary precursors employed for the formation of $SO_4^{\bullet-}$ in water are peroxymonosulfate (PMS) and persulfate (PS). PS and PMS have a sluggish direct interaction with organics, making them unsuitable for pollutant degradation. Energy-based or catalyst-based activation techniques can be used. Light irradiation, ultrasonication, or thermolysis can all be used as energy sources [7,144]. Transition metals, carbonaceous compounds and even alkaline species can be used as activators [145].

When compared to other AOPs, SR-AOPs have more to offer. The SR-AOPs are attractive for practical use due to its adaptability in a pH range from 2 to 8, the extended half-life of

$SO_4^{\bullet-}$ (30–40 ns versus 20 ns for $^{\bullet}OH$), selectivity, strong oxidation potential, and low reactant consumption [146,147]. Furthermore, when compared to HR-AOPs, the interference from natural organic matter (NOM) is less in SR-AOPs [148]. Numerous research have shown how beneficial it is to use PS/PMS oxidants to treat water that is abundant in NOMs and inorganic species. When compared to H_2O_2, it results in a decreased formation of NOM byproducts [149]. Numerous studies have demonstrated that sulfate radical-based oxidation works better than hydroxyl radical oxidation or is comparable in removing TOC and enhancing biodegradability [150,151]. Therefore, SR-AOPs have the potential to address the main limitations of HR-AOPs, such as matrix interference and selectivity for acidic pH, while still maintaining their effectiveness. The types of reactive oxidant species involved in both HR-AOPs and SR-AOPs are illustrated in Fig. 2.6 [152].

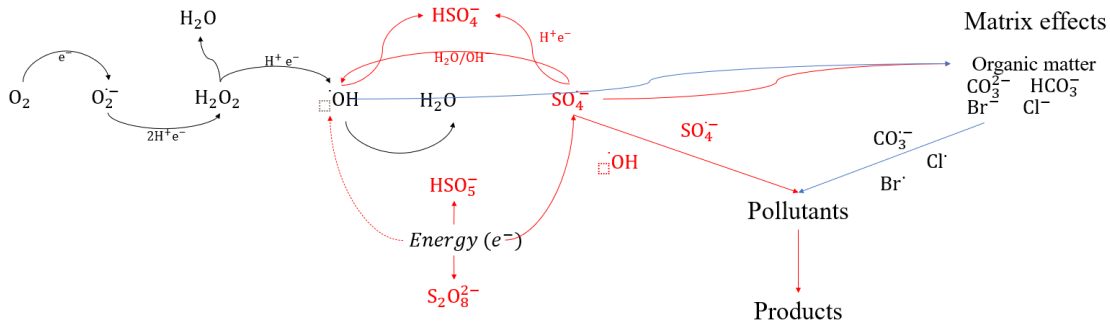

Fig. 2.6. Scheme of the oxidants involved in SR-AOPs and HR-AOPs. Adapted from [152].

In SR-AOPs, $SO_4^{\bullet-}$ is the main radical that contributes to the elimination of the pollutants, although $^{\bullet}OH$ also has an important role, notably during the activation of peroxymonosulfate [153]. $O_2^{\bullet-}$, $^{\bullet}OH$, and carbonate radicals are only a few of the secondary oxidants that SR-AOP uses, in contrast to HR-AOP [152,154]. As seen in Fig. 2.6, secondary radicals like $Cl^{\bullet}$, $Br^{\bullet}$, and $CO_3^{\bullet-}$ may be produced or oxidant scavenging can occur when different water matrix constituents interact [152]. These secondary radicals could also help break down pollutants. Fedorov et al. examined the impact of inorganic anions on the decomposition of aromatic compounds using hydrodynamic cavitation in conjunction with SR-AOP [155]. The inhibitory action was discovered to be in this order: $CO_3^{2-}>SO_4^{2-}>Cl^-$. Cl- ions, as opposed to the other anions, generates $Cl^{\bullet}$ and $Cl_2^{\bullet-}$ radicals that assist break down of aromatic hydrocarbons.

Both $^{\bullet}OH$ and $SO_4^{\bullet-}$ have similar redox potentials, but their chemical reactions differ. SO4•- is more specific and has a higher tendency to bond with organic compounds through the electron transfer pathway.

$^{\bullet}OH$ and $SO_4^{\bullet-}$ have equivalent redox potentials, but their chemistry is different. $SO_4^{\bullet-}$ is more selective and preferentially attaches organics via the electron transport pathway [156]. The much larger molecular size of $SO_4^{\bullet-}$ results in steric hindrance, which increases its energy barriers and selectivity compared to $^{\bullet}OH$ [157]. As a result, the degradation byproducts produced by HR-AOPs and SR-AOPs could be quite different.

2.4.3 Photo-Fenton and photo-Fenton like processes

The *in situ* creation of radicals that oxidize pollutants in aquatic medium and promote complete mineralization, releasing CO_2 and H_2O is a distinguishing property of Fenton processes. By decomposing H_2O_2 in the presence of Fe^{2+} at low pH, the frequently used homogeneous Fenton reaction generates extremely reactive $^{\bullet}OH$ radicals (Eq. 2.5) [158].

$$Fe^{2+} + H_2O_2 \rightarrow Fe^{3+} + {}^{\bullet}OH + OH^- \quad (2.5)$$

The homogeneous Fenton process generates $^{\bullet}OH$ radicals by employing Fe^{2+} as an activator (Eq. 2.5), whereas Fenton-like reactions replenish the Fe^{2+} by reacting Fe^{3+} with H_2O_2 (Eqs 2.6 and 2.7).

$$Fe^{3+} + H_2O_2 \rightarrow Fe^{2+} + HO_2^{\bullet} + H^+ \quad (2.6)$$

$$Fe^{3+} + HO_2^{\bullet} \rightarrow Fe^{2+} + O_2 + H^+ \quad (2.7)$$

Because Fe^{2+} and Fe^{3+} molecules are only soluble at low pH, the homogenous Fenton reactions are limited in their uses. Additionally, the reaction products of these substances may interact with Fe^{3+} to produce long-lasting organic complexes, which would prevent the catalyst from renewing itself [159]. Iron organic complexes may be mineralized and the Fenton catalyst can be renewed by using photo-Fenton techniques, which include UV irradiation. H_2O_2 is more likely to produce $^{\bullet}OH$ radicals when exposed to UVC (260-280 nm) (Eq. 2.8), whereas the concentration of Fe^{2+} ions can be maintained by photo-reduction of Fe^{3+} using near-visible UV light (Eq. 2.9) [158].

$$H_2O_2 \xrightarrow{h\nu} 2{}^{\bullet}OH \quad (2.8)$$

$$Fe(OH)^{2+} \xrightarrow{h\nu} Fe^{2+} + OH^- \quad (2.9)$$

Photo-Fenton-like processes are conducted in similar conditions using persulfate or peroxomonosulfate for sulfate radical generation under UV light (Eq. 2.10). In addition to sulfate radicals, photo-Fenton-like processes system can generate other radicals (Eq. 2.11-13) [160]. Ferrous iron is used to activate persulfate (Eq. 14), while Fe^{3+} can be converted back to Fe^{2+} by UV light (Eq. 15) [9]:

$$S_2O_8^{2-} \xrightarrow{h\nu} 2SO_4^{\bullet-} \quad (2.10)$$

$$SO_4^{\bullet-} + S_2O_8^{2-} \rightarrow SO_4^{2-} + S_2O_8^{\bullet-} \quad (2.11)$$

$$SO_4^{\bullet -} + H_2O \rightarrow SO_4^{2-} + H^+ + HO^{\bullet} \quad (2.12)$$

$$SO_4^{\bullet -} + OH^- \rightarrow SO_4^{2-} + HO^{\bullet} \quad (2.13)$$

$$S_2O_8^{2-} + Fe^{2+} \rightarrow SO_4^{\bullet -} + SO_4^{2-} + Fe^{3+} \quad (2.14)$$

$$Fe^{3+} + H_2O \xrightarrow{hv} Fe^{2+} + HO^{\bullet} + H^+ \quad (2.15)$$

Much study has been conducted on the homogeneous photo-Fenton process using Fe^{2+}. De Luca et al. (2014), for example, successfully eliminated the ubiquitous antibiotic sulfamethoxazole via a photo-Fenton-like method [161]. The pH problems of the Fenton reaction may be avoided by using chelating compounds, which improve the catalyst's solubility at pH 7. In a recent study, Demir-Duz et al. (2019) removed COD up to 88% from actual wastewater from petroleum industry to demonstrate the viability of using sunlight as the radiation source. Furthermore, 95% of the phenol in wastewater was mineralized by employing visible LED irradiation [162]. Recent economic study indicates that the photo-Fenton approach is around 50 times more affordable than photocatalysis utilizing TiO_2 [163]. The homogeneous photo-Fenton method might become even more cost-effective by switching to a less expensive activator source [164].

2.4.4 Photocatalytic AOPs

Numerous studies have focused on utilizing photocatalysis for wastewater treatment, where semiconductors serve as photocatalysts. The addition of H_2O_2 can accelerate the redox reactions catalyzed by the photocatalyst, resulting in the production of oxidants that aid in breaking down organic pollutants. TiO_2 is the most often used catalyst, whereas P25 nanopowder is commercially available [12]. Under UV irradiation, TiO_2-based materials are widely used for the breakdown of many resistant contaminants [165]. TiO_2 requires UV light (380 nm) for excitation due to its 3.2 eV band-gap energy. When the photocatalyst is exposed to light, electrons move from the valence band to the conduction band (as shown in Eq. 2.16). This leads to the formation of hydroxyl radicals in water, as the newly formed electrons in the conduction band (e_{cb}^-) reduce and the newly formed holes in the valence band (h_{vb}^+) oxidize (as seen in Eq-s 2.17 and 2.18). Materials with the larger surface are such as nanoscale catalysts are particularly desirable since both reactions take place at the catalyst's surface. The interaction between e_{cb}^- and O_2 produces the superoxide radical ($O_2^{\bullet -}$), which decreases further to produce $^{\bullet}OH$ [166].

$$TiO_2 + hv \rightarrow e_{cb}^- + h_{vb}^+ \quad (2.16)$$

$$h_{vb}^+ + H_2O \rightarrow HO^{\bullet} + H^+ \quad (2.17)$$

$$e_{cb}^{-} + O_2 \rightarrow O_2^{\bullet -} \quad (2.18)$$

In the last decade, significantly amount of research has been caried out on various semiconductors [15]. Unfortunately, current photocatalysts cannot efficiently absorb sunlight energy as only small fraction of the natural sunlight (> 310 nm) contains the high energy UV light. Therefore, it is crucial to switch from the UV to the visible range in order to optimize photocatalyst performance. The catalysts can be doped with metal ions as well as nonmetal components to achieve this [166].

A few techniques for producing (nano)photocatalysts and immobilizing them on different substrates include hydrothermal treatment, wet impregnation, *in situ* polymerization, anodization, dip coating, and electrodeposition [12], or sol-gel methods [167]. An et al. (2013) transferred Bi and Fe in organic solvent (2-methoxyethanol), then thoroughly mixed the suspension with the mixture of ethylene glycol and citric acid to produce BiFeO3 nanoparticles [167]. The sol was calcined at 500 °C after being dried to create a resin. The catalyst was ground into powder in the final stage.

2.5 Literature gap identification

Based on the existing literature, emerging pollutants pose environmental concern and present in all types of water bodies. Conventional biological treatment technologies are effective in removal of macropollutants, but fail in elimination of certain emerging pollutants. In the last decade, there is an upward trend in research of new technologies for wastewater treatment. The majority of investigations, however, evaluated the performance of the treatment systems by targeting synthetic wastewater omitting the complex structure of real wastewaters. Additionally, the bulk of research only looked at one pollutant in a water solution, giving little thought to the impact of additional organic and inorganic pollutants. As far as authors aware, there are no earlier data on the efficiency of track-etch membranes in the contaminants of emerging concern removal. Moreover, there is a lack of research on the application of sulfate-based advanced oxidation processes with real wastewater and leachates and comparison of Fe-based materials for activation of persulfate. From the literature, it is clear that response surface methodology has been rarely used in wastewater treatment. It is possible to use response surface methodology to improve the efficiency AOPs in the treatment of real wastewater of different origin.

CHAPTER 3: MATERIALS AND METHODS

3.1. Materials and chemicals

Table 3.1 lists the substances and materials utilized in this thesis, as well as their descriptions.

Table 3.1. The list of chemicals and materials.

Name	Description	Supplier
D-Glucose anhydrous	99.5%	
Ammonium bicarbonate	99%	
Potassium bicarbonate	99.9%	Fisher Scientific, USA
Sodium bicarbonate	99.9%	
Iron (III) chloride anhydrous	97%	
Calcium chloride	96%	
Lab Lemco powder		Oxoid, UK
Sodium chloride	98%	Altyn Orda JSC, Kazakhstan
Bisphenol A	99%	
Sulfamethoxazole	99%	
Naproxen	99%	
Caffeine	99%	
Ibuprofen	98%	
Metronidazole	99%	
Carbamazepine	99%	
Potassium chloride	99.9%	Sigma Aldrich, USA
Goethite	99%	
Ammonium persulfate	99%	
Zero valent iron		
Potassium persulfate	99%	
Iron (II) sulfate heptahydrate	99%	
Ammonium chloride	99.9%	
Hydrochloric acid	37%	
Anhydrous potassium monohydrogen phosphate	99.5%	
Titanium dioxide	99.5%, 21 nm	
Disodium hydrogenphosphate dihydrate	99%	
Ammonium iron (II) sulfate hexahydrate	99%	Fisher Chemical, USA
Polycarbonate track-etch flat sheet membranes	10, 50, and 100 nm pore size	It4ip S.A., Belgium
Polyethersulfone phase inversion flat sheet membrane	200 kDa MWCO	Sterlitech, USA

None of the compounds were further purified before usage. With the exception of caffeine, carbamazepine, bisphenol A, naproxen and sulfamethoxazole, commercially available pharmaceuticals were used to prepare synthetic wastewater. Analytical standards were utilized to calibrate high-performance liquid chromatography (HPLC).

3.2. Wastewater composition

3.2.1. Synthetic wastewater for continuous flow activated sludge process and sequencing batch reactor

The specific compositions of the synthetic wastewater were established using the average content of genuine municipal wastewaters used in previous study to examine the influence of drugs on the performance of biological wastewater treatment [90]. 5 g/L of $CaCl_2$, 1 g/L of KCl and 5 g/L of $FeCl_3$ were combined to form trace element solution (TES), 50 μL of which was then mixed with 1 L of freshly made wastewater. Table 3.2 details the composition of the effluent.

Table 3.2. The content of the synthetic wastewater used in the experiments

Content	Concentration, mg/L
Glucose	400
Lab lemco powder	80
Peptone	120
Ammonium bicarbonate (NH_4HCO_3)	40
Potassium bicarbonate ($KHCO_3$)	20
Sodium bicarbonate ($NaHCO_3$)	20

In the experiments using the continuous flow activated sludge process, the synthetic wastewater was supplemented with 30 mg/L of caffeine, metronidazole, and ibuprofen. Similarly, in the sequencing batch reactor experiments, the blank synthetic wastewater was spiked with 3 mg/L of naproxen, bisphenol A, and sulfamethoxazole.

3.2.2. The synthetic municipal wastewater composition for continuous flow photochemical experiments

From the ISO11733 Standard [168], a synthetic wastewater composition was developed. Information regarding its composition is provided in Table 3.3.

Table 3.3. The content of the synthetic wastewater.

Content	Concentration, mg/L
Glucose	19
Lab lemco powder	138
Peptone	192
Ammonium chloride (NH_4Cl)	23
Anhydrous potassium monohydrogen phosphate (K_2HPO_4)	16
Disodium hydrogenphosphate dihydrate ($Na_2HPO_4 \cdot 2H_2O$)	32
Sodium chloride (NaCl)	60
Sodium bicarbonate ($NaHCO_3$)	294
Iron (III) chloride hexahydrate ($FeCl_3.6H_2O$)	4
Carbamazepine	2

The "Astana su arnasy" wastewater treatment plant in Kazakhstan provided the authentic municipal wastewater sample after undergoing mechanical screening in November, 2021. The main properties of both synthetic and authentic municipal wastewater can be found in Table 3.4.

Table 3.4. The main properties of the synthetic and real municipal wastewater, collected in November 2021.

Type of wastewater	Concentration, mg/L			pH
	TC	TOC	TIC	
Synthetic	209.2 ± 3.3	176.3 ± 2.9	32.8 ± 1.2	7.65 ± 0.1
Real	223.6 ± 0.2	145,8 ± 0.2	77.8 ± 0.2	7.51 ± 0.1

3.2.3. The content of the synthetic (SLL) and real landfill leachate (RLL)

The SLL's content closely resembles that of the RLL and was based on the literature [169]. Table 3.5 displays the SLL's recipe.

Table 3.5. The content of the SLL.

Content	**Per 10 L**
Acetic acid	70 mL
Propionic acid	50 mL
Butyric acid	10 mL
K_2HPO_4	300 mg
$KHCO_3$	3120 mg
K_2CO_3	3240 mg
NaCl	14400 mg
$NaNO_3$	500 mg
$NaHCO_3$	30120 mg
$CaCl_2$	28820 mg
$MgCl_2$	14580 mg
$MgSO_4 \cdot 7H_2O$	3200 mg
NH_4HCO_3	24390 mg
$CO(NH_2)_2$ (urea)	6950 mg
Trace metal solution (TMS) (see below)	10 mL
$NaHSO_3$	Titrate to an E_h -120–180 mV
NaOH *	Titrate to a pH 5.8–6.0
H_2O	To make 10 L

Composition of trace metal solution (TMS)

Content	Per 100 mL
$FeSO_4 \cdot 7H_2O$	366 mg
H_3BO_3	5 mg
$ZnSO_4 \cdot 7H_2O$	5 mg
$CuSO_4 \cdot 5H_2O$	4 mg
$MnSO_4 \cdot H_2O$	50 mg
$(NH_4)_6Mo_7O_{24} \cdot 4H_2O$	5 mg
$Al_2(SO_4)_3 \cdot 18H_2O$	3.2 mg
$CoSO_4 \cdot 7H_2O$	15 mg
$NiSO_4 \cdot 6H_2O$	50 mg
96% H_2SO_4	0.1 mL
H_2O	To make 100 mL

Sulfamethoxazole (3 mg/L) has been added to both landfill leachates. The original leachate from real landfills contained a significant amount of TIC, which was made up of substances like carbonates and bicarbonates that can scavenge free radicals [170]. Therefore, it was decided to decrease the amount of TIC by the slight acidification (pH from 8.2 to 6.02) in order to lessen the effect of the scavenging agents. Table 3.6 displays the properties of the

resulting actual landfill leachate and synthetic landfill leachate. Real landfill leachate had conductivity of 42.7 mS/cm and oxidation reduction potential of -78 mV.

Table 3.6. The main properties of the synthetic and real landfill leachate.

Type of landfill leachate	Concentration, mg/L				pH
	TC	TIC	TOC	COD	
Synthetic	5923.7 ± 508	80.16 ± 43	5843.3 ± 524	17580 ± 180	6.03
Real	5406.6 ± 14	204.6 ± 8	5202 ± 22	18560 ± 282	6.02

3.2.4. Poultry slaughterhouse wastewater composition

The wastewater was collected from the poultry farm PC "Izhevsk" (Aqmola region, Kazakhstan). To prevent the growth of harmful microorganisms, the sample was sterilized in a VK-75 autoclave at 1.1 atm and 121°C for 45 minutes. The sterilized wastewater was then stored in a refrigerator at 4°C. The main properties of wastewater can be seen in Table 3.7.

Table 3.7. The properties of the sterile poultry slaughterhouse wastewater.

Type of wastewater	Concentration, mg/L					pH
	TC	TIC	TOC	TN	COD	
Real	115.6 ± 7.4	46.94 ± 1	68.66 ± 9.7	9.52 ± 0.7	155 ± 15	7.53±0.2

3.2.5. Municipal wastewater composition for batch photochemical experiments

The wastewater treatment facility "Astana Su Arnasy" (Astana, Kazakhstan) provided the actual municipal wastewater in April 2021. 20 L of wastewater samples were collected and preserved in a refrigerator at 4 °C to conduct experiments and additional analysis. Prior to the studies, the wastewater was filtered using a paper filter to assure the process's homogeneity and repeatability. The parameters of real municipal wastewater are shown in Table 3.8.

Table 3.8. The properties of the real municipal wastewater collected in April 2021.

Type of wastewater	Concentration, mg/L					pH
	TC	TIC	TOC	TN	COD	
Real	118.5 ± 2.2	98 ± 2.3	20.77 ± 1.7	37.5 ± 2.5	33.5 ± 1.5	7.75±0.3

3.3. Experimental procedure

3.3.1. Continuous flow activated sludge process

The continuous flow biological treatment investigations were carried out in a GUNT CE 705 Activated Sludge Process Bioreactor. A 200 L feed wastewater vessel, an aeration vessel with 34 L aerobic and 17 L anoxic zones, a 30 L secondary clarifier, and an 80 L treated water tank were all part of the system. The reactor's layout is seen in Fig. 3.1.

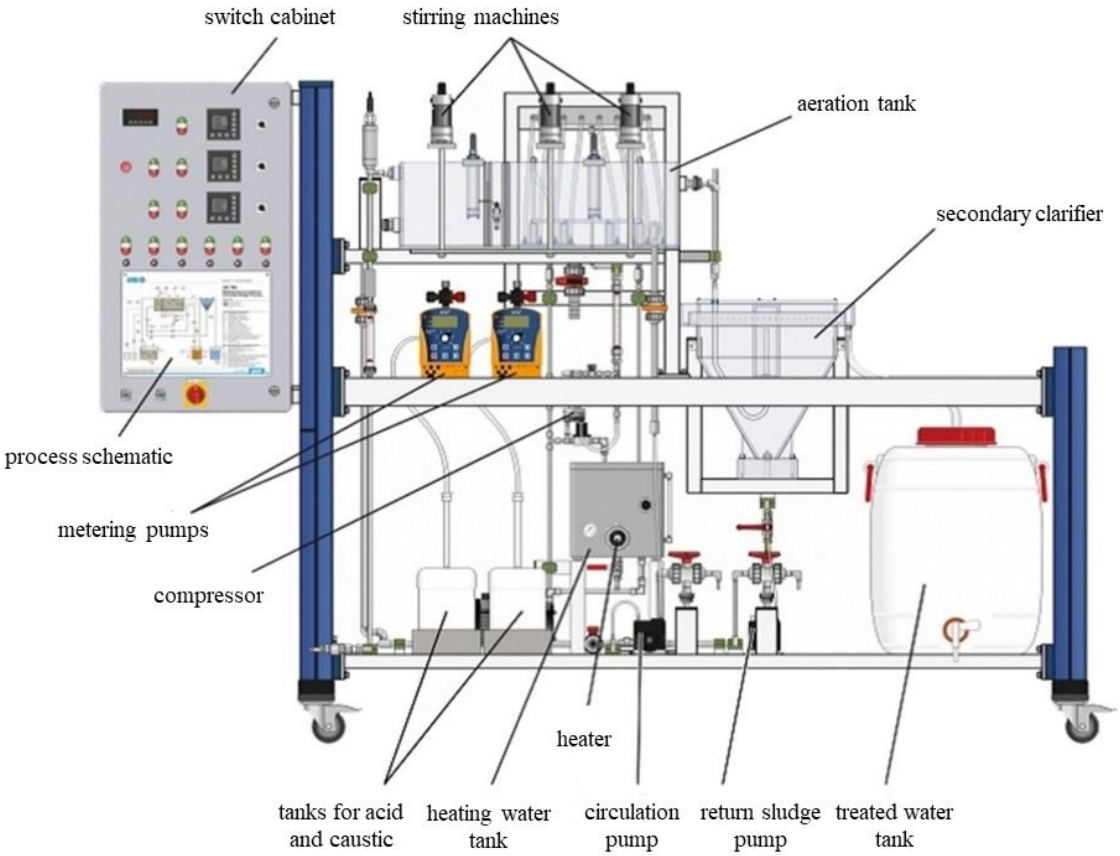

Fig. 3.1. The scheme of CE 705 bioreactor from GUNT (Germany) [171].

The aeration tank was kept at a consistent temperature of 25°C. Both pumps responsible for return sludge and raw wastewater had flowrates of 2 L/h, while internal circulation was kept at 12 L/h. The nitrification zone maintained a dissolved oxygen (DO) concentration of 3.5 mg/L, while the denitrification zone remained at a constant dissolved oxygen concentration of 0.01 mg/L throughout the entire experiment. Every two days, 2 liters of waste sludge were manually removed from the bottom of the clarifier. The concentration of recycle active sludge was 4.3±2.6 g/L and the HRT was 25 hours, with a SRT of 20 days. The TSS in both the nitrification and denitrification zones was consistently measured at 1.9±0.5 g/L. The pH of the inflow was continuously monitored and remained at 7.56±0.2. As part of the practical evaluation of the activated sludge process bioreactor's dynamic response, 10 g/L of NaCL

was continuously added to the reactor vessel from the inflow tank and conductivity was measured.

A six-day blank experiment was carried out. The trial with activated sludge began with no emergent pollutants. Ibuprofen, metronidazole, and caffeine were each added at 30 mg/L in each of the three phases. Finally, all three pollutants were mixed at 10 mg/L concentrations while keeping a constant total organic carbon by partially eliminating glucose from the system.

Activated sludge (5 L) was provided by the "Astana Su Arnasy" wastewater treatment plant in Astana, Kazakhstan. The activated sludge was given 26 days to acclimate and for the reactor to reach steady-state. Each stage of the emerging pollutants research lasted for 10 days, during which frequent samples were taken and analyzed. After the 10-day test, the reactor was run for three days with synthetic wastewater without any emerging contaminants to remove their concentration from the system.

3.3.2. Sequencing batch reactor and membrane filtration experiments

"Astana su arnasy wastewater treatment plant in Astana, Kazakhstan provided samples of recycled activated sludge with a total suspended solids (TSS) range of 6-8 g/L during the winter of 2021. Following sample collection, 200 mL of synthetic wastewater was combined with 2 L of recycled activated sludge (RAS) and kept under aeration overnight. Next day, aeration was stopped and after 2 hours of sedimentation, the supernatant was removed. Then, the amount of withdrawn liquid was replaced with the distilled water. This procedure was done twice. Batch experiments were carried out with Armfield W11 SBR, which are, essentially, plexiglass cylinders measuring 30 cm in height and 24 cm in diameter. The solution was mixed using vertical agitators from Daihan (model HS-120 A) and pumped into and out of the reactor vessel using a peristaltic pump (Cole-Parmer, USA). Each reactor had built-in aerators on the bottom that could aerate at a rate of 3 L/min, with an eight-hour hydraulic retention period. The biological treatment process consisted of 1 hour of FILL stage, 7.5 hours of REACT stage, 1 hour of SETTLE stage and 30 minutes of DRAW stage. The aerobic REACT stage lasted 5 hours, while anoxic REACT stage lasted 2.5 hours. There was no mixing during the SETTLE and DRAW steps. To start the SBR, 5 L of feed solution was supplied using a pump with peristaltic action, and 5 L of wastewater that had been treated was pumped out after each cycle. The SBR effluents were kept at 4 °C for subsequent study after each cycle. In total, there were 6 cycles for each experimental condition with and without emerging pollutants.

In this investigation, a membrane filtration system comprised of a peristaltic pump, membrane holder (Sterlitech, USA), and stirrer plate was employed. To make a homogenous solution, the feed was agitated on the plate, and the permeate was collected in the vessel on the electronic balance. The experiments were conducted in dead-end mode with a filter area of 4 x 4 cm2, and each lasted for six hours. Track-etch membranes as well as phase inversion membrane were used for membrane filtration. Before the experiments, the membranes were pre-conditioned by soaking them in deionized water at 37 °C for one day.

3.3.3. Batch photochemical treatment

The batch photochemical reactor (Toption Instrument Co., Ltd.) used for the studies is depicted in Fig. 3.2. Inside the photoreactor, there were lamps with 30 W of power for 254 nm UV irradiation and 500 W for 365 nm UV irradiation. At the beginning of each run, certain amount of the wastewater was supplied to the reactor along with the appropriate concentrations of chemicals. The treated solution was continuously mixed using the magnetic stirrer. With the UV lamp turned on, the experiment begun. At the completion of the experiments, aliquots from the reaction mixture were obtained and delivered immediately to the analyzer. The cooling of the reactor is carried out by the flow of the tap water through the reactor jacket,

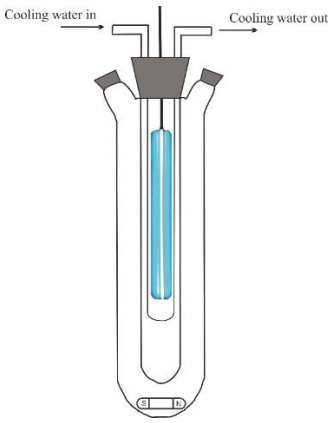

Fig. 3.2. The experimental setup of the batch photochemical reactor.

3.3.4. Continuous flow photochemical treatment

The continuous flow photochemical reactor configuration is shown in Fig. 3.3. A 10 W UV light source (254 nm) and a 300 mL glass cylinder made up the photoreactor. The flow rates of 0.54 L/h, 0.45 L/h, and 0.3 L/h were corresponding to the space times of 20, 40, and 60 min, respectively.

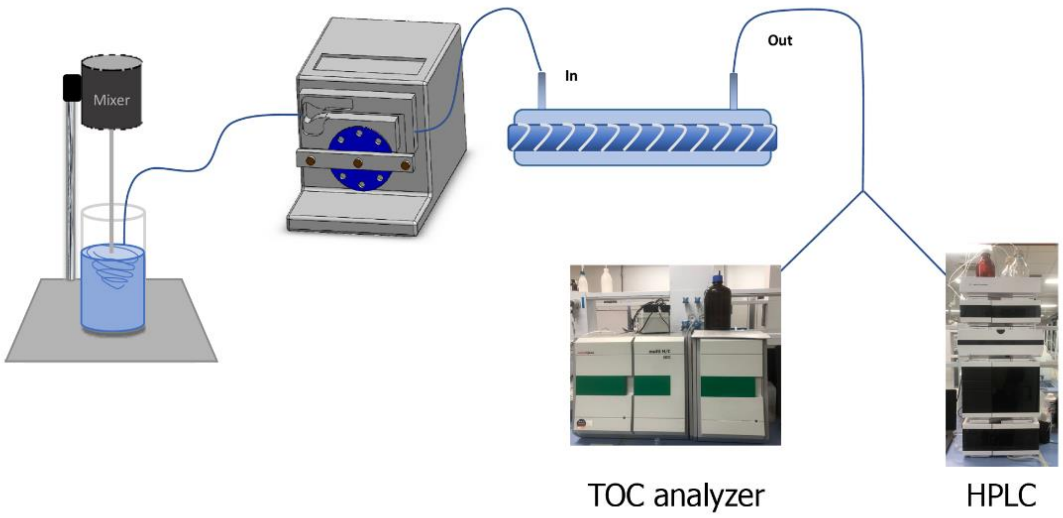

Fig. 3.3. The continuous flow photochemical photoreactor's schematic.

3.4. Analytical methods

3.4.1. Analytical methods

Prior to HPLC, Ion Chromatography (IC), TC, and TN analysis, samples were filtered using 20-micron Chromofil syringe filters. The Agilent 1290 Infinity HPLC, USA, was used to measure the amounts of naproxen (NPX), carbamazepine (CBZ), bisphenol A (BPA), sulfamethoxazole (SMX), caffeine (CAF), ibuprofen (IBU), and metronidazole (MNZ). The details of HPLC analysis in further were previously reported [171–174] and shown in Table 3.9.

Table 3.9. The details of HPLC analysis.

Parameter	NPX	BPA	SMX	CBZ	CAF	MNZ	IBU
Column	ZORBAX Rapid resolution high definition column (Agilent), phase SB-C8, internal diameter = 2.1 mm, length = 100 mm, particle size = 1.8 μm						
Injection volume (μL)	1	1	1	1	1	1	10
Eluent	60% H_2O 40% CH_3CN					50% H_2O 50% CH_3OH	65% H_2O 35% CH_3CN
Flow rate (mL/min)	0.4	0.4	0.4	0.35	0.4	0.1	0.7
Column temperature	Left side: 25 °C, right side: 25 °C						
Detector wavelength (nm)	228.5	230	258	225	280	292	222
Retention time (min)	3.746	2.680	1.372	1.056	0.742	3.357	4.687

Thermo Scientific Dionex ICS-6000, USA, was used to measure the levels of ions. TC and TN concentrations were quantified using the Multi N/C 3100 analyzer (Analytik Jena AG, Germany). The specifics of the IC analysis and TC and TN analysis were reported previously [171].

3.4.2. Catalysts characterization

Zeiss Crossbeam 540 scanning electron microscope with energy dispersive spectroscopy (SEM-EDS) and SmartLab, Rigaku X-ray diffraction spectrometer were used to analyze the surface morphology and elemental contents of catalysts. Using a Nitrogen Porosimeter at 77.35 °K, the specific surface area of the materials and their pore size were calculated. The Mastersizer 3000 was used to gather data on particle size distribution.

3.4.3. Measurement of other parameters

Dissolved oxygen concentration, conductivity and pH was measured by multi-parameter WTW inoLab 9310 IDS (Germany). The samples were filtered through 1.2 m GF/F glass microfiber filters under vacuum to determine the total suspended solids (TSS). TSS was determined by drying the sample in an oven at 105 °C until the weight remained constant.

The quantity of volatile suspended solids (VSS) in the sample was evaluated by calcining it at 550 °C for 30 minutes.

The Hach DRB 200 dry thermostat reactor and Hach DR 3900 spectrophotometer were used to measure the COD concentration. Additionally, Malvern Panalytical AxiosmAX X-ray fluorescence spectrometer was used to characterize the wastewater. Agilent Cary 600 Series FTIR was utilized to identify functional groups present in the pollutants of the wastewater. Analysis of the metals was conducted using Analytik Jena ContrAA 700 atomic absorbance spectrometer. A Lumex pyro-915+ mercury analyzer was used to determine the amount of mercury present in wastewater.

3.5. Statistical methods

Design-Expert (13.0) was utilized to create the model for selecting experiments and optimizing experimental conditions in this study. The screening process in this study involved the use of Plackett-Burman Design (PBD) along with the linear regression model (Eq. 3.1) [175]:

$$Y = \beta_0 + \sum \beta_i \chi_i \quad (3.1)$$

where the response variable, which represents the removal of pollutants, is denoted as Y. The mean response is represented by β_0, while the linear coefficient for each independent factor is represented by β_i. The level of each independent factor is represented by χ_i.

The PBD is a widely used method for screening because of its simplicity and ability to identify the most important factors compared to other methods [176]. This initial stage helps to simplify a process and provides direction for further development [175]. The PBD model is represented by a matrix with four factors and two levels each (high and low or +1 and -1), as shown in Table 3.10.

Table 3.10. PBD factors and levels used in landfill leachate treatment using UV/PS/Goethite

Factors	**Levels**	
	-1	**1**
UVA	OFF	ON
Time, h	1	3
PS, mM	150	450
Goethite, g/L	0.5	2.5

In addition to screening, optimization plays a crucial role in evaluating a process. The regression equation derived from optimization can offer valuable insights such as accurate

forecasts of the actual process, the interplay between the components involved, and their levels of significance [176]. Following the screening experiments, the Box-Behnken design (BBD) was acquired in a three-factor format with three levels. The three levels were coded as -1, 0, and +1, as presented in Tables 3.11, 3.12 and 3.13.

Table 3.11. BBD factors and levels used in landfill leachate treatment using UV/PS/Goethite

Factors	Levels		
	-1	**0**	**1**
Time, h	3	6	9
PS, mM	200	400	600
Goethite, g/L	0.5	1	1.5

Table 3.12. BBD factors and levels used in batch photochemical wastewater treatment using UV/PS/Fe^{2+}.

Factors	Levels		
	-1	**0**	**1**
Time, min	60	100	140
pH	3	5.35	7.7
$K_2S_2O_8/Fe^{2+}$ molar ratio	7.5	10	12.5
$K_2S_2O_8$ concentration, mM	10	20	30

The Box-Behnken design (BBD) is an important tool for optimizing processes [176]. Despite requiring a small number of tests, the BBD can offer extensive and detailed information, including the effects of operational factors on all outcomes and their interactions.

In order to estimate the outcomes of the tests, a polynomial model based on the connection between outputs and variables (Eq. 3.2) was used [22]:

$$Y = \beta_0 + \sum_{j=1}^{k} \beta_j \chi_j + \sum_{i<j} \beta_{ij} \chi_i \chi_j + \sum_{j=1}^{k} \beta_{jj} \chi_j^2 + \varepsilon \qquad (3.2)$$

In this equation, Y is the outcome variable, β_0 denotes a constant coefficient, β_i a coefficient that determines the linearity, β_{ij} is a parameter which determines the quadratic effect, β_{jj} denotes an interactive regression coefficient, χ_i and χ_j denote coded variables, and ε denotes an error. The Minitab Software (19.0) was utilized to construct a Pareto chart.

CHAPTER 4: TREATMENT OF SYNTHETIC WASTEWATER WITH CONTINUOUS FLOW ACTIVATED SLUDGE PROCESS AND ADVANCED OXIDATION PROCESSES

4.1. Introduction

The majority of emerging contaminants are pharmaceutical chemicals [5]. Pharmaceutical chemicals are typically found in wastewater from healthcare facilities, the pharmaceutical production sector, agricultural waste, and household trash [29,30]. It is known that certain pharmaceuticals are not removed by traditional WWTPs.

Caffeine may be found in coffee, tea, and many other soft drinks and is frequently used as a psychostimulant. Urine and domestic plumbing are two ways that caffeine reaches aquatic environments. As much as 16 μg/L of it was discovered in Singapore groundwater tests [177]. Caffeine's potentially harmful consequences when released into the environment without adequate management have been well documented [178]. When consumed with polluted water, caffeine has been demonstrated to negatively impact an animal's neurological system and gastrointestinal tract [179]. Additionally, irrigation with water that contains caffeine reduces soil fertility [180]. Although many microbes have been shown to be hindered by caffeine, the case has been reported when fungi and aerobic bacteria have effectively degraded caffeine by utilizing it as a source of nitrogen [181].

Metronidazole (MNZ) is an antibiotic and anti-inflammatory drug with proven efficiency. It has a variety of applications and has been discovered in wastewater all over the world [182]. This antibiotic has a poor biodegradation rate and is harmful to the environment. In high dosages and after prolonged usage, it is thought to be a chemical that may be mutagenic and carcinogenic at high concentrations [100]. Because of its antimicrobial characteristics and recalcitrance, typical wastewater treatment systems only partially remove metronidazole. It interferes with the nitrification processes and the development of microbes found in activated sludge process, reducing the plant's overall effectiveness [183].

Ibuprofen (IBU) is frequently used as a pain reliever to lower fever and inflammation and one of the pharmaceutical pollutants with the most extensive investigation [13]. Ibuprofen can interfere with an aquatic animal's ability to reproduce and disturb their endocrine system [184]. It has also been asserted that conventional methods including chlorination or coagulation were not efficient at eliminating of this compound [97].

The majority of WWTPs use the activated sludge technique and can successfully remove organic impurities that are biodegradable. However, a quite number of drugs are not biodegradable, and some of them have resistant characteristics [91]. The efficiency of activated sludge process was previously shown in Table 2.3. As a result, effective pre-

treatment or post-treatment systems have been used to completely remove emerging contaminants in wastewaters. These systems include advanced oxidation processes (AOPs) and membrane bioreactors [20].

AOPs refers to a large set of efficient technologies used to clean industrial wastewater and tainted drinking water. Hydroxyl and sulfate radicals are the typically used oxidants in AOPs. Different organic contaminants can be oxidized by these oxidative radicals [185].

4.2. Focus of the chapter.

This chapter's goal was to assess the MBR, AOPs, and activated sludge technology for wastewater treatment. By monitoring the concentration of TSS, TC, TN, NH_4^+ and NO_3^- as well as the content of the organic pollutants, it was possible to assess the impact of the target pollutants (CAF, MNZ, and IBU) on the processes separately as well as together. The effectiveness of AOPs for the wastewater treatment involving MNZ has not been the subject of any systematic or controlled investigations, to the authors' knowledge. Also, no prior study has been done to examine the joint impact of CAF, MNZ and IBU on nitrogen reduction processes during the biological wastewater treatment.

4.3. Preliminary blank experiments

The aim of the blank test was to evaluate the impact of the reactor on the treatment of the synthetic wastewater excluding the activated sludge. TC and TN removals were monitored during this test which is illustrated in Fig. 4.1.

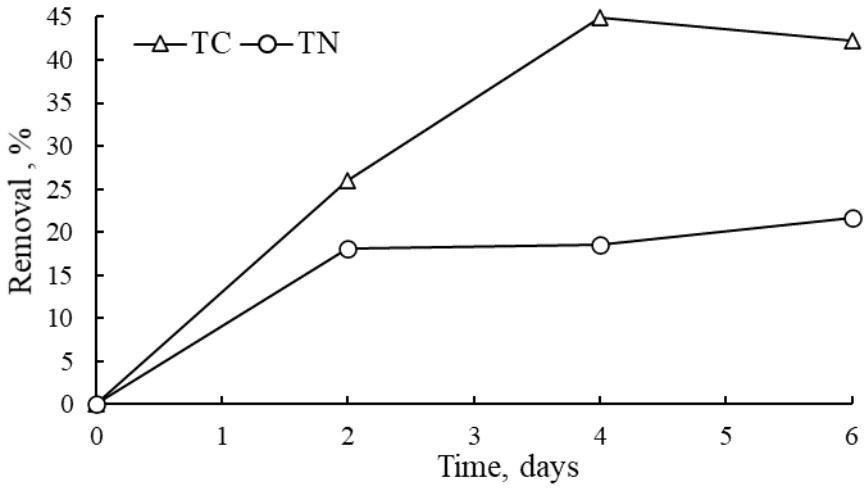

Fig. 4.1. The removal of TC and TN in the blank experiments.

After day 6, TC removal of 43% and TN removal of 22% has been achieved during the blank test. The mean TC and TN values in the influent were corresponding to 265±31 mg/L and

26±2 mg/L. The significantly high TC elimination is largely linked with the contamination with microbes in the feed tank and, in a lower degree, to aeration-induced elimination. There are just a few studies in the literature that involve blank tests with activated sludge bioreactors. SBR was employed to treat palm oil industry wastewater and a COD reduction of 35% was obtained after 40 days, which the authors explained with foaming [186].

In a work utilizing analogous synthetic wastewater, the effect of air stripping was assessed using SBR [90]. They found that the removal of TC was 44% after 21 h of air stripping. Moreover, the elimination of chlorophenols were in range of 10 to 29% [90]. The literature indicates that caffeine, ibuprofen, and metronidazole have Henry solubility (Hcp) values that are significantly lower than those of chlorophenols. In light of this, we can assume that that the aforementioned target pollutants utilized in the study were largely stable to evaporation and that there was little chance that evaporation would result in a considerable loss of them. A step input change experiment with sodium chloride as a tracer has been carried out to investigate the hydrodynamic profile of the continuous flow reactor. Fig. 4.2 displays the tracer studies' outcomes.

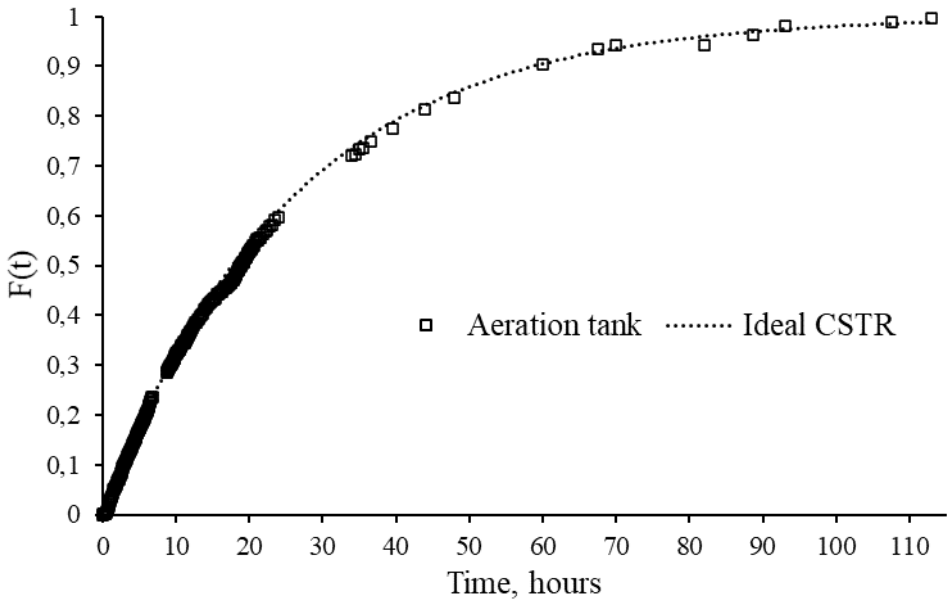

Fig. 4.2. The results of the step input change experiment.

In essence, a continuous stirred tank reactor (CSTR) correlate how the activated sludge bioreactor operated. Experimentally, the aeration tank had a residence time of 25.6 h, while the predicted residence time was 25.5 h. After 3 days of the experiment, the NaCl concentration in the solution inside the reactor amounted 94% of the feed solution concentration. Therefore, it was considered that the reactor reached the steady state

functioning. Based on that 10-day experiments with emerging pollutants and 3-day washing out experiments without emerging pollutants have been selected.

4.4. TC and TN removal

Significant TC and TN removal as well as effective TSS were accomplished throughout the acclimatization phase (Fig. 4.3). In particular, TC and TN were removed on average at rates of 79.7% and 64.2%, respectively. pH and DO during the process are shown in Fig. S4.1 and S4.2.

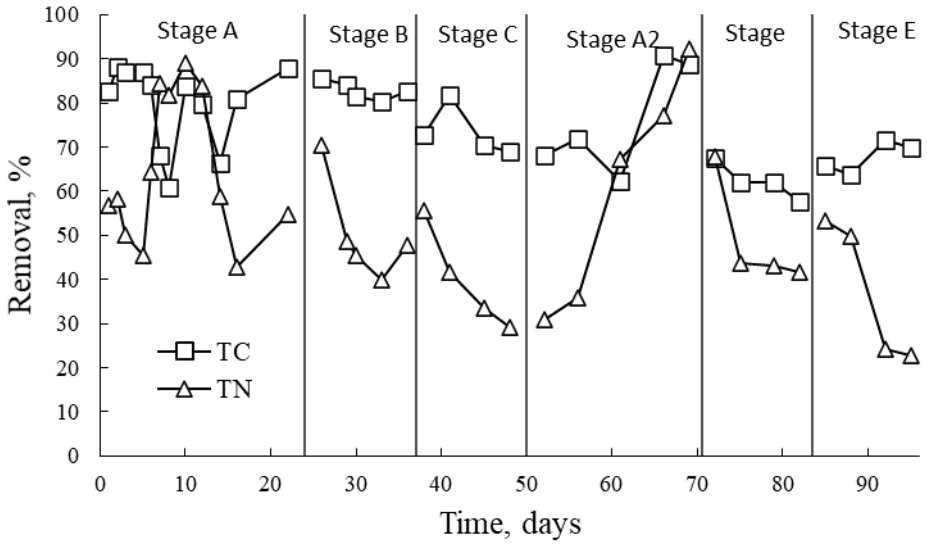

Fig. 4.3. TC and TN removal efficiencies over time: A and A2 (without emerging pollutants), Stage B (CAF 30 mg/L), Stage C (MNZ 30 mg/L), Stage D (IBU 30 mg/L) and Stage E (CAF, MNZ, IBU 10 mg/L each).

The average TSS concentration was in range of 1.5-2.0 g/L in both nitrification and denitrification zones during the whole experiment (Table 4.1).

Table 4.1. TC, TN removals and TSS values over stages.

Stages	TC rem. (%)	TN rem. (%)	TSS, g/L	
			Nitrification	Denitrification
A (without emerging pollutant)	79.7±9.3	64.2±16.3	1.9±0.7	1.8±0.7
Stage B (CAF 30 mg/L)	82.1±1.7	45.5±4.0	2.0±0.6	1.8±0.5
Stage C (MNZ 30 mg/L)	73.7±6.9	34.7±6.3	2.0±0.3	2.0±0.3
A2 (without emerging pollutant)	76.4±12.7	60.7±26.5	1.6±0.5	1.5±0.3
Stage D (IBU 30 mg/L)	60.5±2.5	42.8±1.1	1.75±0.3	1.85±0.4
Stage E (CAF, MNZ, IBU 10 mg/L each)	68.8±4.1	32.3±15.2	1.6±0.2	1.6±0.2

After caffeine was introduced to the system, no improvement in TC removal efficiency was seen (Table 4.1). Caffeine is known to have negative impact bacteria responsible for ammonium oxidation, which possibly caused the dramatic decline in TN elimination efficiency down to 46% [126]. Additionally, due to caffeine's potential to improve some microbes' capacity to produce biomass, the average TSS concentration also slightly increased [187].

In the activated sludge bioreactor, there was no discernible decrease in the effectiveness of TC removal during the course of Stage C, while TN removal decreased by double the amount compared to Stage A, when emerging contaminants were absent (Table 4.1). Given that metronidazole is an antibiotic and a resistive substance, this was anticipated. It can have a negative impact on bacterial development, and a 2 mM concentration of metronidazole was shown to six-fold inhibit denitrifying bacteria's rate of growth [188]. Metronidazole significantly decreased the process' effectiveness, therefore, acclimatization stage (A2) was conducted again to reach the steady state performance again. 76% TC removal and 61% TN removal was reached during the course of the acclimatization stage.

Similar to Stage C, the mean TN removal fell sharply to 41% when 30 mg/L of ibuprofen was introduced from the feed tank (Fig. 4.3). Additionally, the TC removal was negatively impacted and fell to 60%. The elimination of TN was also greatly affected in Stage D. These findings are consistent with the literature, which found that high concentrations of ibuprofen (0.5 and 1 g/L) significantly affected the microbial activity of aerobic microorganisms [189].

Finally, using 10 mg/L for each chemical, the combined effect of the EPs on the removal ability of the biological treatment was examined. Mean TC and TN removal in this stage fell to 68% and 32%, respectively (Table 4.1). As was already mentioned, all three of the chemicals hindered the effectiveness of TN elimination when used individually. As a result, the combination of pollutants reduced the effectiveness of TN elimination, lowering it to 22% on day 10 of Stage E. The mean TC removal was in range of 60% to 82%, as shown in Table 4.1. Due to the reactor's adaptability and ability to operate at a high retention time, it was possible to prevent the loss of the biomass and maintain a sufficient TSS.

4.5. Nitrification and denitrificafion

The effects of EPs on the biological activities have been examined in a number of research. Caffeine, ibuprofen, and their by-products have harmful effects on riverine microbial populations [190]. It was also reported that denitrifying bacteria could be affected by the presence of ibuprofen in the solutions, whereas metronidazole may have harmful impact on aerobic bacteria [188,189].

Figures 4.4 and 4.5 display the removal capabilities of ammonium nitrogen and nitrate nitrogen, respectively.

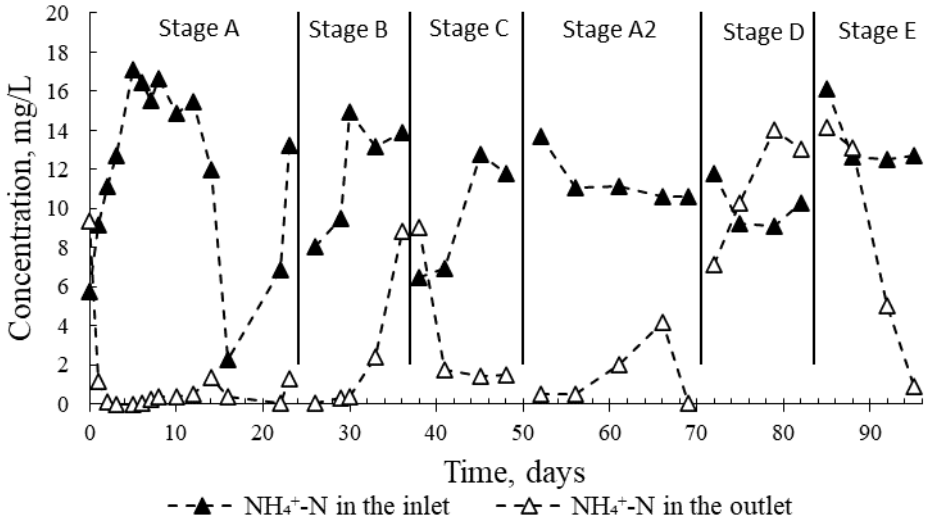

Fig. 4.4. Efficiency of NH_4^+-N removal in an activated sludge bioreactor: A and A2 (without emerging pollutant), Stage B (CAF 30 mg/L), Stage C (MNZ 30 mg/L), Stage D (IBU 30 mg/L) and Stage E (CAF, MNZ, IBU 10 mg/L each).

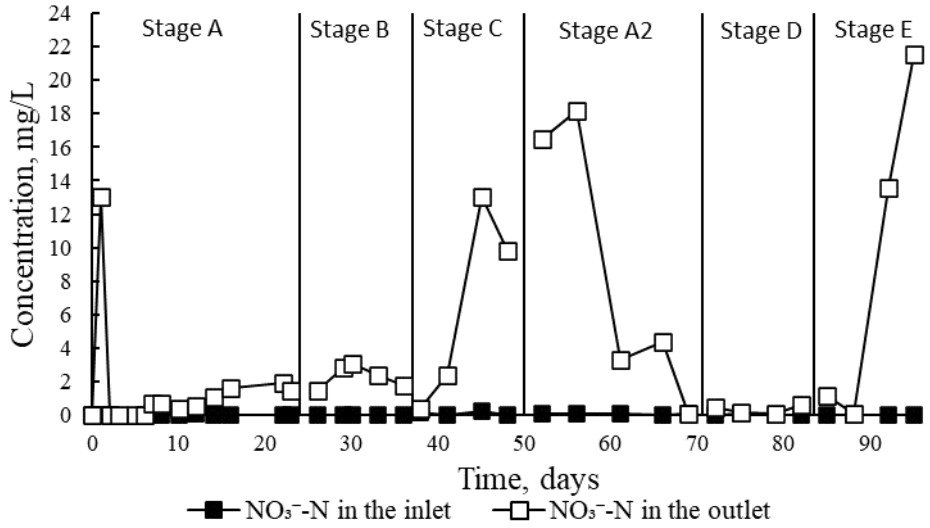

Fig. 4.5. Efficiency of NO_3^--N removal in an activated sludge bioreactor: A and A2 (without emerging pollutant), Stage B (CAF 30 mg/L), Stage C (MNZ 30 mg/L), Stage D (IBU 30 mg/L) and Stage E (CAF, MNZ, IBU 10 mg/L each).

Stage A led to the establishment of effective nitrification and denitrification processes. With emerging contaminants, the removal efficiency of TN was limited at all stages, and this appears to be due to various causes for each one. The NH_4^+-N in the effluent rose in the presence of caffeine up to 9 mg/L, as shown in Fig. 4.4. This rise can be attributed to the reduction of activity of the microorganisms responsible for the nitrification [126]. In the effluent, the NO_3^--N content varied from 1 to 3 mg/L. (Fig. 4.5).

In Stage C, ammonium nitrogen content in the effluent was around 1.6 mg/L. Effluent nitrate nitrogen rose dramatically from 2 to around 13 mg/L. These findings are consistent with the literature, where metronidazole reduced the biological activity of the autotrophic and heterotrophic microorganisms, which are responsible for denitrification and nitrification [188].

The rise in nitrates was only noticed only for metronidazole. Metronidazole has a low molecular mass, which makes it easy to enter both anaerobe and aerobe cell membranes. Reactive intermediates created during metronidazole's reduction cause damage to the DNA of the bacteria. Metronidazole's selective action against anaerobic microbes is explained by the presence of ferri-doxin system in anaerobes, which facilitates the drug's reductive process [76]. Therefore, it is very possible that metronidazole impacts the denitrification, which increases the concentration of the nitrates in the effluent.

NO_3^--N and NH_4^+-N were almost absent in the outlet when the metronidazole input was discontinued. Fig. 4.4 makes it abundantly evident that at Stage D, the concentration of NH_4^+-N increases to 13 mg/L. This indicates that the ammonium oxidation was significantly

impacted by ibuprofen. Given that the generation of nitrates was inhibited, it is unknown if ibuprofen suppresses the denitrifying bacteria. According to the findings in the literature, ibuprofen is known to inhibit the action of bacteria that create ammonium and nitrite [189]. Lastly, a combination of caffeine, ibuprofen, and metronidazole was investigated. Fig. 4.4 demonstrates how, during the course of Stage E, the ammonium nitrogen content in the outlet reduced from 14 to 1 mg/L. Due to the reduced concentrations of caffeine and ibuprofen, it is possible that nitrifying autotrophs were not inhibited. The quantity of NO_3^--N in the outlet, on the opposite, grown considerably from 1 to 21 mg/L when metronidazole was present, as shown in Fig. 4.5. As was previously noted, metronidazole had a significant impact on the denitrifying bacteria. According to nitrification/denitrification experiments, it is essential to remove EPs prior to biological wastewater treatment in order to prevent disruption of the TN removal efficiency.

4.6. Emerging contaminants' fate in the activated sludge process

Ibuprofen and caffeine were fully eliminated from the system, however metronidazole remained resistant to biological decomposition (Table 4.2).

Table 4.2. The results on the removal of the EPs

Experimental stage	**Stage B**	**Stage C**	**Stage D**	**Stage E**		
	Biodegradation of EPs, %					
Time, days	CAF	MNZ	IBU	CAF	MNZ	IBU
3	98.3	27.4	100	100	56.5	83.8
7	100	12.2	100	100	51.65	100
10	98.8	12.4	100	100	52.1	100
Mean removal, %	99.0±0.7	17.3±7.1	100	100	53.4±2.2	94.6±7.7
Mean concentration, mg/L	28.1±0.5	26.3±0.4	26.7±1.2	10.6±0.15	9.4±0.15	10.3±0.3

Caffeine was entirely biodegradable, as evidenced by the average removal rate in Stage B of 99%. This outcome is consistent with the literature, where the activated sludge technique was employed to completely remove caffeine [191]. In another study, the membrane

bioreactor was applied to treat leachate [192]. They were able to remove 99.9% of the caffeine, and they concluded that this was related to its high biodegradability.

Between 12 to 27% of the metronidazole is eliminated in Stage C. The poor metronidazole elimination percentage may be attributed to the antibiotic's ability to inhibit the bacteria [183]. Imidazoles are potent bactericides that prevent microorganisms from synthesizing nucleic acids. They are mutagenic to fungi, rodents, and anaerobes as well [76]. Other authors also produced similar to our study findings on metronidazole removal using activated sludge such as 15% removal after 10 days [101] and 22% removal after 9 days [100]. The stability of the imidazole ring is thought to be responsible for metronidazole's recalcitrance [182]. The formation of exopolymeric molecules, which are crucial for the adsorption of metronidazole, is connected with its biological elimination. The ability of the bacteria to degrade metronidazole is, however, limited [193].

During Stage D, ibuprofen was completely eliminated. Ibuprofen is easily biodegradable, and even at 12°C, elimination of up to 99% of 10 mg/L of the drug was achieved in 24 hours [98]. 50 mg/L ibuprofen suppresses the microbiological activity, according to other investigations on the effects of high ibuprofen concentrations [194].

Finally, in Stage E, all concentrations of the biodegradable substances caffeine and ibuprofen were eliminated. Metronidazole had an average clearance effectiveness of 53.4±2.2%. The decrease in its concentration can be used to explain this rise in removal rate. Additionally, the use of ibuprofen during Stage D of the bioreactor may have raised the prevalence of bacteria resistant to antibiotics, which may have boosted the microbial activity of activated sludge [194].

4.7. Photochemical treatment of activated sludge effluents containing metronidazole

As metronidazole has not been completely removed by the activated sludge process in Stage C, it was decided to further treat the effluents with metronidazole (19.44 mg/L) using photochemical treatment. Hydrogen peroxide, potassium persulfate, titanium dioxide and ferrous iron were applied for this purpose under UV. Figures 4.6. and 4.7 display the TOC removal and MNZ degradation profiles.

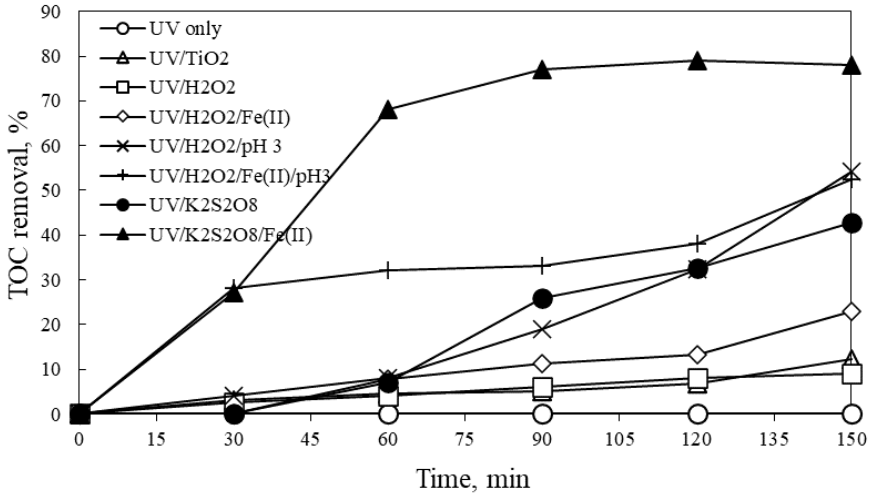

Fig. 4.6. Removal of TOC using photochemical treatment ($[H_2O_2]$ = 8 mM, $[K_2S_2O_8]$ = 5 mM, $[Fe^{2+}]$ = 5 mg/L, $[TiO_2]$ = 1 g/L.

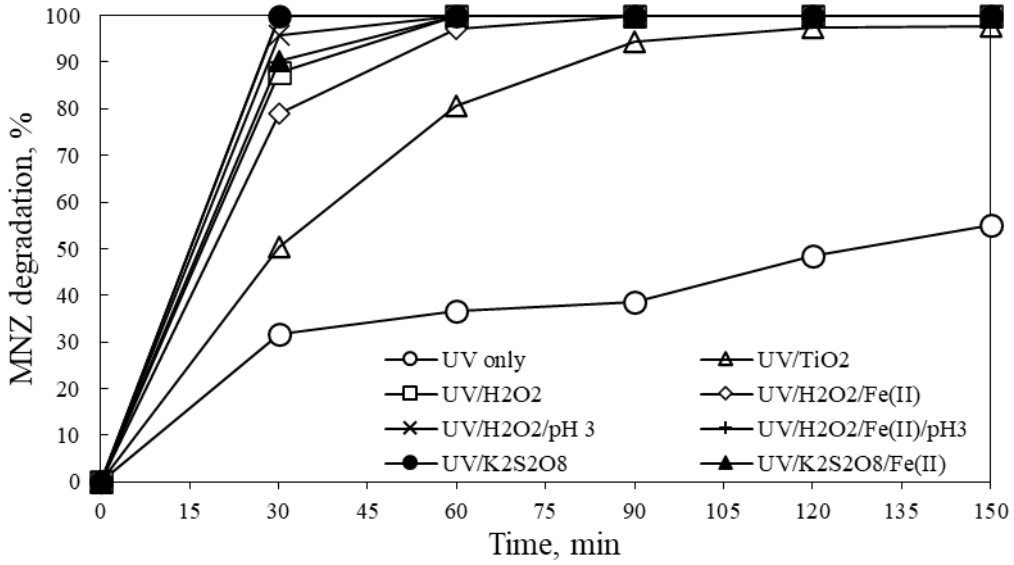

Fig. 4.7. Degradation MNZ using photochemical treatment ($[H_2O_2]$ = 8 mM, $[K_2S_2O_8]$ = 5 mM, $[Fe^{2+}]$ = 5 mg/L, $[TiO_2]$ = 1 g/L.

UV photolysis did not result in the significant removal of TOC. Similar to the UV photolysis, the application of H_2O_2 (8 mM) proved ineffective in significantly mineralizing the wastewater (TOC removal of 8%). The UV/H_2O_2 method was more effective and removed 54% TOC after 150 minutes when the pH was lowered to 3. Changes in pH have an influence on the nature and light absorption of the compounds in water. Contaminants in the solution only partially absorb radiation at an acidic pH, therefore the bulk of irradiation is used to cause hydrogen peroxide to break down and produce hydroxyl radicals. Additionally, TIC, containing hydroxyl radical scavengers, is reduced by acidic pH [152].

In the following experiment, Fe(II) was added at a concentration of 5 mg/L to begin photo-Fenton reactions, which improved the UV/H_2O_2 process. Using this method led to 23% TOC removal, while TOC removal climbed to 53% when UV/H_2O_2/Fe^{2+} was used at pH 3. It must be noted that as iron is more soluble at acidic pH ranges, the photo-Fenton reaction benefits from them. Additionally, the application of UV aids in avoiding the formation of organic iron complexes that could prevent Fe(II) regeneration [152].

Another source of powerful oxidizing radicals was $K_2S_2O_8$. The scavenging elements (natural organic matter, alkalinity) in solution have less of an impact on SO_4^{2-} radicals than on OH radicals. UV/$K_2S_2O_8$ achieved 43% removal of TOC, while introduction of Fe^{2+} to this system increased TOC removal to 78%. To the end of the treatment effluent's pH dropped to 2.88 due to the production of sulfate radicals and this was advantageous for the conversion of Fe^{3+} to Fe^{2+}. Lastly, 12% TOC was removed in photocatalytic tests using 1 g/L TiO_2.

MNZ degradation findings (Fig. 4.7) show that in all studies except UV photolysis and UV/TiO_2, 100% MNZ degradation was attained. After 150 minutes of exposure, 98% and 55% of MNZ were decomposed by UV/TiO_2 and UV photolysis, respectively.

4.8. Summary of the chapter

This chapter examined the biodegradability and inhibitory properties of three common commercial medications that are present in wastewater effluents: ibuprofen, caffeine and metronidazole. Activated sludge process was run on a continuous flow mode for 95 days.

Almost complete removal of caffeine and ibuprofen was obtained throughout the separate treatment and when treated in combination. In case of metronidazole only 17% removal was achieved during the separate treatment and 53% removal was achieved when treated together with caffeine and ibuprofen. The TC elimination efficiency was shown to be lowered by the introduction of ibuprofen and metronidazole to the wastewater, but not by the addition of caffeine. Nevertheless, the efficacy of TN removal was reduced at all testing phases with emerging pollutants. According to the IC results, the presence of caffeine, ibuprofen, and metronidazole affected nitrification while inhibiting denitrification. Inefficient TC (around 70%) and TN (around 30%) removal efficiency were the result of the synthetic wastewater's cumulative inclusion of caffeine, metronidazole, and ibuprofen. It was discovered that the confluence of emerging contaminants damaged denitrification, causing the abundance of unconverted nitrates in the effluent.

The elimination of metronidazole was 100% after 60 minutes and 78% for TOC after 90 minutes in the photochemical treatment of the activated sludge process effluents using

$UV/K_2S_2O_8/Fe^{2+}$. The study demonstrated that AOPs are effective methods for treating biological treatment effluents, but they need additional in-depth study to comprehend the mechanisms of removal. These findings were published in *Journal of Chemical Technology and Biotechnology* with a research paper titled “The effect of caffeine, metronidazole and ibuprofen on continuous flow activated sludge process” and in *Chemical Engineering Transactions* with a paper titled “Treatment of a biological effluent containing metronidazole”.

CHAPTER 5: INTEGRATED TREATMENT OF SYNTHETIC WASTEWATER WITH MEMBRANE BIOREACTOR AND ADVANCED OXIDATION PROCESSES

5.1. Introduction

In general, the types of residential and industrial activities that take place might affect the composition of wastewaters from one location to another. In any case, the organic debris, pathogens, nutrients (nitrogen and phosphorus), hazardous pollutants (both organic and inorganic), and dissolved minerals may be distinguished as the elements of the wastewater matrix [30]. Emerging organic pollutants can cause substantial harm to the ecosystem and pose serious health hazards to humans when they are present in aquatic environments such as sewage, surface water, groundwater, and drinking water [71].

A significant number of organic pollutants have been released into the environment since the beginning of industrialization. The outcome of their current involvement is still uncertain as they haven't been commonly detected before. The increasing number of refractory infections and the potential carcinogenic and/or endocrine-disrupting consequences of these substances pose a serious danger to the immune systems of living things [73]. SDG 6 places a strong emphasis on how urgent the situation is, and by 2030 it aims to reduce the amount of untreated municipal wastewater by half, stop pollution, stop the discharge of new contaminants into water bodies, accomplish smart recycling, and reuse water safely around the world [25]. This puts a lot of pressure on the scientific community to create solutions to eliminate the danger of organic pollutants that are affordable, ecologically acceptable, useful, and implementable on a broad scale.

Sequencing batch reactors (SBRs) garnered the initial wave of attention for the purpose in the latter part of the 20^{th} century. This technique involves adding wastewater and chemicals to a vessel for a predetermined period of time, after which the wastewater is released [195]. The "fill-and-draw" operations used in the traditional activated sludge treatment method, where raw sewage is used as the feed, gave rise to this technology. Aeration, settling, and clarification are further chemical processes that SBR systems imply doing repeatedly [89].

Although adaptable and having good removal efficiency values for total suspended solids (TSS), phosphates, COD, and biological oxygen demand (BOD), this process has weak selectivity, making it unpromising for the removal of chemical micropollutants [36,38,40]. When Kolecka et al. evaluated the SBR system at the Swarzewo WWTP, they found that 94.4–99.5% of conventional pollutants were removed [196]. But there was a lot of variation in the removal of pharmaceuticals; for example, the removal efficiency for naproxen ranged

from 3.6 to 100%c. Even negative removal efficiency values were noted for diclofenac. The elimination of non-steroidal anti-inflammatory drugs was shown to be ineffective using batch treatment techniques and activated sludge processes [196].

The membrane bioreactor (MBR) has been used as an effective wastewater treatment technique [17]. System is identical to batch reactor, but treated water is selectively and preferentially filtered via membrane with embedded active biomass treatment [19]. Standard membranes for membrane bioreactors are often created using the phase inversion approach. Using this method, it is challenging to manage membrane pore size distribution, density, and shape [16,118]. It has been suggested that these restrictions may be circumvented using the track-etch membrane technique [20]. The productivity of the wastewater treatment plants has risen thanks to incorporating membrane bioreactor technology [116,118]. Membrane fouling, a phenomena where pollutants are deposited inside and on the surface of the membrane matrix, reduces the permeability effectiveness of membrane pores, and is the fundamental drawback of MBRs [17]. Pre-treatment procedures are thus preferred to avoid fouling and increase the lifespan of membranes.

Advanced oxidation processes are one of the strategies that has a lot of potential for post-treatment of emerging contaminants. They are drawing attention because they are so effective in destroying the target organic pollutants. The actual process often depends on a mixture of oxidants that produce active species, most frequently radicals, and catalysts (photoactive metals and metal oxides) [7,144]. Catalysts are also activated by other factors, such as thermolysis, sonolysis, photolysis, etc. The goal of each of these techniques is to produce active radicals [159]. Historically, the major oxidation sources for these processes was the hydroxide radicals created by the breakdown of hydrogen peroxide. However, the need for alternative oxidants was driven up by the danger that the latter causes during its transit, storage, and use. Given their promising oxidizing capability, persulfate salts quickly attracted attention [142].

5.2. Focus of the chapter

The evidence in existing literature highlights the gravity of the issue regarding emerging pollutants and the inadequacy of existing methods of wastewater treatment to address this problem individually. Therefore, it is imperative to seek out effective combined water treatment technologies. This section delves into the utilization of MBR along with AOPs for the treatment of wastewater containing organic pollutants such as sulfamethoxazole, naproxen, and bisphenol A. To the best of the authors' knowledge, there are no published

studies on the integration of track-etch membrane bioreactors and advanced oxidation processes.

5.3. SBR process

At the start of the study, tests were conducted without activated sludge to assess the influence of the reactor's structure and the possibility of organic compounds being released due to aeration. Fig. 5.1 illustrates how EP degrades and how TOC, TC, and TN are removed in an abiotic environment.

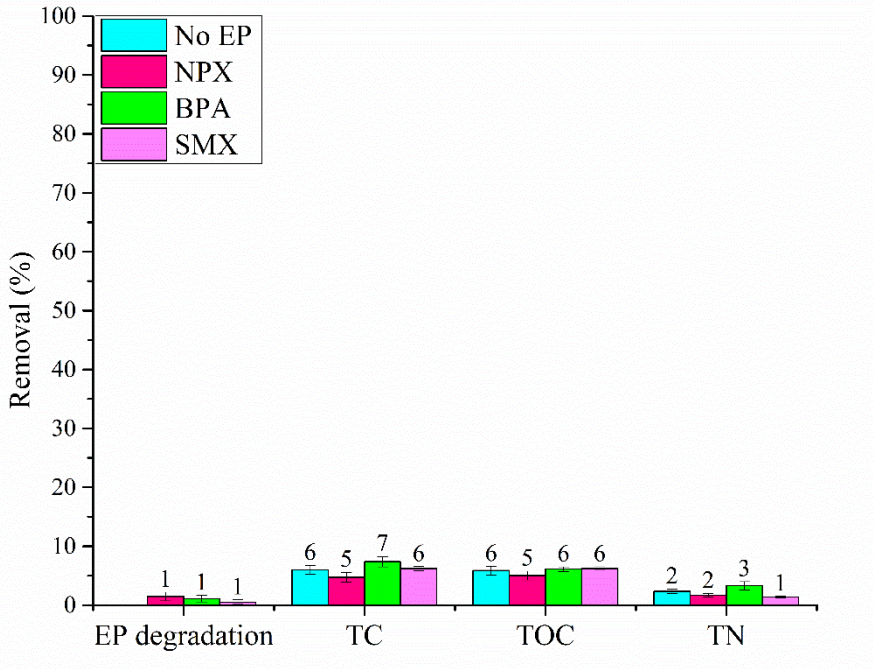

Fig. 5.1. Abiotic control experiments using SBR.

Insignificant amounts of organic matter and nitrogen were removed as a result of hydrolysis and volatilization. It is important to note that only organic substances with Henry's law constants above 0.005 can be removed from solutions through air stripping [197]. Therefore, these chemicals' volatilization as a result of air stripping did not aid in their elimination.

The studies with and without EPs had average TSS values between 2.4 and 2.9 g/L (Fig. 5.2).

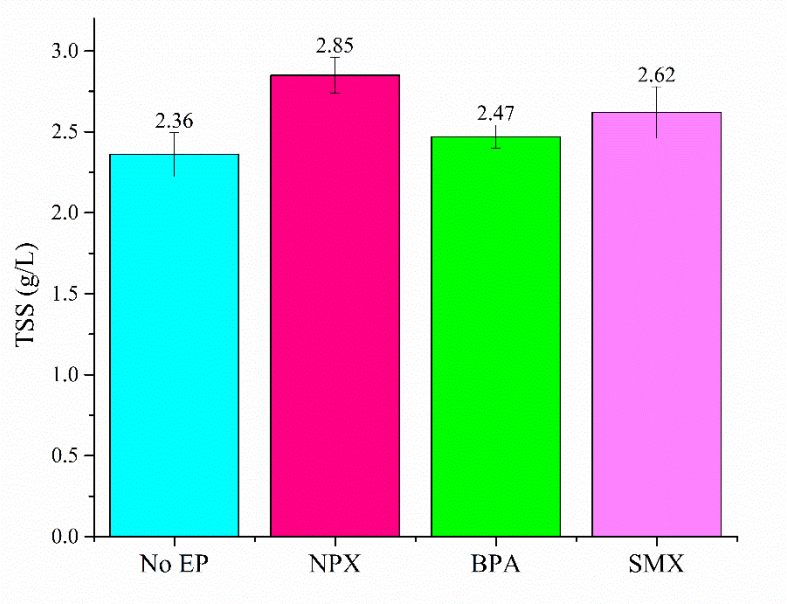

Fig. 5.2. The concentration of TSS during the SBR experiments.

TSS was composed of around 80% volatile suspended solids (VSS), also known as biological solids. Fig. 5.3 displays the outcomes of SBR tests using activated sludge.

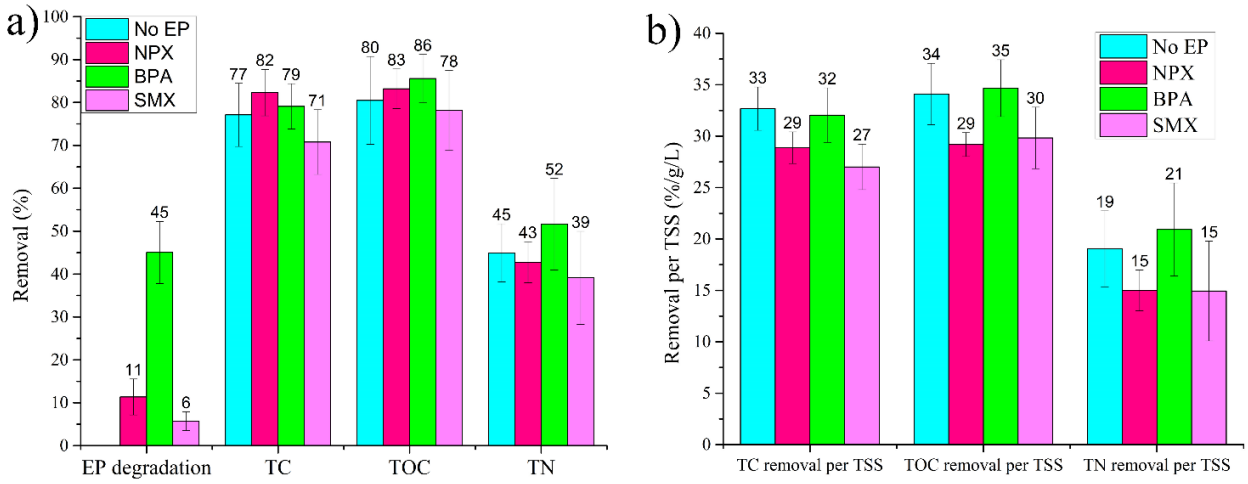

Fig. 5.3. SBR experiments: a) removal of TOC, TC and TN and degradation of EPs; b) removal of TOC, TC and TN and degradation of EPs normalized per TSS, 1g/L.

The removal efficiencies of TC, TOC, and TN were comparable for experiments with and without EP. The studies with NPX, BPA, or SMX showed TOC removal of 83%, 86%, and 78%, respectively, compared to the control experiment without EPs, which had a TOC removal of 80%. TN removals ranged from 39 to 52%. The TOC and TN elimination were in agreement with earlier findings. Doskaliyev et al. observed TC removal from synthetic wastewater ranging from 80 to 95% and TN removals ranging from 20 to 80% [90]. In a

different research, Sajjad and Kim employed SBR to treat synthetic wastewater and were successful in removing 84% TOC and 71% TN [198].

For EPs, the biodegradation values were highly variable. SBR was able to degrade BPA by 45%, but NPX and SMX degraded BPA by only 11% and 6%, respectively. Previous research has demonstrated that the inclusion of nitriles, aromatic alcohols and esters can enhance biodegradability, while the presence of nitro-, azo-, aromatic amine-, halogenic and sulfo- groups can hinder biodegradability [138,199]. The chain elongation also improves the compound's degradation because the side chain can be easily broken to initiate the compound's disintegration [37]. The organic molecules' biodegradability is additionally aided by the compounds' branching structure and large molecular weight [16]. Degradations of 60% or more have been observed for compounds having MW greater than 300 [37].

Guerra et al. looked into the effectiveness of the water treatment facilities in Northern America and reported about 1% to 77% BPA degradation [200]. BPA has also been shown to have inhibitory effects on activated sludge at high concentrations (53–100 mg/L) [109,201]. In batch sorption tests, Tang et al. showed NPX (200 g/L) removal of 11% after 10 min, and by 25 min, practically all of the NPX was degraded utilizing the activated sludge method [202]. Around 70% degradation of NPX from municipal wastewater was found by other researches [105]. When treating human metabolite solutions including SMX with activated sludge, Geng et al. found that 3.1% of the SMX was mineralized and that 50% of the SMX was adsorbed [203]. Collado et al. employed SBR to treat SMX (50 g/L) and got 20–50% elimination of SMX [204]. Overall, the outcomes of this work's elimination of EPs were consistent with those of earlier research. The removals per TSS were normalized as an additional method of comparing the collected data. As shown in Fig. 5.3b, the study conducted with BPA had the highest effectiveness per TSS. However, due of the minor variations between the trials, it was obvious that the presence of EPs at 3 mg/L had no effect on the SBR process.

5.4. Membrane filtration

The PIM and TEM were used to filter the SBR effluents. Fig. 5.4 displays the outcomes of the filtration experiments.

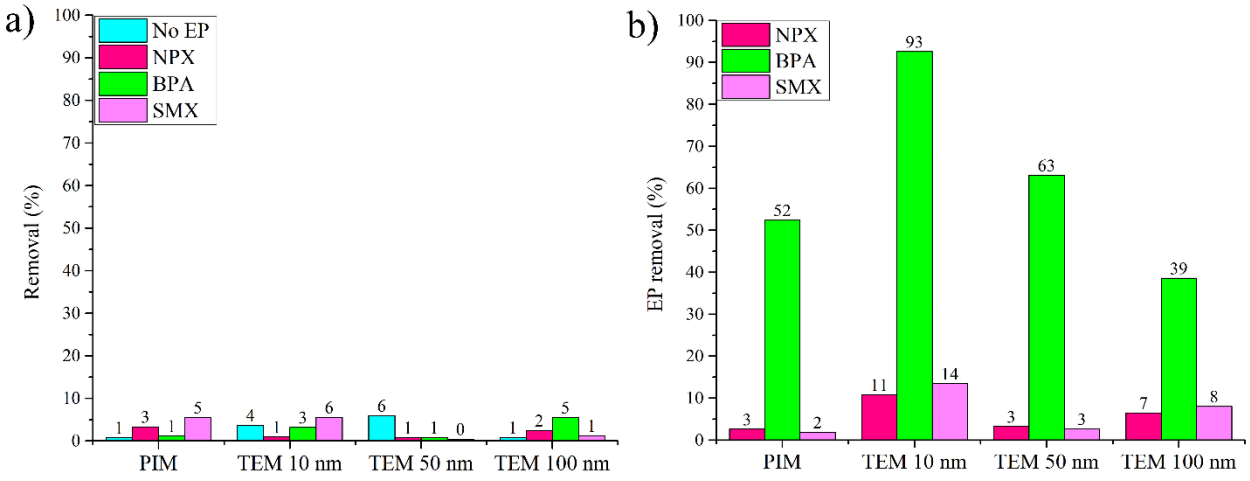

Fig. 5.4. The results of the membrane filtration experiments conducted for 6 hours in dead-end mode: a) removal of TOC and b) removal of emerging pollutants.

For all membranes, there was no discernible TOC reduction. The TOC reduction was between 0% and 6%. However, the elimination of EPs was more successful than that of TOCs. There was a definite trend toward BPA elimination utilizing various TEM sizes. The amount of BPA removed was higher when the TEM was smaller in size. When a 10 nm TEM was employed, the maximum BPA elimination recorded was 93%. Furthermore, 11% of NPX and 14% of SMX could be eliminated by 10 nm TEM. BPA was removed by 52% when PIM was used, but just 3% when NPX and SMX were used.

González-Pérez et al. observed that the removal of NPX was greater than 95% using MBR at high hydraulic- and sludge-retention times [205]. Under aerobic circumstances, 98% of the BPA was degraded in the MBR system [206]. Under aerobic and anoxic conditions, Hai et al. used MBR to remove 65% of SMX [207].

The membrane used in this study is known to remove non-polar compounds through sorption and retention, while polar compounds are primarily removed through biodegradation due to limited sorption [16]. The pore size of the membrane used in this study was 10 nm, which is larger than the size of the EP molecules studied. However, the results showed that as the pore size decreased, the removal of EPs increased. This could be attributed to membrane fouling, as seen in previous studies where the use of a fouled membrane resulted in higher retention of pollutants compared to a clean membrane [208]. This is because fouling can reduce the pore size and increase retention through size exclusion [209]. Additionally, the high electropositivity of BPA molecules allows them to strongly attach to organic matter and fouling cakes, further contributing to their retention [209]. Therefore, it can be assumed that both physical retention and sorption mechanisms play a role in the removal of EPs. However,

due to the complexity of EP removal, the exact mechanism of filtration cannot be determined [16].

It was anticipated that there would be varied water flux patterns because the membranes had different pore sizes and types. Gravimetric measurements were used to obtain the combined profiles of water flux displayed in Fig. 5.5.

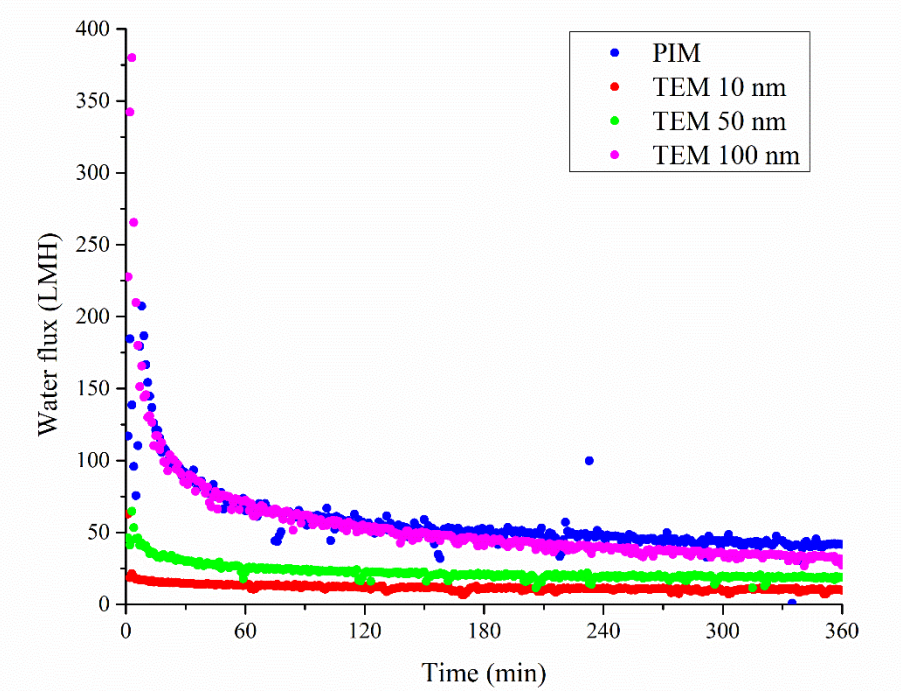

Fig. 5.5. The overall water flux during the filtration process in dead-end mode of the SBR effluents using different membranes.

For each membrane, the initial water flow varied between 46 and 380 L/m^2/h (LMH). On average, water flux went in the following sequence from greatest to lowest value: PIM, TEM 100, TEM 50, and TEM 10 nm. PIM was the most stable of these 4 membranes, while being capable of rejecting 200 kDa particles. PIM started with a water flow of 207 LMH and ended with one of 41 LMH after six hours. Initially, 100 nm TEM had a larger flux than other membranes due to its largest pore size, but with time, as a result of membrane fouling, the flux substantially dropped. The average water flow at TEM 100 nm after 6 hours of operation was 31 LMH.

Fig. 5.5 shows that the water flow experienced a dramatic reduction at the start of the filtration. This might be explained by the fact that faster convective flow transported a large concentration of pollutants to the membrane pores or surfaces, blocking or constricting the membrane pores [210]. Fig. 5.6 displays SEM pictures of TEM 100 nm before and after filtering.

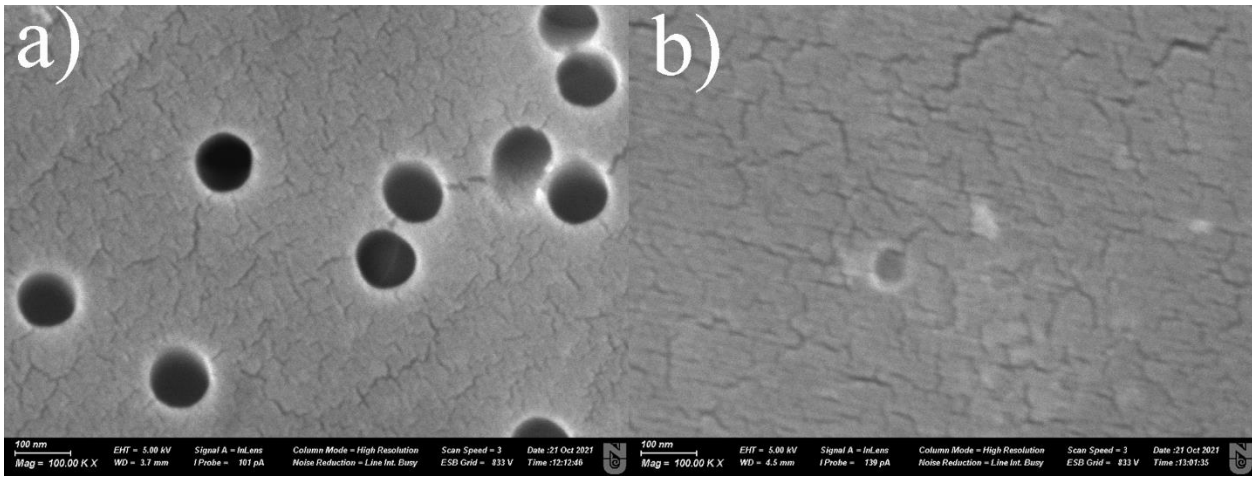

Fig. 5.6. SEM image of 100 nm TEM before (a) and after (b) membrane filtration.

The water flux patterns for TEM 10 nm and TEM 50 nm were similar during the filtration process. Initially, the water flux for TEM 50 nm and TEM 10 nm were 65 LMH and 62 LMH, respectively. After 6 hours, the water flux decreased to 19 LMH for TEM 50 nm and 10 LMH for TEM 10 nm. Table 5.1 shows the TSS and particle size distribution of the SBR effluents before and after being filtered through the membranes.

Table 5.1. The TSS and particle dimensions of the SBR wastewater before and after being filtered through a membrane.

SBR effluent	TSS, mg/L				Median particle size, d.µm			
	No EP	NPX	BPA	SMX	No EP	NPX	BPA	SMX
Initial	68.5	51.1	81.1	65.5	67.4	59.5	59.6	47.6
PES	<2	<2	<2	<2	0.39	0.44	0.54	0.38
TEM 10 nm	<2	<2	<2	<2	0.45	0.45	0.84	0.50
TEM 50 nm	<2	<2	<2	<2	0.29	0.47	0.60	0.46
TEM 100 nm	<2	<2	<2	<2	0.19	0.35	0.37	0.46

The use of membrane filtration effectively eliminated all TSS from the SBR effluents. The median size of particles in the SBR effluent samples varied from 47.6 to 67.4 µm, but after filtration, the median size of the particles in the solution decreased to a range of 190 nm to 840 nm. Despite the fact that the membranes had a pore size considerably smaller than the reported particle size (10-100 nm), it is possible that particles agglomerated after filtration. This suggests that the larger particles were successfully captured by the membrane, resulting in a shift from microscale to nanoscale in the median particle size.

5.5. Photochemical treatment of the SBR effluents

The UV/PS process was investigated for its ability to remove organic materials from SBR effluents. Fig. 5.7 displays TOC removal curves for varying PS concentrations.

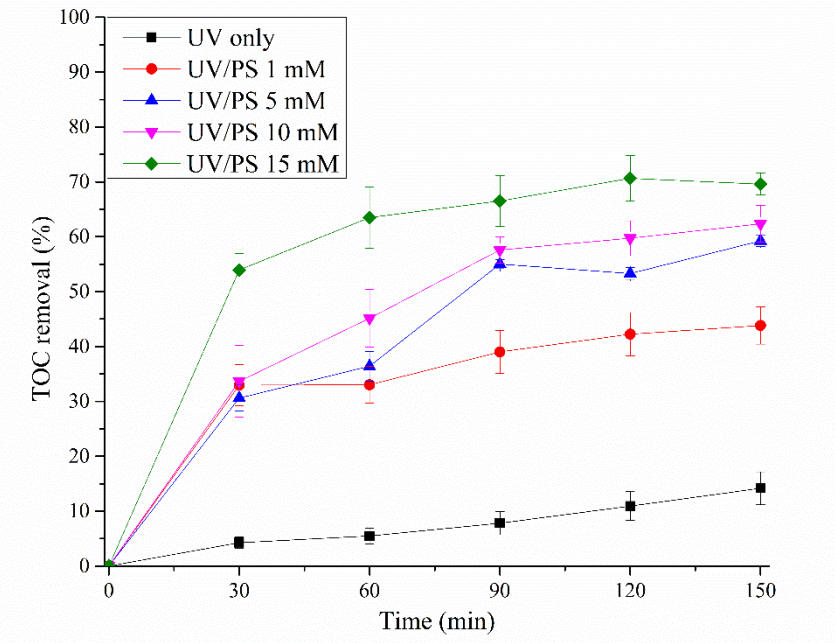

Fig. 5.7. The results of the photochemical treatment of the SBR effluents using UV/PS process.

Only 14% of the TOC was removed after 150 minutes when UV irradiation was used alone. After 150 minutes, the addition of 1 mM PS to the system dramatically boosted TOC removal by up to 44%. Final TOC removals with the usage of 5 mM and 10 mM PS were 59 and 62%, respectively. This could be a result of the recombination of hydroxyl radicals that have been produced in excess [211]. When 15 mM PS was employed, the greatest TOC reduction (70%) was found.

Further research was done on the possibility of utilizing different PS activators. For this, the effects of goethite, ZVI, and iron (II) sulfate heptahydrate were examined. Persulfate oxidation results with various iron sources are shown in Fig. 5.8.

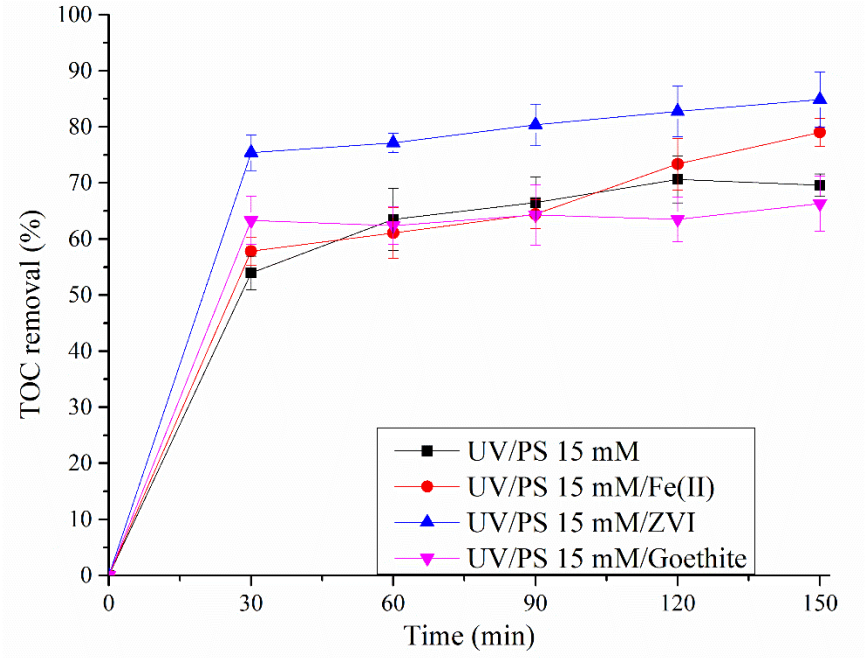

Fig. 5.8. The results of the photochemical treatment of the SBR effluents using UV/PS and various iron sources, each with an iron content of 37.5 mg/L.

The use of UV/PS/Goethite resulted in the lowest reduction of TOC, at only 66%. This is because UV light can activate persulfate to produce sulfate radicals (Eq. 5.1), but the process may be less efficient due to the extra step needed to regenerate the ferric ion (Fe^{3+}) in goethite into ferrous ion (Fe^{2+}). These ions are responsible for activating persulfate (Eq.5.2-3). Overall, the interaction between these three factors can be represented by the following equations [172]:

$$S_2O_8^{2-} \xrightarrow{hv} 2SO_4^{\bullet-} \quad (5.1)$$

$$Fe^{3+} + H_2O \xrightarrow{hv} Fe^{2+} + HO^{\bullet} + H^{+} \quad (5.2)$$

$$S_2O_8^{2-} + Fe^{2+} \xrightarrow{hv} SO_4^{\bullet-} + SO_4^{2-} + Fe^{3+} \quad (5.3)$$

It is important to note that the presence of highly complex water matrices and inorganic mineral ions may have an impact on these reactions [172]. The combination of UV/PS/Fe^{2+} led to a 79% reduction of TOC after 150 minutes. The most efficient system was UV/PS/ZVI, which achieved a TOC removal of 85%. These systems also showed complete degradation of all EPs within 30 minutes of treatment, compared to 60 minutes when using UV alone.

5.6. Photochemical treatment of the membrane filtration effluents

The UV/PS/ZVI system was used to treat the PIMBR and TEMBR effluents in order to combine the membrane bioreactor with AOPs. The outcomes of the experiments are displayed in Fig. 5.9 and 5.10.

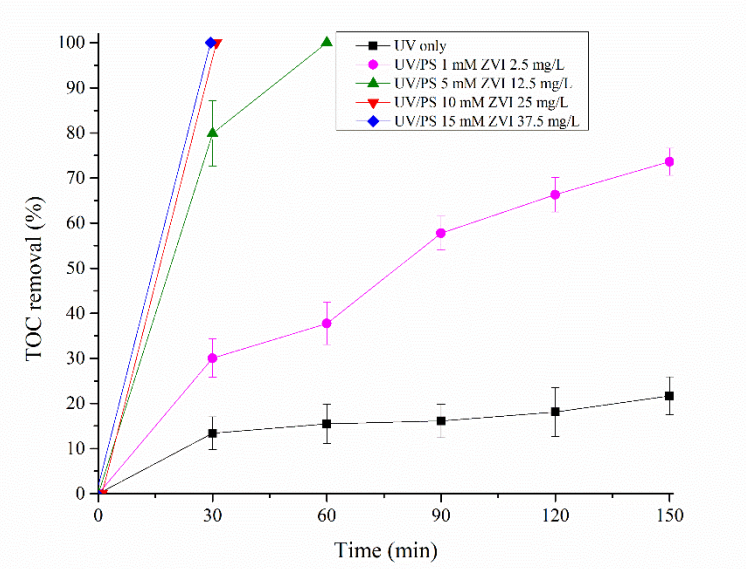

Fig. 5.9. The results of the photochemical treatment of the TEMBR effluents using UV/PS/ZVI process.

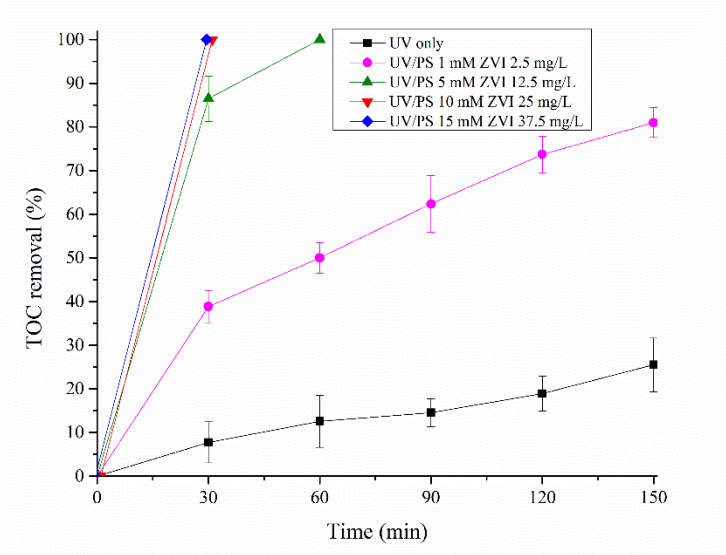

Fig. 5.10. The results of the photochemical treatment of the PIMBR effluents using UV/PS/ZVI process.

It should be noted that whereas the MBR effluents had TSS less than 2 mg/L, the effluents after SBR had significantly higher TSS up to 80 mg/L. As a result, increased UV/PS/ZVI system efficiency was anticipated. Organic carbon was removed from TEMBR and PIMBR effluents by UV irradiation in amounts of 22 and 26%, respectively. Compared to SBR

effluents, this was nearly twice as high. In case of TEMBR and PIMBR effluents, 74% and 81% of organic carbon was removed using UV/PS 1 mM/ZVI 2.5 mg/L. These outcomes were similar to those obtained by the UV/PS 15 mM/ZVI 37.5 mg/L procedure used for SBR effluents (85%). Membrane filtration may thereby effectively lower the amount of chemicals utilized as photochemical oxidants and activators, as well as the associated expenses. At higher PS concentrations, TOC was completely removed from both effluents within 30 to 60 minutes.

Advanced oxidation processes have been utilized successfully to remove organic contaminants. The initial concentrations of sulfamethoxazole, naproxen, bisphenol A in TEMBR effluents were 2.7 mg/L, 2.9 mg/L, and 0.1 mg/L, respectively, while PIMBR effluents contained 2.7 mg/L, 2.8 mg/L, and 0.8 mg/L, respectively. The use of UV treatment alone demonstrated significant removal of emerging pollutants, with removal rates ranging from 55.8% to 100%. However, full degradation of TOC was not achieved, suggesting that certain pollutants, such as NPX, BPA, and SMX, may have been transformed into photodegradation byproducts. In contrast, the implementation of UV/PS 1 mM/ZVI 2.5 mg/L resulted in complete degradation of emerging pollutants within a short time frame of 30 minutes. The comparison with the literature is given in Table 5.2.

Table 5.2. Comparison of the results of the persulfate oxidation of the emerging pollutants in the TEMBR effluents with the literature.

The process	EP concentration	Removal, %	Ref.
UV only for 160 min	BPA (5 mg/L)	80	[212]
UV/PS 1 mM for 5 min	BPA (2 mg/L)	60	[213]
UV only for 30 min	NPX (25 μM)	10	[214]
UV only for 40 min	NPX (10 μM)	100	[215]
UV only for 20 min	SMX (10.87 mg/L)	100	[216]
UV/PS 1 mM/ZVI 2.5 mg/L for 30 min	SMX (2.7 mg/L), NPX (2.9 mg/L) and BPA (0.1 mg/L)	100	This work

In summary, the degradation rates of emerging pollutants in this study were consistent with previous findings. Given the potential risks posed by emerging pollutants and their by-products to the environment and human health, it is crucial to achieve complete mineralization of the organic carbon in effluent. The MBR-AOPs system utilized in this study successfully achieved this objective, making it a promising approach for further wastewater treatment investigations.

The integration of AOPs with traditional technologies has led to advancements in environmental friendliness and operability [217]. However, the homogeneous Fenton

method faces challenges with iron-containing sludge and low pH levels, making it less favorable for scaled-up processes. The photo-Fenton process has shown high efficiency in degrading complex organic compounds, but strict pH control and the consumption of oxidizing reagents and chemicals for pH adjustment limit its industrial application and increase costs. The operation of the process under low pH requires tubes, pipes and reactor vessels made of acid-resistant materials. Moreover, additional post-treatment is required after AOPs to increase the pH of the wastewater and remove sulfate ions using ion exchange or other methods [218]. AOPs and integrated AOPs are being compared to other technologies for wastewater treatment [219]. Combination processes are more efficient, but different pretreatment and combinations are needed for each type of wastewater. For now, limitations of AOPs have hindered their industrial use and more research should be done until it reaches the point of economic efficiency.

5.7. Summary of the chapter

In this chapter, sequencing batch reactor, membrane filtration, and advanced oxidation methods were used to treat synthetic wastewater with and without emerging contaminants. For wastewater with and without emerging contaminants, the sequencing batch reactor, running on HRT 8 h, obtained TOC removal ranging from 78 to 86% and TN removal ranging from 39 to 52%. It was possible to draw the conclusion that the emerging contaminants at concentrations of 3 mg/L had no impact on the biological treatment process since the variation between the removals was within a standard deviation range. Additionally, a sequencing batch reactor was able to partially remove emerging contaminants. For instance, while NPX and SMX had average removal rates of 11% and 6%, respectively, BPA had an average removal rate of 45%.

Additionally, phase inversion membrane and track-etch membranes with pore diameters of 10 nm, 50 nm, and 100 nm were employed to filter the SBR effluents. For all four types, the average removal of organic carbon was negligible, falling between 1 and 6 percent. However, membrane filtration had an efficiency comparable to the SBR for the removal of emerging contaminants. When TEM 10 nm was employed for filtration, the maximum level of pollutant removal was seen since almost complete removal of BPA (93%) was achieved and fractions of NPX (11%) and SMX (14%) were degraded. Sorption and size exclusion may play a main role in the removal of BPA employing membranes. Additionally, all membranes were successful in removing TSS and bringing particulate matter down from the micro to the nanoscale. The phase inversion membrane had the highest average water flux, which was most likely due to its increased hydrophilicity in comparison to the other track-

etch membranes. However, SEM examination revealed that all membranes had pore blockage during the first 20 minutes, which caused a dramatic drop in the water flux.

After SBR, TEMBR, and PIMBR, advanced oxidation processes based on persulfate were used for the subsequent treatment of the effluents. The UV/PS 15 mM treatment resulted in the highest final TOC reduction of 70%. ZVI was the most effective PS activator evaluated, with an 85% final TOC removal. After TEMBR and PIMBR, the effluents were finally passed for the photochemical treatment. After 150 min UV/PS 1 mM/ZVI 2.5 mg/L eliminated 74% and 81% of TOC from the TEMBR and PIMBR effluents, respectively. Moreover, BPA, NPX, and SMX were completely degraded after 30 minutes in both effluents. These results were published in *Journal of Water Process Engineering* with a research paper titled "Membrane bioreactor and advanced oxidation processes for combined treatment of the synthetic wastewater containing naproxen, bisphenol A, and sulfamethoxazole".

CHAPTER 6: PHOTOCHEMICAL TREATMENT OF POULTRY SLAUGHTERHOUSE WASTEWATER

6.1. Introduction

High concentrations of several contaminants are common characteristics of wastewater discharged from a slaughterhouse plant. Remaining blood, urine, and feces are the primary sources of organic nitrogen, whereas skin lipids and oils are the main sources of organic carbon. The presence of phosphorus in this effluent is influenced by disinfectants, detergents, blood, and manure [220]. Poultry slaughterhouse wastewater may also contain a variety of harmful bacteria, including *Salmonella*, *Staphylococcus*, and *Clostridium* [221].

The treatment of the industrial wastewater has evolved into a critical concern for the poultry processing sector as a result of tighter rules on water disposal and growing consumer environmental consciousness. Biological treatment is used in the majority of poultry slaughterhouse wastewater treatment facilities. An activated sludge method [171] and membrane bioreactor [116,222] can all be used to obtain a COD removal rate of more than 80%. Treatment of wastewater using biological technologies is successful globally. In situations involving substantial loading of organic pollutants, they are very efficient and affordable [114,132]. In general, aeration uses around 50 to 60% of the energy, activated sludge treatment uses between 15 and 25 %, whereas another 15% of the energy is dedicated for the secondary clarifier [223]. Pharmaceuticals, vaccinations, cleaning supplies, and other organic contaminants found in slaughterhouse effluent may prevent microbial activity of the activated sludge and escape the treatment, which might have detrimental effects on aquatic life [3,224]. The investigation of complementary water purification methods, such as AOPs, is motivated by the potential obstruction related to biological treatment and the strengthening of disposal rules.

Using electrocoagulation with the addition of H_2O_2, Eryuruk et al. [221] examined the treatment of actual slaughterhouse wastewater. Authors reported that it was possible to remove 95% of COD under optimal conditions (0.2M H_2O_2, 0.5 g/L polyelectrolyte and 50 mA/cm^2).

Davarnejad and Nasiri also did a study on the use of the electrochemical oxidation to treat slaughterhouse wastewater. In their efforts, they were able to remove COD by 92% and color by 88% [22]. Thirugnanasambandham et al. discovered that pH 3, 20 mL/L H_2O_2, 10 mA/cm^2, and 30 minutes of electrochemical reaction produced the best treatment results, which removed 93% and 97% of the turbidity and COD, respectively [225].

Bustillo-Lecompte et al. [226] carried out a similar investigation into the improvement of continuous flow UV/H_2O_2 process of slaughterhouse wastewater. 81% of TOC removal was achieved under ideal conditions, as established by the central composite design.

6.2. Focus of the chapter

This chapter describes the use of AOPs to photochemically treat actual slaughterhouse effluent utilizing hydroxyl and sulfate radicals as the main oxidants. To study the photocatalytic degradation, TiO_2 and iron-doped TiO_2 catalysts were utilized. Additionally, the impact of starting pH and various H_2O_2 concentrations on the treatment of wastewater was assessed. Even though there are several research on the conventional slaughterhouse wastewater treatment, very few of them are pertinent to the application of AOPs. The research indicates that no published studies have yet been done on the use of sulfate radicals for the treatment of slaughterhouse effluents.

6.3. Slaughterhouse wastewater characterization

Poultry slaughterhouse wastewater had COD and TOC values of 155 mg/L and 68.7 mg/L, respectively. This indicates that the wastewater was low-strength. The World Bank and European legislations suggest that the COD outflow limitations for slaughterhouse wastewater not exceed 125 mg/L. Australian discharge regulations are even stricter, which requires the TOC of the discharge effluent be under 10 mg/L [227].

High-strength slaughterhouse wastewater is often treated anaerobically. However, it frequently finds it difficult to adhere to the typical discharge limitations [228]. Additionally, refractory substances like disinfectants, antibiotics, and detergents may evade the biological treatment process [38,177,229]. In order to completely remove contaminants, post-treatment is therefore required.

Vidal et al. conducted similar studies, first using anaerobic digestion to produce effluents with TOC of 52 mg/L from the slaughterhouse wastewater [230]. The TOC was subsequently reduced to 2 mg/L using the solar photoelectro-Fenton method to treat the effluents.

Tables 6.1 provide a summary of the findings of the IC investigations.

Table 6.1. The IC results of the sterile poultry slaughterhouse wastewater.

Ion	Na^+	NH_4^+	K^+	Mg^{2+}	Ca^{2+}	F^-	Cl^-	SO_4^{2-}	Br^-	NO_3^-	PO_4^{3-}
Content, mg/L	141.87	0.84	14.86	67.27	132.43	10.46	213.88	236.11	0.22	2.98	1.78

The findings of IC show that poultry slaughterhouse wastewater includes significant levels of alkali and alkaline earth metals, fluoride, chloride, and sulfates. Moreover, the traces of the ammonium, bromine, nitrate and phosphate were also present. Sulfate and hydroxyl radicals are reported to be scavenged by Cl^- and Br^- [7]. Additionally, Cl^- and Br^- may lead to the creation of harmful chlorate and bromate oxyanions [7]. Both bicarbonate and carbonate ions, which make up total inorganic carbon, have the ability to scavenge hydroxyl and sulfate radicals [231].

Fig. S6.1 displays the FTIR data of the slaughterhouse wastewater. The wastewater included substances with the following functional groups, according to the FTIR data (Table S 6.1): O–H, ≡C-H, C-N, C=C, C=O, N-H, C-Br and C-I. Both IC and FTIR tests revealed the presence of bromine species, which can be derived from sanitizers that include bromine and are frequently used to eliminate harmful bacteria in buildings and machinery [232].

6.4. UV/H_2O_2 process

The poultry slaughterhouse wastewater was initially treated with 0-196 mM of H_2O_2 while being exposed to UV light. The findings are displayed in Fig. 6.1. UV photolysis had TOC removal of 3% after 150 min. Hydroxyl radicals produced by hydrogen peroxide's dissociation should is responsible for the degradation of organics in the wastewater (Eq. 6.1) [158].

$$H_2O_2 \xrightarrow{h\nu} {}^{\bullet}OH \tag{6.1}$$

TOC removal increased from 47% to 74% with the increase in the concentration of hydrogen peroxide from 49 to 98 mM. Because hydrogen peroxide itself has a scavenging effect on the generated hydroxyl radicals, as has already been seen in earlier experiments, a further increase in H_2O_2 was also not beneficial [13]. Fig. S6.3 shows the pH development during these experiments. In all experiments with H_2O_2 a starting value was around 7.5, then pH dropped to around 6.7, while in the experiment without H_2O_2, pH practically remained constant. The effective operation of AOPs at circumneutral pH is essential due to the possibility of applications on a greater scale [231].

In another study, the optimal ratio of influent TOC to H_2O_2 for eliminating the most TOC (81%) was 35.8 (mg/L TOC/mg/L H_2O_2) [226]. These results are close to those found in our investigation employing a batch photoreactor (Fig.6.1).

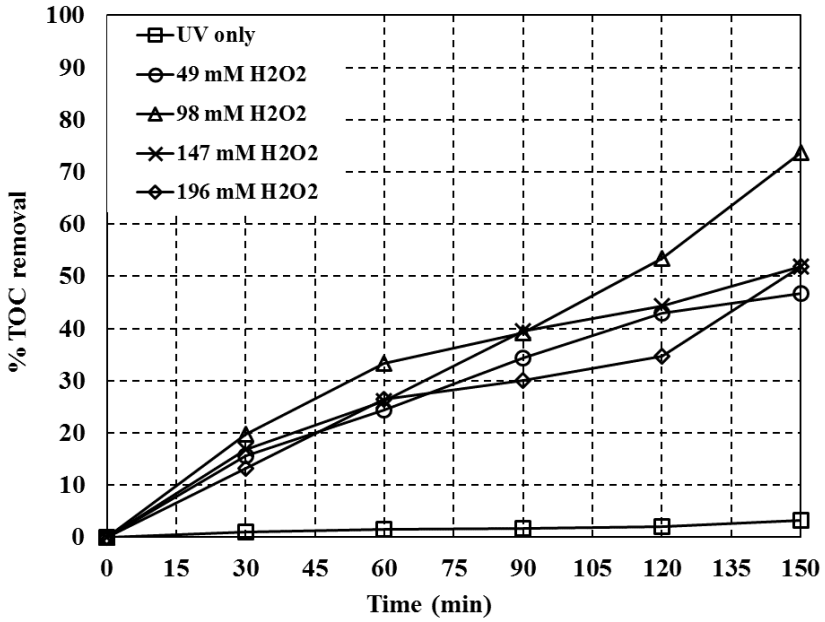

Fig. 6.1. Time-dependent TOC elimination throughout the UV/H_2O_2 process.

Fig. 6.2 displays the outcomes of the computations of energy per order. The use of 98 mM H_2O_2 had the least energy spent (324 kWh/m^3/order).

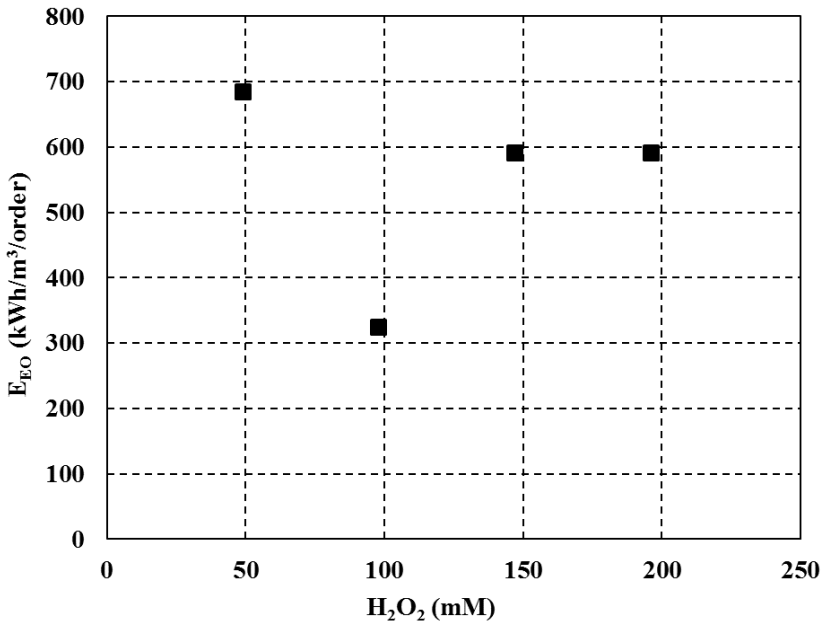

Fig. 6.2. The impact of H_2O_2 starting concentration on the UV/H_2O_2 process's electrical energy consumption

The wastewater's initial pH was then adjusted to lower levels in an effort to see whether it was possible to achieve the same level of TOC removal (74%) while using less H_2O_2, hence lowering the process's cost. The impact that pH has on how hydroxyl radicals are produced is crucial. It is evident from Fig. 6.3 that the process was not enhanced by lowering the wastewater's original pH. In extremely acidic aqueous conditions, $H_3O_2^+$ is created when

H_2O_2 is present (Eq. 6.2), which enhances the stability of H_2O_2 and reduces the production of $^{\bullet}OH$ radicals [233]. Additionally, HO_2^- competes with $^{\bullet}OH$ for H_2O_2 (Eq. 6.3-4) [234].

$$H_2O_2 + H^+ \rightarrow H_3O_2^+ \quad (6.2)$$

$$H_2O_2 + HO_2^- \rightarrow H_2O + O_2 + OH^- \quad (6.3)$$

$$^{\bullet}OH + HO_2^- \rightarrow OH^- + \bullet\ ^{\bullet}HO_2 \quad (6.4)$$

The findings are in correlation with the recent study [235].

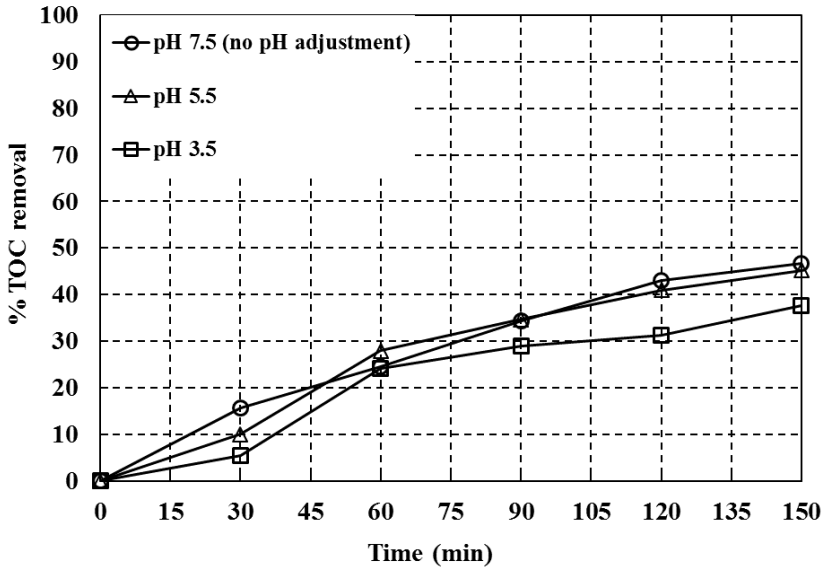

Fig. 6.3. The impact of pH on TOC removal during the UV/H_2O_2 49 mM process.

6.5. UV/H_2O_2/Fe^{2+} process

The AOP that has been the subject of the most investigation is the UV/H_2O_2 process, in which hydrogen peroxide is photolyzed to produce hydroxyl radicals [146,147]. Nevertheless, the process is constrained by H_2O_2's low UV photon absorption. Iron can enhance the process overall by enhancing photon absorption by starting photo-Fenton reactions [236].

In order to conduct photo-Fenton studies, 98 mM H_2O_2 was employed. In this series of tests, H_2O_2 and Fe^{2+} were used (Fig. 6.4). The initial pH was once changed to 3.3. The procedure only benefited from the increment in Fe^{2+} content from 5 to 20 mg/L during the first 90 minutes of the treatment, then the TOC removal eventually stabilized at a value of about 67% for both concentrations. The highest TOC removal obtained (82.5%) was significantly boosted by the first pH adjustment to 3.3. A pH level close to 3 has been demonstrated to enhance Fenton reactions in a prior publication [237]. The Fenton oxidation process is strongly influenced by the production of $[Fe(OH)]^{2+}$ at pH values between 2.8 and 3.5.

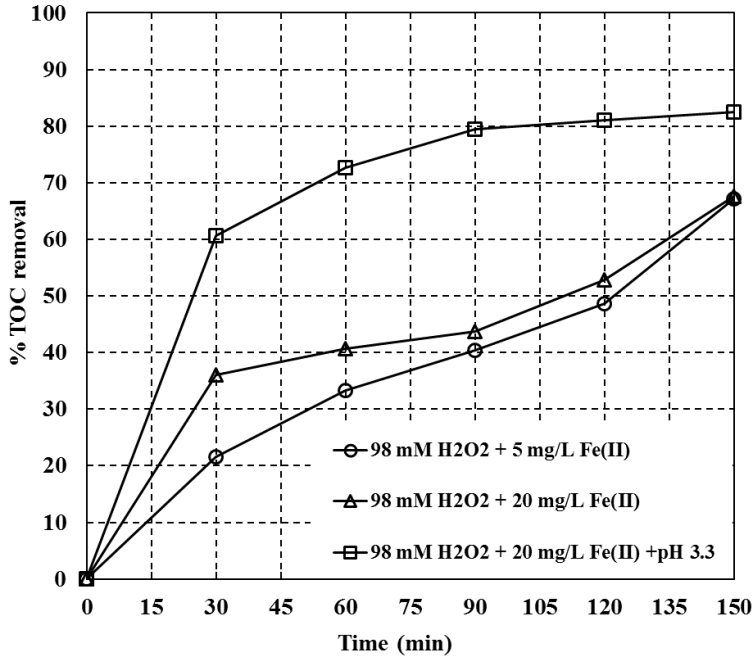

Fig. 6.4. Time-dependent TOC elimination throughout the UV/H_2O_2/Fe^{2+} process.

According to calculations, the lowest E_{EO} values for the photo-Fenton experiment was 248 kWh/m^3/order after the adjustment of pH.

6.6. UV/TiO_2 process

The treatment of the wastewater also involved TiO_2-mediated photocatalysis. In particular, 0.5 and 1.0 g/L TiO_2 and 0.5 g/L Fe(4%wt.)/TiO_2 were utilized as catalysts under UV light. In the past, the Fe/TiO_2 catalyst outperformed the pure TiO_2 catalyst in the oxidation of 4-tert-butyl phenol in solution [238]. The outcomes are displayed in Fig. 6.5.

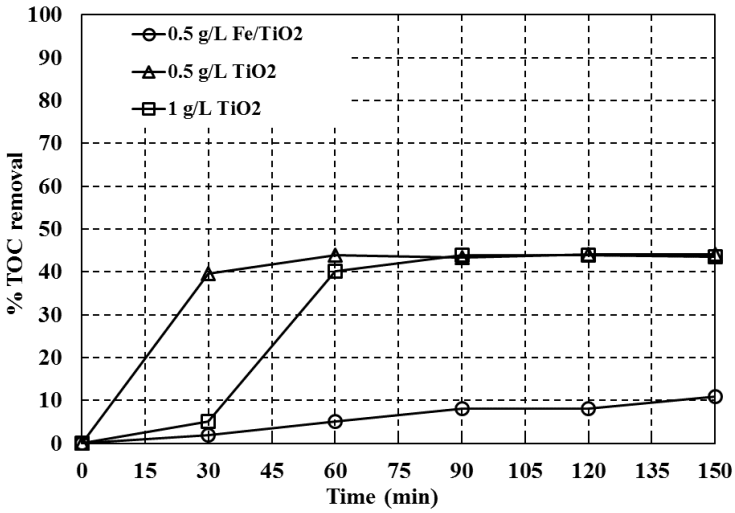

Fig. 6.5. Time-dependent TOC elimination throughout the UV/TiO_2 process.

According to the findings, the undoped catalyst was more effective at removing TOC than the iron-doped catalyst. After 60 minutes, using 0.5 g/L and 1 g/L TiO_2 reduced TOC by 44% and 40%, respectively. However, monitoring TOC levels after 150 minutes showed no discernible improvement. Increased turbidity in the solution as a consequence of a rise in catalyst concentration decreased ability of the UV light to penetrate the solution and reach the catalyst [12,165].

Fe-doped TiO_2 treatment resulted in a TOC elimination of 10% after 150 minutes, which was far low to be of real significance. Fe-doping has various effects on the effectiveness of wastewater treatment, according to the literature. Different Fe dopant concentrations were also synthesized by Chen et al. [239]. In the photocatalytic treatment of effluent from papermaking industry, the catalysts with lower Fe contents (0.01%, 0.03%, and 0.05%) were more efficient than the undoped TiO_2. The improvement in electron-hole separation efficiency brought about by the introduction of Fe^{2+} may be used to explain why the photocatalytic activity has increased [239].

In another study, Bukhari et al. used pure TiO_2 (1 g/L) to photocatalyze the treatment of slaughterhouse wastewater and were able to remove 72% of the COD, but addition of Ag did not have significant effect [240].

6.7. UV/$K_2S_2O_8$

$K_2S_2O_8$ was utilized at doses from 1 to15 mM. In addition, under UV irradiation, a photo-Fenton-like reaction was employed by combination of Fe^{2+} and K_2S_2O8. (Fig. 6.6).

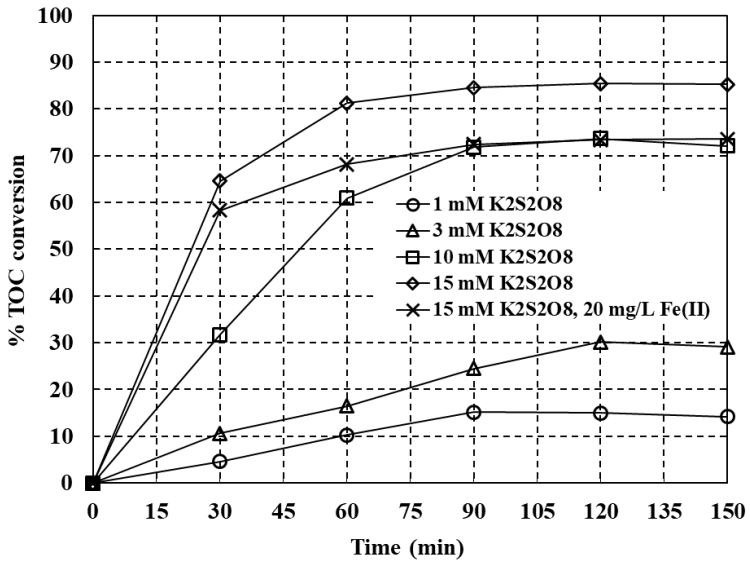

Fig. 6.6. Time-dependent TOC elimination throughout the UV/$K_2S_2O_8$ process

The rise in oxidant concentration led to an increase in TOC elimination. 15 mM $K_2S_2O_8$ successfully eliminated 85% of the TOC after 150 min, outperforming earlier experiments employing 98 mM H_2O_2 (74% TOC removal). Sulfate radicals ($^{\bullet}SO_4^-$, 30-40 μs) have a half-life that is significantly longer than that of hydroxyl radicals (10^{-3} μs). As a result, while working with actual wastewaters, $^{\bullet}SO_4^-$ is less susceptible to being scavenged by unintended molecules, which makes $^{\bullet}SO_4^-$ more alluring to $^{\bullet}OH$ [6,139].

Previous research has compared the performance of $^{\bullet}SO_4^-$ and $^{\bullet}OH$ based photocatalytic processes. During photochemical treatment of sodium diatrizoate with 10 mM $K_2S_2O_8$ and 10 mM H_2O_2, Velo-Gala et al. [241] obtained 78% and 77% decomposition of sodium diatrizoate at circumneutral pH, respectively. The pH rise had a negative impact on the UV/H_2O_2 system's degrading performance, in contrast to the UV/$K_2S_2O_8$ system. The degradation of sulfamethazine (SMZ) with the help of UV/H_2O_2 and UV/$K_2S_2O_8$ was compared by Acosta-Rangel et al. After 60 minutes of the experiment, it was shown that using 0.147 mM $K_2S_2O_8$ and 0.147 mM H_2O_2 caused an 80% and 89% degradation of SMZ, respectively [242].

The effectiveness of the several AOPs used for treating the wastewater from slaughterhouses has been examined and is displayed in Fig. 6.7 in a comparison of TOC and COD removal.

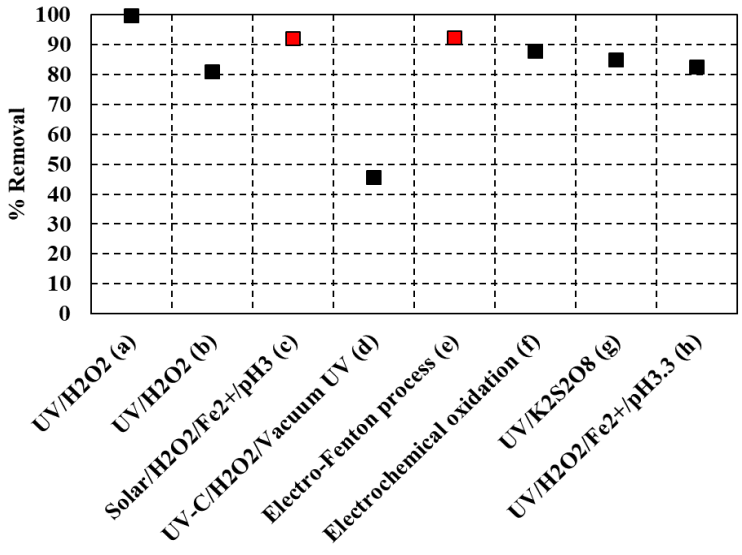

Fig. 6.7. The removals of COD (in red) and TOC (in black) by various AOPs used for the treatment of the slaughterhouse wastewater (Ref-s: a) [243]; b) [226]; c) [244] d) [245]; e) [22]; f) [246]; g-h) current study).

According to Fig. 6.7, the majority of the projects effectively treated slaughterhouse wastewater, with pollutant removal rates ranging from 81 to 99%. The UV/H_2O_2/Fe^{2+}/pH3 and UV/$K_2S_2O_8$ processes utilized in the current study both had removal efficiencies that

were within the specified range. Table S 6.2 provides more information on these processes' experimental settings and effluent characteristics.

Calculations revealed that the EEO values for the UV/$K_2S_2O_8$(15 mM) and UV/$K_2S_2O_8$(15 mM)/Fe^{2+}(20mg/L) were 226 kWh/m^3/order and 325 kWh/m^3/order, respectively. Table S 6.3 lists the reported E_{EO} values for persulfate-based AOPs from the literature.

Evidently, model solutions were used for the majority of the works [223,247–254]. The UV/persulfate technique is now seen as being close to a full-scale wastewater treatment application [139]. The E_{EO} results should be considered as suggestive, and pilot-scale testing is required to ascertain whether it is feasible on a greater scale.

6.8. Formation of intermediates

The amounts of formic and acetic acid were quantified using IC. These substances are the final intermediates that can be found before all of the organic molecules have completely mineralized. The following material balances were used to indirectly compute the amounts of organic carbon (OC) in intermediates and mineralized CO_2:

$$\mathrm{OC_{intermediates}} = \mathrm{final(TOC - TOC_{formic\ acid} - TOC_{acetic\ acid})} \quad (5)$$

$$\mathrm{OC_{CO_2}} = \mathrm{initialTOC - finalTOC} \quad (6)$$

The outcomes are displayed in Fig. S6.3. During the UV/H_2O_2 process, the lowest concentration of intermediates was discovered at 98 mM of H_2O_2, while the production of acids increased as H_2O_2 concentration increased. The generation of acids increased when the pH was changed from neutral to acidic levels. Similar to this, the intermediate concentration marginally dropped when Fe(II) concentration increased during the UV/H_2O_2/Fe^{2+} process from 5 to 20 mg/L. Additionally, the CO2 production was increased by combining this process with pH adjustment. The UV/H_2O_2/Fe^{2+} technique at pH 3.3 produced the least amount of undetected intermediates (10% of TOC), while formic acid concentrations of 1.2 mg/L and acetic acid concentrations of 17.9 mg/L were found.

In the final solutions after testing using the heterogeneous catalysts, no formic acid nor acetic acid was found. According to Fig. S6.3, the increase in $K_2S_2O_8$ concentration sped up the breakdown of the intermediates by intensifying the generation of CO_2. Lastly, the UV/$K_2S_2O_8$ process did not become more effective with the inclusion of Fe^{2+}, in contrast to the UV/H_2O_2/Fe^{2+} process.

6.9. Summary of the chapter

In this study, a poultry slaughterhouse wastewater was treated using several photochemical treatment methods. The main objective of this work was to apply different AOPs and select the most effective photochemical system for the treatment of wastewater with a complex matrix in terms of organic carbon removal. While employing UV photolysis and the UV/4% Fe-TiO_2 process had negligible TOC removal, using undoped TiO_2 removed 44% of the TOC after 60 minutes. The UV/H_2O_2 technique removed 74% of the TOC when the H_2O_2 concentration was increased to 98 mM. Higher iron concentrations were used, however this did not improve the process' effectiveness. The TOC removal with H_2O_2 (98 mM) and Fe^{2+} (20 mg/L) at pH 3.3 reached 82.5% after 150 min under UV light.

After 150 minutes in the UV/$K_2S_2O_8$ system, 15 mM $K_2S_2O_8$ removed 85% of the TOC, whereas 73.5% of the TOC was removed using $K_2S_2O_8$ (15 mM) and Fe^{2+} (20 mg/L). The UV/$K_2S_2O_8$ process demonstrated E_{EO} value of 226 kWh/m3/order, which was the lowest in this work. The UV/$K_2S_2O_8$ treatment's effluent quality was within the legal limitations for disposal set by the United States, Australia, and European nations. In order to fulfill discharge requirements and recycle the effluents, the UV/$K_2S_2O_8$ procedure may be used after biological wastewater treatment. The research findings from these investigations are published in the *Journal of Water Process Engineering* under the title “Treatment of a poultry slaughterhouse wastewater using advanced oxidation processes”.

CHAPTER 7: PHOTOCHEMICAL TREATMENT OF MUNICIPAL WASTEWATER

7.1. Introduction

In recent years, it has been clear that the discharges from urban wastewater treatment plants represent a significant source of new micropollutants, including hormones, medications, and items for personal care [3]. Traditional WWTPs are unable to remove micropollutants at a rapid pace, since they are resistant to biodegradation despite their extremely low concentration [4]. Currently, strategies for eliminating these chemicals from MWW are being considered [4].

In recent years, scientists have been interested in a novel kind of oxidizing agent such as persulfate [6]. The metal activation approach only produces 50% of the sulfate radicals that may be produced when using the equal molar concentration of persulfate by heating or UV activation of persulfate (Eq.7.1-2). Fe^{2+} and Fe^{3+} are the most frequently utilized metals [9].

$$S_2O_8^{2-} \xrightarrow{h\nu} 2SO_4^{\bullet-} \tag{7.1}$$

$$S_2O_8^{2-} + Fe^{2+} \rightarrow SO_4^{\bullet-} + SO_4^{2-} + Fe^{3+} \tag{7.2}$$

Sulfate and hydroxyl radicals each have distinct reaction patterns, although both are highly reactive entities with short lifetimes. When reacting with organic materials, $^{\bullet}OH$ has a propensity to remove hydrogen from C-H bonds or attach to C=C bonds, whereas sulfate radicals have a propensity to remove electrons from the molecule, which subsequently results in the formation of organic radical cations [255]. Eq-s 7.3 and 7.4 show how hydroxyl radicals are produced by sulfate radicals [160].

$$SO_4^{\bullet-} + S_2O_8^{2-} \rightarrow SO_4^{2-} + S_2O_8^{\bullet-} \tag{7.3}$$

$$SO_4^{\bullet-} + H_2O \rightarrow SO_4^{2-} + H^+ + HO^{\bullet} \tag{7.4}$$

Additionally, under alkaline circumstances, sulfate radicals might generate more hydroxyl radicals [255]. In contrast to hydrogen peroxide (H_2O_2), persulfate also has the ability to directly oxidize certain organic compounds [7].

In order to degrade sodium diatrizoate in an aqueous medium, Velo-Gala et al. [241] investigated the efficiencies of UV/H_2O_2 and UV/$K_2S_2O_8$-based oxidation processes. With larger rate constants, the UV/$K_2S_2O_8$ process was discovered to be more effective than the UV/H_2O_2 system [241]. In order to effectively degrade dye pollutants in actual wastewater treatment, Pervez et al. [256] used a novel Fe_3O_4@GO+$K_2S_2O_8$ system. Persulfate-activated iron-based heterogeneous catalysts have gathered significant attention as a foreseeably cutting-edge and sustainable system for water treatment.

7.2. Focus of the chapter

In light of research on energy usage, persulfate-based oxidation procedures have lately been claimed viable for full-scale application [139]. Even though, it is crucial to assess the procedure' effectiveness using actual wastewaters. Consequently, the objective of this work was to evaluate the effectiveness of AOPs that treat municipal wastewater utilizing Fe and potassium persulfate under UV light. No research using the UV/$S_2O_8^{2-}$/Fe^{2+} procedure to remediate real municipal wastewaters have been reported. The photochemical treatment of the real wastewater was optimized using the response surface methodology (RSM).

7.3. Experimental design results

Table 7.1 displays the results as well as the Box-Behnken design that was generated by the program. 95% two-sided confidence intervals were presented in Table S7.1.

Table 7.1. Box-Behnken design matrix and results.

Run	Experimental variables				Response (Y, %)					
	X_1	X_2	X_3	X_4	Actual			Predicted		
	Time	pH	$K_2S_2O_8$, mM	$K_2S_2O_8/Fe^{2+}$	TC	TOC	TN	TC	TOC	TN
1	60	5.35	30	10	56.35	45.79	9.42	54.77	46.43	34.86
2	100	3	30	10	50.80	27.98	10.87	48.18	34.35	15.79
3	140	5.35	20	7.5	60.69	58.06	6.97	57.54	60.27	26.40
4	100	3	10	10	68.35	53.03	6.35	65.51	58.62	30.66
5	140	3	20	10	58.50	46.89	6.63	64.53	52.78	14.46
6	140	5.35	30	10	71.31	73.9	10.05	63.57	65.80	15.49
7	100	5.35	20	10	50.96	55.74	35.66	47.52	55.87	45.65
8	100	7.7	10	10	39.86	76.27	5.07	37.30	69.55	12.25
9	100	5.35	20	10	47.17	59.64	46.13	47.52	55.87	45.65
10	60	5.35	20	7.5	68.24	46.06	8.13	64.30	49.37	28.64
11	60	3	20	10	65.61	24.68	39.52	66.28	25.72	26.26
12	60	5.35	10	10	57.39	56.96	21.4	63.29	57.82	17.70
13	140	5.35	20	12.5	61.69	63.61	53.35	60.46	59.94	44.94
14	100	7.7	20	12.5	46.36	72.34	11.49	46.99	74.68	39.83
15	100	3	20	7.5	60.63	37.45	46.66	58.16	38.51	20.06
16	140	7.7	20	10	49.32	67.99	21.08	55.67	68.90	20.50
17	100	3	20	12.5	57.51	55.8	51.61	58.75	52.85	54.42
18	100	5.35	20	10	44.44	52.23	55.15	47.52	55.87	45.65
19	100	7.7	20	7.5	55.07	79.09	33.43	51.99	85.45	32.36
20	60	5.35	20	12.5	59.01	55.83	59.26	56.98	53.26	51.93
21	100	5.35	10	7.5	46.11	60.96	23.24	48.80	55.44	21.98
22	100	5.35	30	12.5	44.19	53.94	57.89	48.52	56.41	45.31
23	60	7.7	20	10	56.21	87.31	39.61	57.20	78.37	17.94
24	100	7.7	30	10	60.79	98.15	44.14	58.46	92.20	31.93
25	100	5.35	10	12.5	54.74	66.9	60.13	51.81	71.27	57.30
26	100	5.35	30	7.5	45.98	76.1	49.81	55.93	68.68	38.80
27	140	5.35	10	10	51.47	65.26	51.53	51.21	56.03	27.83

The equations of the models were presented below (in coded units):

$$\text{TC removal (\%)} = 47.52 - 4.48X_2 + 9.62X_1^2 + 8.6X_2{*}X_3 \quad (7.5)$$

$$\text{TOC removal (\%)} = 55.87 + 4.92X_1 + 19.61X_2 + 6.04X_3^2 + 2.4X_4^2 - 10.38X_1{*}X_2 + 11.73X_2{*}X_3 - 7.02X_3{*}X_4 \quad (7.6)$$

where, in descending order, X_1, X_2, X_3, and X_4 stand for, respectively, time (min), pH, $K_2S_2O_8$ (mM), and molar ratio of $K_2S_2O_8$ to Fe^{2+}. In equations, X_2, X_1^2 and X_2X_3 terms for TC removal and X_1, X_2, X_3^2, X_1X_2, X_2X_3 and X_3X_4 terms for TOC removal were significant according to the analysis of variance. No parameters for TN removal were determined to be essential especially to the model's poor fit. Confidence intervals for BBD model coefficients were provided in Tables S7.2 and S7.3.

The normal probability versus residuals for removals are depicted in Fig. 7.1. They demonstrate how all three models' data match the normal probability distribution. Fig. 7.2, respectively, displays the experimental and estimated data for the removals. These numbers show that the actual and anticipated statistics for TC and TOC elimination have a fair degree of consistency. The regression quadratic model, however, does not appear to have a straight-line pattern in Fig. 2c, suggesting that it is not suitable for the TN model.

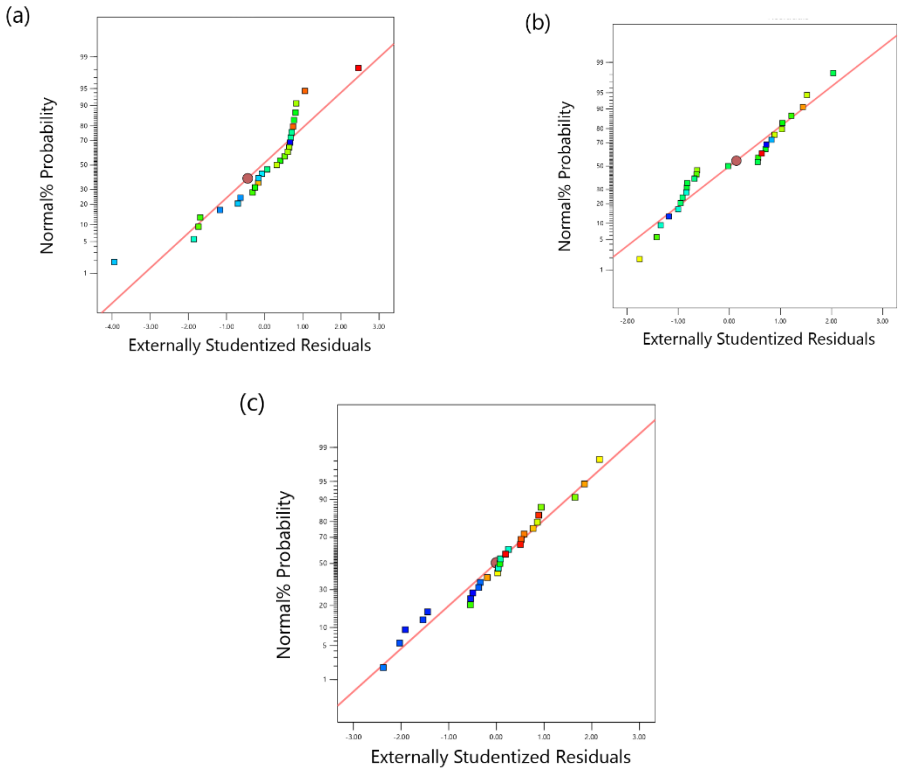

Fig. 7.1. Normal probability plot of the residuals for (a) TC removal, (b) TOC removal, and (c) TN removal.

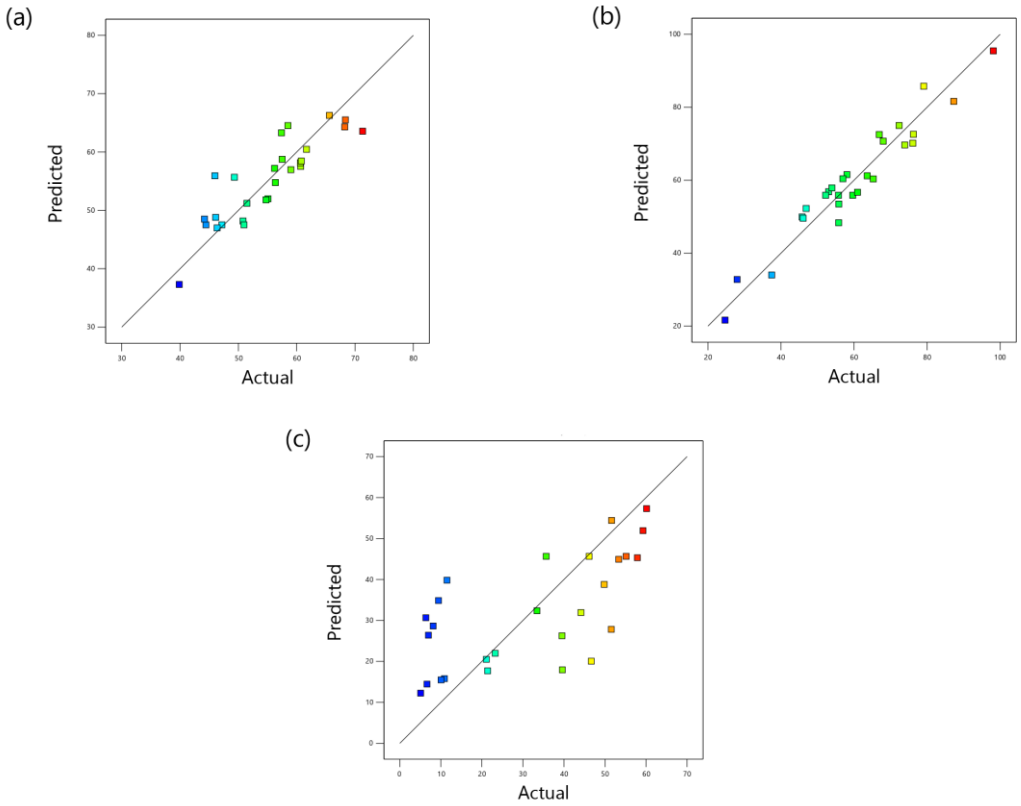

Fig. 7.2. Actual vs predicted plot: (a) TC removal, (b) TOC removal, and (c) TN removal.

7.4. ANOVA Analysis

Using the ANOVA, the model's suitability was evaluated. Calculating and evaluating regression coefficients (R^2), F- and p-values are all included in the study. Table 7.2 lists the outcomes of the ANOVA.

Table 7.2. ANOVA test for the different models.

Response	Source	Sum of Squares	Degrees of Freedom	Mean Square	F-Value	*p*-Value
TC removal	Model	1344.37	14	96.03	2.84	0.039
	Error	405.90	12	33.83		
	Lack of fit	384.45	10	38.45		
	Pure error	21.44	2	10.72		
TOC removal	Model	6659.09	14	475.65	11.64	0
	Error	490.32	12	40.86		
	Lack of fit	462.84	10	46.28		
	Pure error	27.48	2	13.74		
TN removal	Model	4664.4	14	333.17	0.70	0.739
	Error	5697.3	12	474.77		
	Lack of fit	5507.3	10	550.70		
	Pure error	190.3	2	95.14		

The models' main parameters include regression coefficients. R^2 was 0.7681, 0.9314, and 0.4502 for the elimination of TC, TOC, and TN, respectively. Generally, the value of the regression coefficient should be closer to 1. R^2 value of the TOC removal model was greater than 0.8 and could be considered for further optimization. In case of TN removal, the model could explain only 45% of the entire variance in the TN removal.

Model predictions are generally considered statistically significant when p is less than 0.05, while p is greater than 0.1 indicates that the model does not adequately capture the experimental data [22]. The models employed to predict the TC and TOC reductions have P-values of 0.039 and 0.0001, respectively, indicating that they are significant for both responses. F and p values for the TN elimination indicate that the model is inappropriate for the further optimization.

Overall, the quadratic model accurately captured the process when the ANOVA findings were taken into consideration, and it may be used to enhance the TC and TOC reductions.

7.5. Visualization of the regression models

Surface plots in three dimensions show how the factors interact with the response. The models were graphically demonstrated in Fig. 7.3-7.4.

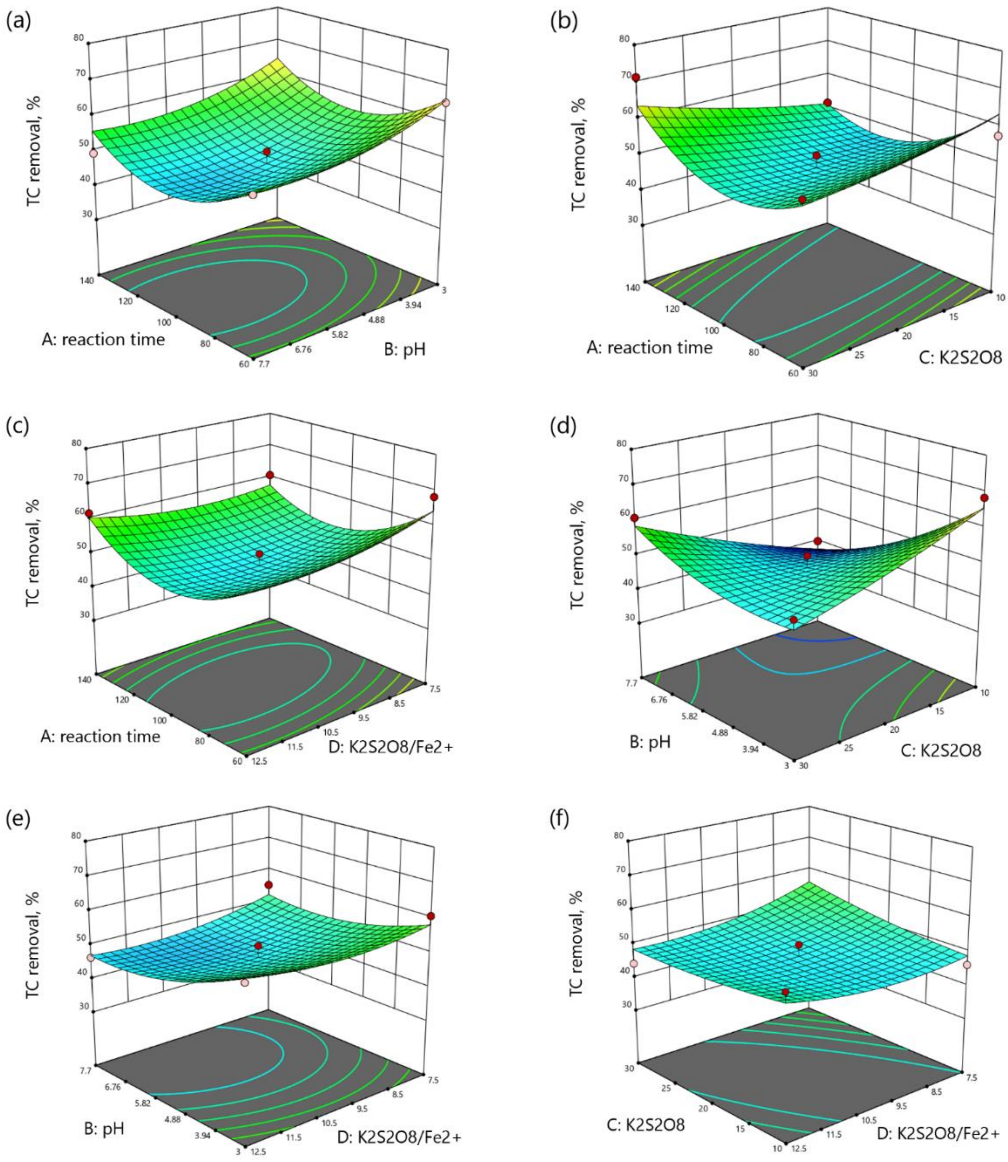

Fig. 7.3. Surface plots for TC removal model: (a) time and pH, (b) time and $K_2S_2O_8$ content, (c) time and $K_2S_2O_8/Fe^{2+}$, (d) pH and $K_2S_2O_8$ content, (e) pH and $K_2S_2O_8/Fe^{2+}$, (f) $K_2S_2O_8$ content and $K_2S_2O_8/Fe^{2+}$ ratio.

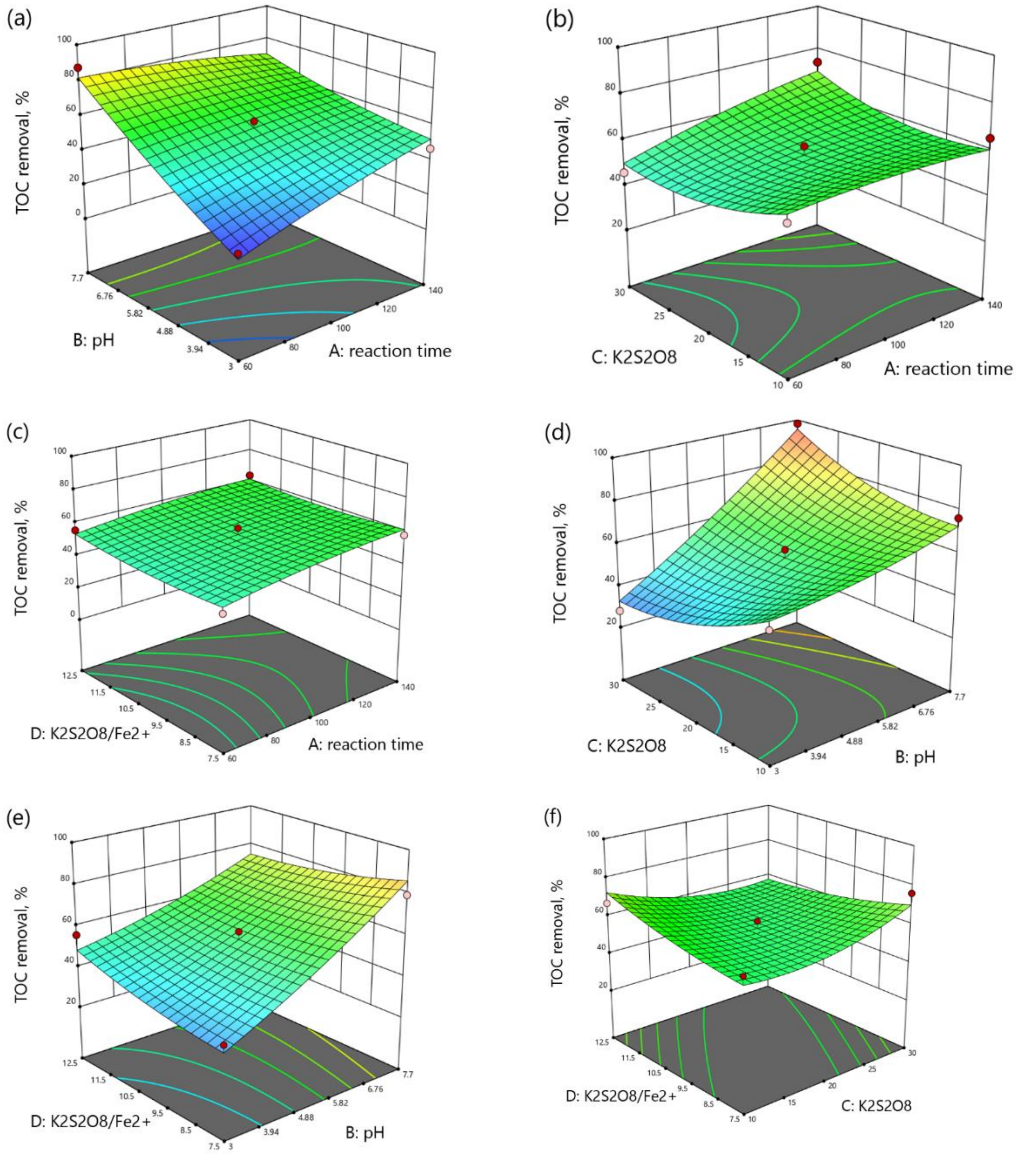

Fig. 7.4. Surface plots for TOC removal model: (a) time and pH, (b) time and $K_2S_2O_8$ content, (c) time and $K_2S_2O_8/Fe^{2+}$, (d) pH and $K_2S_2O_8$ content, (e) pH and $K_2S_2O_8/Fe^{2+}$, (f) $K_2S_2O_8$ content and $K_2S_2O_8/Fe^{2+}$ ratio.

The interplay of time and pH is depicted in Fig. 7.3a. It is clear that the TC removal was marginally reduced by an increase in reaction time and pH. Fig. 3b shows that TC removal increased from 56.3% to 71.3% at 30 mM $K_2S_2O_8$ and dropped from 57.4% to 51.5% with time at concentration of $K_2S_2O_8$ at 10 mM. Fig. 7.3c displays a comparable pattern, where the removal of TC increased at high molar ratios and reduced at low molar ratios with time. Fig. 7.3d illustrates how pH and $K_2S_2O_8$ interact. When $K_2S_2O_8$ concentration was increased at an acidic pH, TC removal decreased from 68.4% to 50.8%, but when it was increased at a neutral pH, TC removal increased from 39.9% to 60.8%. The connection between pH and molar ratio is shown in Fig. 7.3e, where TC removal reduced with an increase in pH. The interplay of oxidant dose and ratio of the oxidant to the Fe^{2+} on TC elimination is shown in

Fig. 7.3f. At low molar ratios, TC removal enhanced with the $K_2S_2O_8$ rise; at high molar ratios, it declined.

Fig. 7.4a shows that TOC removal in acidic conditions improved with reaction duration and reduced at neutral pH. Fig. 7.4b depicts the gradual rise in TOC removal with time at low ranges (57% to 65%), as well as the abrupt increase from 46% at 60 minutes to 74% at 140 minutes and 30 mM $K_2S_2O_8$. The effects of the time and the $K_2S_2O_8/Fe^{2+}$ on TOC removal are depicted in Fig. 7.4c. In any range, the TOC removal got greater with time and molar ratio increase.

The relationship between pH and oxidant dose is depicted in Fig. 7.4d. In actuality, the TOC removal at any range was improved by the pH rise. The increase in oxidant concentration decreased the TOC removal from 53% to 28% at acidic pH and from 76% to 98% at neutral pH. According to Fig. 4e, the molar ratio of $K_2S_2O_8/Fe^{2+}$ had less of an impact on TOC removal than pH did. The TOC removal increased with pH increment from 37% to 79%, but it decreased with molar ratio increase from 79% to 72% at a neutral pH.

The effect of $K_2S_2O_8$ amount and $K_2S_2O_8/Fe^{2+}$ ratio on TOC removal is shown in Fig. 7.4f. At a concentration of 10 mM $K_2S_2O_8$, the increment in $K_2S_2O_8/Fe^{2+}$ enhanced the removal of TOC from 61% to 67%. On the other hand, the TOC removal was reduced from 76% to 54% by the molar ratio increase at 30 mM of $K_2S_2O_8$.

7.6. The effect of the parameters involved in the photo-Fenton-like oxidation.

Reaction time had a varied impact on TC, TOC, and TN elimination. The rise in reaction time improved the elimination of TOC as seen in Fig. 7.4. This is due to the fact that it takes time for organic substances to fully oxidize. After that, at 106 min, the removal of TOC started to decline. On the other hand, TC removal declined as reaction time rose.

In this study, the maximum TC and TN removal rates were obtained at a pH of 5.35 and 100% TOC removal at a pH of 7.7, respectively. Persulfates lower the pH throughout the reaction and are less reliant on pH adjustment. Due to the enhanced solubility, this generates the ideal operating conditions for Fe^{2+} [9].

The $K_2S_2O_8$ amount and $K_2S_2O_8/Fe^{2+}$ ratio substantially influenced TC and TOC elimination, according to the ANOVA findings. Fig. 7.4f illustrates how increasing the $K_2S_2O_8$ concentration reduced the TC removal from 55% to 44% and from 46.1% to 46% at different molar ratios. Thus, 10 mM $K_2S_2O_8$ and a 12.5 $K_2S_2O_8/Fe^{2+}$ ratio were the ideal ratios for removing TC.

At a low molar ratio, TOC elimination increased with the rise in oxidant dosage from 61% to 76.1%, while at a high molar ratio, it declined from 66.9% to 54%. The ideal $K_2S_2O_8$

concentration for TOC removal was 30 mM, and a molar ratio of 7.5 was used. This was probably brought on by too many iron ions consuming sulfate radicals, which led to the creation of ferric iron and sulfate ions (Eq. 7.7) [9].

$$SO_4^{\bullet -} + Fe^{2+} \rightarrow SO_4^{2-} + Fe^{3+} \quad (7.7)$$

7.7. Optimization and Validation

At the next stage, the RSM was used to predict the optimal removal conditions (Table 7.3).

Table 7.3. RSM-calculated ideal conditions and experimental confirmation for the wastewater treatment.

Target	Time, min	pH	$K_2S_2O_8$, mM	Molar ratio $K_2S_2O_8/Fe^{2+}$	Removal, %		Error
					Actual	Predicted	
TC	60	3	10	12.5	52.78	84.24	31.46
TOC	106.06	7.7	30	7.5	100	100	0
TN	97.98	4.33	15.05	12.5	56.29	63.87	7.58

The optimal removal conditions were determined using the RSM. The optimal conditions for 100% TOC removal, according to RSM, were a pH of 7.7, a time of 106 min, a oxidant concentration of 30 mM, and a $K_2S_2O_8/Fe^{2+}$ ratio of 7.5. These parameters were employed for the trials, and Table 7.3 demonstrates that there is high agreement between the actual and anticipated data for TOC removal. On the contrary hand, RSM miscalculated the ideal circumstances for the elimination of TC and TN. This is due to the models for TC and TOC not fitting the experimental data, where the R^2-coefficients were less than 0.8.

Ion chromatography was used to determine the amounts of formic and acetic acids. Equations (7.8) and (7.9) were used to calculate the intermediate and the mineralized organic carbon following the photochemical treatment:

$$OC_{\text{intermediates}} = \text{final}(TOC - TOC_{\text{formic acid}} - TOC_{\text{acetic acid}}) \quad (7.8)$$

$$OC_{CO_2} = \text{initial}TOC - \text{final}TOC \quad (7.9)$$

The results of the quantification of the intermediates are summarized in Table S 7.4. Complete mineralization was achieved in experiments using RSM optimization. Furthermore, it is clear that the only acetic acid was present in the organic carbon after run #17 (pH 7.7, 60 min, 20 mM $K_2S_2O_8$, and $K_2S_2O_8/Fe^{2+}$ of 10). Even though run 17 did not result in complete TOC mineralization, the time and resource economies may benefit from these circumstances.

Similarly, UV/$K_2S_2O_8$/ZVI was utilized to treat synthetic and real municipal wastewater using the continuous flow photochemical reactor. Table 7.4 displays the anticipated ideal experimental settings for TOC elimination.

Table 7.4. RSM optimal conditions and experimental verification for UV/$K_2S_2O_8$/ZVI process.

Municipal wastewater	Space time, min	PS, mM	PS/ZVI molar ratio	Removal, %			Error
				TOC		CBZ	
				Actual	Predicted	Actual	
Synthetic	60	60	15	71.14	65	100	6.14
Real	50	50	15	60.48	65	100	4.52

For TOC removal, RSM predicted the following process variables: a space time of 60 min; a PS content of 60 mM; and a PS/ZVI ratio of 15. The model projected a 65% TOC reduction for the synthetic municipal wastewater under these processing parameters. In actuality, a removal of TOC of 71.14% was accomplished. Next, using the RSM-derived parameters, real wastewater was treated. By comparing them to the TOC of the real wastewater, the space time and PS concentration parameters for the effective treatment of the synthetic wastewater were recomputed. The following parameters were attained: a PS content of 60 mM, a PS to ZVI molar ratio of 15, and a space time of 60 min. The PS/ZVI ratio remained consistent since it was PS concentration-dependent. When compared to the synthetic municipal wastewater, 60.48% less TOC was removed under these parameters. The fact that real wastewater has a higher concentration of radical scavengers (TIC of 77.8 mg/L) than model wastewater (TIC of 32.8 mg/L), which might reduce process efficiency, could be the cause for this drop in TOC removal. Under these conditions, CBZ was entirely eliminated from both synthetic and real wastewater.

7.8. Summary of the chapter

Response surface methodology has been used to optimize the wastewater treatment process. The RSM found that the optimal parameters for the complete mineralization of TOC in a batch photochemical reactor were a time of 106 min, a pH of 7.7, a $K_2S_2O_8$ dosage of 30 mM, and a $K_2S_2O_8$ to Fe^{2+} ratio of 7.5. However, the RSM model miscalculated the optimum parameters for TC and TN elimination. The highest removal of TC (71.3%) has been observed at $K_2S_2O_8$ dosage of 30 mM and $K_2S_2O_8$ to Fe^{2+} ratio of 10 at pH 5.35 after 140 min. In case of TN, the highest TN elimination was obtained at $K_2S_2O_8$ dosage of 10 mM and $K_2S_2O_8$ to Fe^{2+} ratio of 12.5 at pH 5.35 after 100 min. Using ANOVA, the crucial

elements of the photochemical process have been determined. All relevant factors and interactions between time, pH, and $K_2S_2O_8$ had an impact on TOC removal. These results were published in *Catalysts* in publication titled “Photo-Fenton-like treatment of municipal wastewater”.

The application of continuous flow UV/$K_2S_2O_8$/ZVI process was conducted for synthetic and real municipal wastewater for the first time. The study utilized RSM to examine the effects of various process factors, including space time, K_2S_2O8 concentration, and $K_2S_2O_8$/ZVI molar ratio, on the reduction of TOC. Synthetic municipal wastewater was initially used for the experiments, and a model was created using RSM based on the collected data. Carbamazepine was also added to both synthetic and actual municipal wastewater to observe its fate during treatment with the UV/$K_2S_2O_8$/ZVI system. The results showed that in synthetic wastewater, a 71% reduction in TOC and complete elimination of carbamazepine were achieved. In actual municipal wastewater, a space time of 50 minutes, a $K_2S_2O_8$ concentration of 50 mM, and a $K_2S_2O_8$/ZVI ratio of 15 resulted in a 60% reduction in TOC and complete elimination of carbamazepine. The difference in TOC removal between the two types of wastewaters may be attributed to the complex composition of real wastewater and the presence of radical-reducing agents. These results were published in *Catalysts* in publication titled “UV and zero-valent iron (ZVI) activated continuous flow persulfate oxidation of municipal wastewater”.

CHAPTER 8: PHOTOCHEMICAL TREATMENT OF LANDFILL LEACHATE

8.1. Introduction

The production of landfill leachate, a liquid that results from the decomposition of solid waste, and its infiltration with water to aquatic environment or other exposed-to-environment sites are two of the primary concerns created by urban waste. Dissolved organics and inorganics, heavy metals, and ammonia make up the majority of transferred contaminants [169]. Moreover, it has been documented that the wastewaters contain emerging contaminants such sulfamethoxazole [59].

Ecosystems are put in danger when landfill leachate is released into the environment untreated [169]. The COD of an actual landfill leachate might vary between 100 mg/L for a more than ten-year-old leachate to over 70000 mg/L for a young leachate according to the literature [257]. Old dumpsites (Marseille, France) have a TN content of 5 mg/L, but new landfill sites (Jiangsu, China) have a TN content of 13000 mg/L [257]. For aquatic species and microbes involved in biological wastewater treatment, NH3-N concentrations more than 100 mg/L have been observed to be hazardous [258]. Upon reaching biological treatment centers, the actual landfill leachate must get appropriate pretreatment.

Sulfate radical-based AOPs (SR-AOPs), which may break down organic compounds in landfill leachate by using active species like sulfate ($SO_4^{\bullet-}$) and hydroxyl ($HO^{\bullet}$) radicals, have recently attracted a lot of attention [7,8]. Sulfate radicals are produced by persulfate (PS) and peroxomonosulfate (PMS). Given their reliability, affordability, and comparatively low reaction conditions, PS and PMS are often favored over H_2O_2 [7,8]. Sulfate radical has a typical redox potential between 2.5 and 3.1 V [142].

Ishak et al. examined the two SR-AOPs while treating pre-treated leachate under the identical circumstances and found that PS and PMS under UV light, respectively, removed 63.0% and 60.4% of COD from the sample [259]. Heat, ultrasonic (US), microwaves, UV rays, pH, or transition metals can all be used to initiate sulfate radical production [160]. Because to its accessibility and thermodynamic stability, goethite was also used to activate PS [9]. Eq-s 8.1, 8.2, and 8.3 [160] depict the processes that happen in the photo-Fenton-like oxidation:

$$S_2O_8^{2-} \xrightarrow{hv} 2SO_4^{\bullet-} \tag{8.1}$$

$$Fe^{3+} + H_2O \xrightarrow{hv} Fe^{2+} + HO^{\bullet} + H^{+} \tag{8.2}$$

$$S_2O_8^{2-} + Fe^{2+} \xrightarrow{hv} SO_4^{\bullet-} + SO_4^{2-} + Fe^{3+} \tag{8.3}$$

Goethite is also reported to be the most thermodynamically stable iron oxide mineral. Because of its large surface area and abundance in nature, goethite is seen to be a potential

substitute for present persulfate activators [260]. The continued development of affordable, environmentally acceptable technology for the leachate and wastewater treatment can be made feasible by the cheap price of goethite.

8.2. Focus of the chapter

In this investigation, UV light, PS, and goethite are used to remediate both synthetic and actual landfill leachate. The sulfonamide antibiotic sulfamethoxazole was spiked into the landfill leachates. Sulfamethoxazole has previously been detected in landfill leachate and municipal wastewater [261]. In this study, it was employed as the target emerging pollutant to examine its fate after the application of the photo-Fenton-like oxidation to treat a landfill leachate. Using the RSM together with the Plackett-Burman and Box-Behnken designs, evaluation and improvement of the photochemical treatment was carried out. There are currently no published works utilizing UV and goethite to remediate landfill leachate and activate PS.

8.3. Characterization of the catalyst

XRD, nitrogen porosimetry, and SEM-EDS were used to characterize the structural properties of goethite (Fig. 8.1). The goethite XRD spectrum is shown in Fig. 8.1a, along with the acquired diffraction peaks that match those mentioned in the literature (JCPDS No. 29-0713). Strong intensity and a small half-peak breadth on the diffraction peaks demonstrated the stability of the crystal structure. The XRD investigation revealed no additional phases.

The adsorption-desorption isotherm of goethite, which is shown in Fig. 8.1b, may be categorized as a type IV with H3 hysteresis loops. This suggests the presence of mesoporous materials [262]. The detailed results of the nitrogen porosimeter is presented in Table S 8.1. The BET surface area (S_{BET}) was 11.4 m^2/g. The pore volume was determined to be 0.044 cm^3/g. The material's ability for catalysis increases as surface area increases because more active surfaces are exposed. In the literature, goethite's S_{BET} varies; for instance, Ding et al. (2020) employed goethite with a specific surface area of 68.2 m^2/g to activate PS in the breakdown of bisphenol A [262]. Goethite was produced by Hadi et al. (2020) by modifying iron (II) sulfate heprahydrate. The goethite that was created had a 3.49 m^2/g specific surface area and was employed in a heterogeneous Fenton-like system for the breakdown of 4-chlorophenol [263].

In Fig. 8.1c–d, the SEM–EDS evaluation is displayed. Goethite was made up of needle-shaped particles with sizes ranging from 50 nm to 500 nm in width and 200 nm to 1.5 m in length. EDS was used to calculate the elemental analysis of goethite.

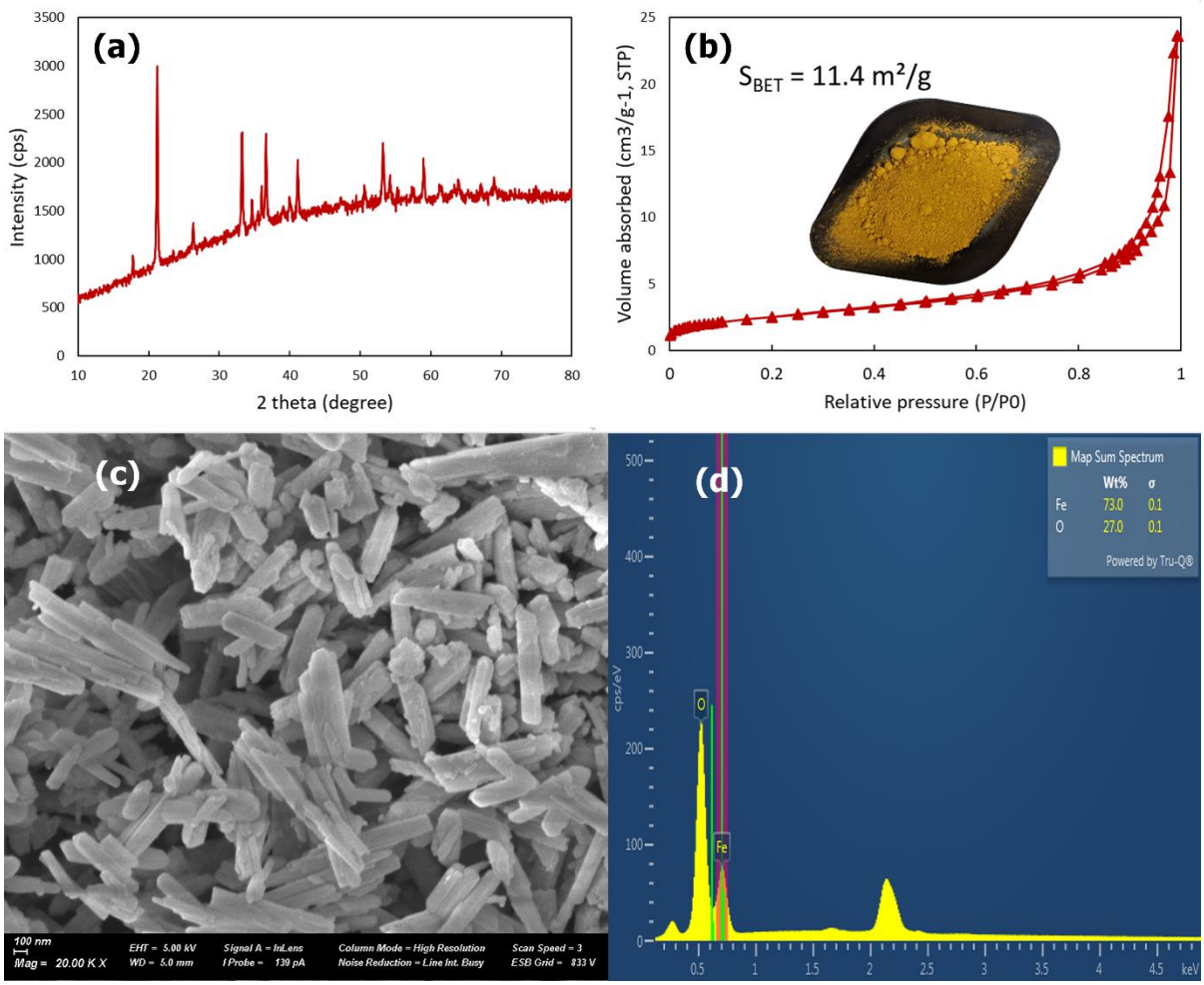

Fig. 8.1. Goethite characterization: a) X-ray diffraction; b) Nitrogen porosimetry; c) SEM; d) EDS.

The distribution of goethite's particle size followed a unimodal curve (Fig. S8.1). 10% of the goethite particles are 0.39 µm in size or smaller, 90% of the particles had a diameter less than 3.47 µm. The median size of goethite particles is 1.06 µm. While the volume average diameter was discovered to be 1.68 µm, the Sauter mean diameter was determined to be 0.83 µm.

8.4. Plackett-Burman design (PBD)

In the preliminary experiment, the elimination of TOC and sulfamethoxazole (SMX) in the synthetic landfill leachate samples upon exposure to UV radiation served as a measure of the efficiency of the treatment. To determine the experimental range for the factorial experiments, four synthetic landfill leachate experiments were conducted with PS

concentrations from 50 to 750 mM prior to the design experiments. The outcomes were included in the supporting information as Fig. S8.2. This graph shows that the TOC removal increased as the PS concentration was raised from 50 mM to 450 mM, but did not rise further when the PS concentration was raised to 750 mM.

PBD is utilized to filter the processes' influencing components. Also, this design offers details on potential ideal experimental circumstances. The PBD experimental matrix and the experiment's findings are displayed in Table 8.1. 95% two sided confidence intervals were presented in Table S8.2.

Table 8.1. Screening experiments with PBD.

Run	Experimental variables				Removals, %				pH	
	PS (mM)	Time (h)	Goethite (g/L)	UV light	Real		Expected			
					TOC	SMX	TOC	SMX	Starting	Final
	X_1	X_2	X_3	X_4						
1	450	3	0.5	Off	0.36	100	5.82	91.76	5.80	5.65
2	450	3	0.5	On	63.1	100	43.12	100	6.00	1.64
3	150	3	2.5	On	43.73	100	41.87	98.15	5.90	3.87
4	150	1	0.5	On	32.39	100	32.96	100	6.14	2.09
5	150	1	2.5	Off	1.95	89.67	0	88.56	6.00	5.62
6	450	1	0.5	On	20.5	100	33.95	100	5.90	5.70
7	150	3	0.5	Off	0	100	4.83	94.64	5.72	5.69
8	450	1	2.5	On	33.21	100	33.69	95.52	6.14	2.09
9	150	1	0.5	Off	0	89.45	0	94.89	5.88	5.73
10	150	3	2.5	On	34.52	100	41.87	98.15	5.72	4.72
11	450	1	2.5	Off	0	92.1	0	85.68	5.90	5.73
12	450	3	2.5	Off	1.36	69.73	5.56	85.43	5.88	4.72

Eq. 8.4 present the PBD model (in coded units) for TOC removal that was acquired from Design-Expert software:

$$\text{TOC removal (\%)} = 19.26 + 0.495*X_1 + 4.585*X_2 - 0.132*X_3 + 18.648*X_4 \quad (8.4)$$

where X_1, X_2, X_3, and X_4 stand for, respectively, reaction time, PS content, goethite dosage, and UV switch (On/Off). Confidence intervals for the screening model coefficients were provided in Table S8.3.

ANOVA was used to evaluate how suitable the models were. Significant metrics, including regression coefficients (R^2), F- and p-values, were identified throughout this analysis. The outcomes of the ANOVA are reported in Table 8.2.

Table 8.2. ANOVA test for the different PBD models.

Response	Source	Sum of squares	Degrees of freedom	Mean square	F-value	P-value
TOC removal	Model	4428.54	4	1107.13	9.89	0.0052
	Residual	783.69	7	111.96		
	Lack of fit	741.28	6	123.55	2.91	0.4207
	Pure error	42.41	1	42.41		
	Adequate precision = 6.9869					
SMX degradation	Model	435.69	4	108.92	1.62	0.2705
	Residual	470.43	7	67.20		
	Lack of fit	470.43	6	78.40		
	Pure error	0.0000	1	0.0000		
	Adequate precision = 3.6466					

Regression coefficient values around one demonstrate the strong model validity. The elimination of TOC and sulfamethoxazole had R^2 values of 0.8496 and 0.4808, respectively. An F-value of 9.89 and a p-value of 0.0052 were determined to the TOC removal model. Models and model terms are regarded as “trusted” when the p-value <0.05, whereas models with p-values >0.05 are regarded as non-significant [22]. As a result, the synthetic landfill leachate treatment might be optimized further using the PBD model of TOC removal.

Sulfamethoxazole degradation model's p-value, on the other hand, was 0.2705. Moreover, pred-negative R^2's value suggested that the aggregate mean of the answers could be able to provide predictions that were more accurate than that model. The sulfamethoxazole degradation could not, therefore, be further optimized using the model.

Fig. S8.3 indicates a strong connection between the actual and anticipated values. Fig. S8.4 shows the normal probability vs residuals for TOC removal where a straight-line trend can be seen that the normal probability distribution is followed by the PBD model for TOC removal.

The contour plots were generated to illustrate the findings of the Plackett-Burman design (Fig. S8.5). It is clear that under "dark" conditions (without UV), sulfamethoxazole virtually completely degraded. Dark trials did not, however, result in a considerable elimination of TOC. At best, just 2% of TOC was eliminated in the absence of light after 1 hour with PS of 150 mM and goethite of 2.5 g/L. According to these findings, goethite was unable to activate PS and cause the production of sulfate radicals. The conversion of Fe^{3+} into Fe^{2+} required an

extra chemical or energy source, which sped up the production of sulfate radicals [231]. UVA is hence a crucial factor that is required for the oxidation of TOC.

With regard to other variables, it is evident that the TOC removal increased as the PS concentration and reaction duration rose. In contrast, the rise in goethite content resulted in decreased TOC removals, which, in accordance with Eq. 8.5, might be explained by the extra Fe^{2+} consuming sulfate radicals [264]:

$$SO_4^{\bullet-} + Fe^{2+} \rightarrow SO_4^{2-} + Fe^{3+} \quad (8.5)$$

The color of the goethite solution may also be the cause of this. The solution became more turbid as the goethite concentration rose. The procedure became less successful as a result of the reduction of UVA radiation delivery.

Overall, it was determined to conduct the trials under UVA with an extended irradiation time, raise the PS concentration, and lower the goethite dosage.

8.5. Box-Behnken design (BBD) with RSM

Table 8.3 displays 15 studies' BBD settings, including various factors, actual response values, and expected response values. 95% two sided confidence intervals were presented in Table S8.4.

Table 8.3. The synthetic landfill leachate treatment experiments using BBD

Run	Experimental variables			Removals, %				pH	
	PS (mM)	Time (h)	Goethite (g/L)	Real		Expected			
				TOC	SMX	TOC	SMX	Starting	Final
	X_1	X_2	X_3						
1	200	3	1	50.39	100	51.70	98.33	6.08	3.23
2	400	9	0.5	68.60	100	67.95	99.17	6.37	1.47
3	200	6	1.5	56.41	100	54.46	100	6.16	1.79
4	200	6	0.5	62.78	100	61.93	100	6.51	1.78
5	600	6	1.5	70.64	100	71.49	99.17	6.85	1.51
6	200	9	1	47.69	100	49.18	100	5.87	1.70
7	400	3	1.5	53.99	100	54.64	100	6.12	2.75
8	600	9	1	75.87	93.33	74.56	95.00	5.99	1.31
9	600	6	0.5	67.85	100	69.80	99.17	5.93	1.51
10	400	3	0.5	72.97	100	72.51	100	5.95	1.62
11	400	9	1.5	79.57	100	80.03	99.17	5.87	1.51
12	400	6	1	78.39	100	75.79	100	6.07	2.75
13	600	3	1	52.70	100	51.21	100	6.07	2.75
14	400	6	1	71.97	100	75.79	100	5.97	1.56
15	400	6	1	77.01	100	75.79	100	5.78	1.52

Figs. 8.2 and 8.3 illustrate how accurately the BBD models predicted TOC removal. As shown in Fig. 8.2, the BBD model for TOC elimination matched the normal probability distribution. The BBD model's calculated values also clearly match the experimentally measured values, as shown by Fig. 8.3. The BBD model for sulfamethoxazole degradation was inadequately created because almost all runs led to the complete destruction of the pollutant.

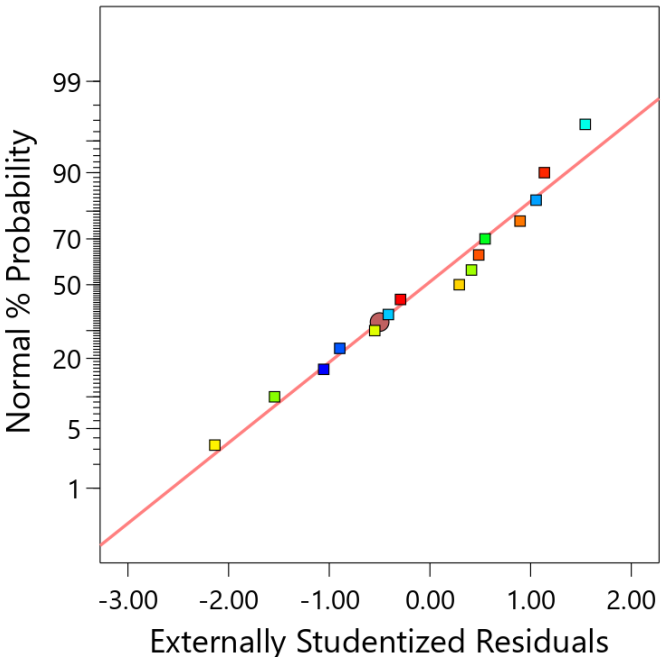

Fig. 8.2. Normal probability plot of the residuals for TOC removal.

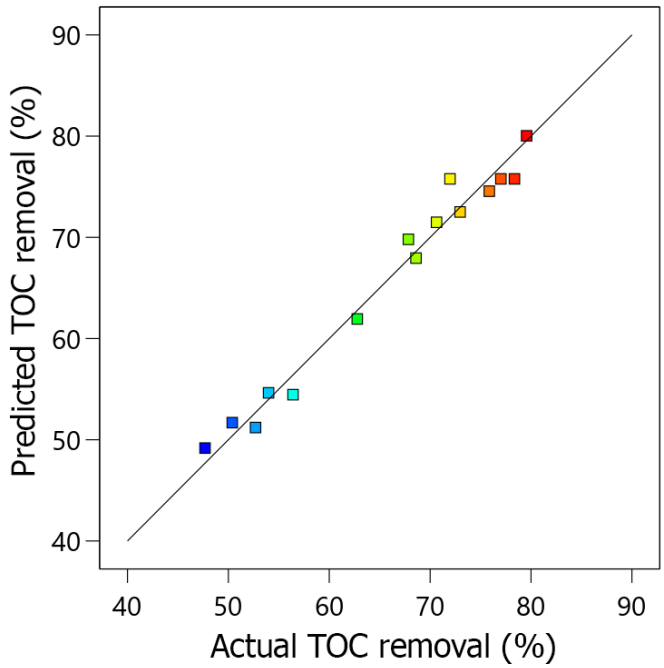

Fig. 8.3. Actual vs predicted plot for TOC removal.

ANOVA, results of which is shown in Table 8.4, was used to evaluate the BBD model's quality of fit.

Table 8.4. ANOVA test for the different BBD models.

Response	Source	Sum of squares	Degrees of freedom	Mean square	F-value	P-value
TOC removal	Model	1632.34	9	181.37	22.19	0.0016
	Residual	40.86	5	8.17		
	Lack of fit	18.17	3	6.06	0.5341	0.7034
	Pure error	22.69	2	11.34		
	Adequate precision = 13.2173					
SMX degradation	Model	30.40	9	3.38	1.52	0.336
	Residual	11.12	5	2.22		
	Lack of fit	11.12	3	3.71		
	Pure error	0.00	2	0.00		
	Adequate precision = 4.7926					

X_2, X_1, X_2X_1, X_2X_3, X_2^2, and X_1^2 are significant model variables in the ANOVA for the response surface model. The regression coefficient for TOC removal model was 0.9755, indicating a good approximation. Furthermore, the F-value of 22.13 and the p-value of 0.0016 suggested that the model was significant. The lack of fit of the model with a p-value of 0.7049 was not significant. Nevertheless, because the p-value for the sulfamethoxazole degradation BBD model was more than 0.05, it was not significant.

Eq. 8.6 show the BBD models (in coded units) for TOC removal produced using the Design-Expert program.

$$\text{TOC removal (\%)} = 75.789 + 6.224*X_1 + 5.21*X_2 + 6.467*X_1X_2 + 7.488*X_2X_3 - 11.744*X_1^2 - 7.382*X_2^2 \quad (8.6)$$

where X_1, X_2, and X_3 stand for, respectively, PS content, time and goethite dosage.

To illustrate the important variables and their interactions in the BBD model for TOC removal, a Pareto graph was created (Fig. S8.6). According to this graph, important model parameters are X_1, X_2, X_1X_2, X_2X_3, X_1^2, and X_2^2. Confidence intervals for the BBD model coefficients were provided in Table S8.5. Overall, the landfill leachate treatment was properly represented by the model for TOC removal, which was then utilized to further optimize the method.

8.6. 3D plots for the BBD-RSM model

Due to the non-significant results of the BBD model for sulfamethoxazole degradation, only the TOC removal surface plots are shown in Fig. 8.4.

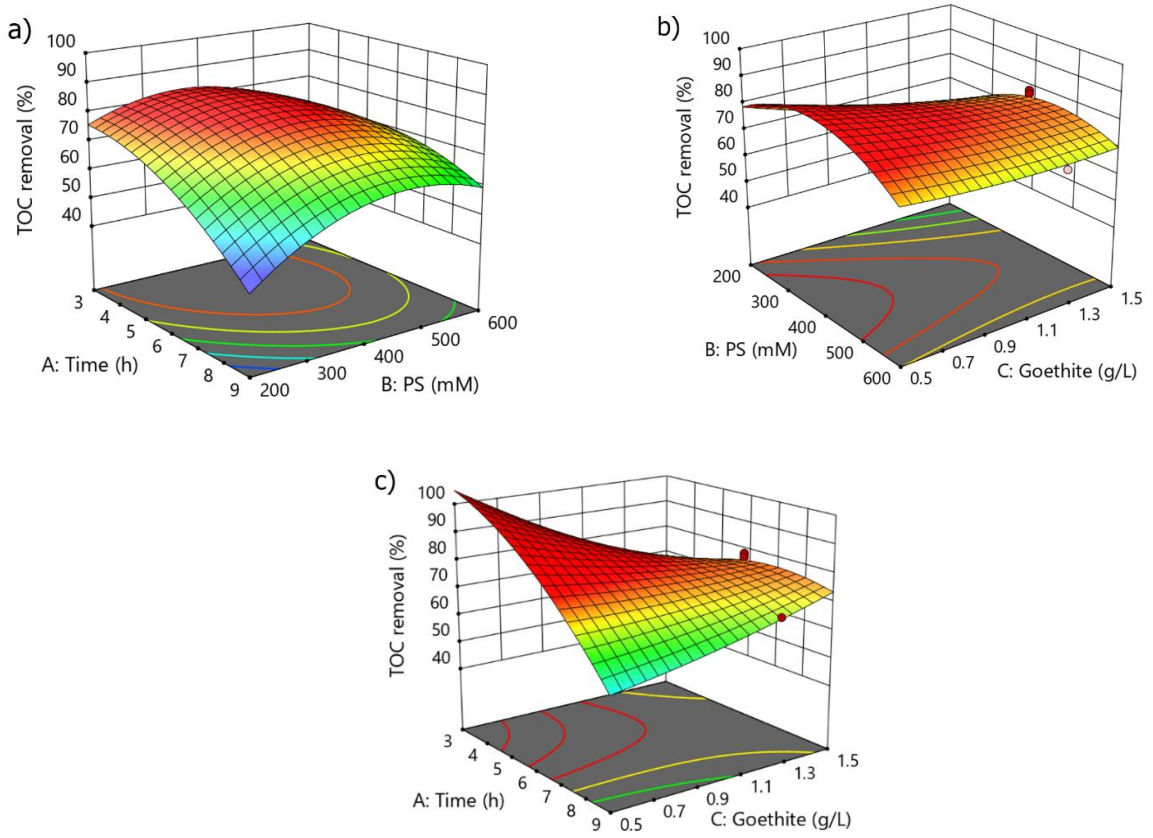

Fig. 8.4. Surface plots for TOC removal model: (a) time and PS content, (b) PS content and goethite dosage, and (c) time and goethite dosage.

Fig. 8.4a demonstrates that the removal of TOC did not change much with an increase in the amount of time at PS content of 200 mM (around 50%). On the other hand, at PS concentration of 600 mM, the TOC removal rose dramatically with time increasing from 53% to 76%. After 6 hours, the 400 mM PS concentration achieved a better TOC removal (78%) than with the 600 mM PS concentration. This may be explained by the fact that an increase in PS concentration causes the pH to fall even more, favoring the creation of $Fe(H_2O)^{2+}$, which in turn reduces the production of ferrous iron [158].

Moreover, an overabundance of PS may cause the production of PS radicals rather than the weaker sulfate radicals, which would cause the scavenging of sulfate radicals to occur (Eq. 8.7 and 8.8) [263]:

$$SO_4^{\bullet -} + SO_4^{\bullet -} \rightarrow S_2O_8^{2-} \quad (8.7)$$

$$SO_4^{\bullet -} + S_2O_8^{2-} \rightarrow SO_4^{2-} + S_2O_8^{\bullet -} \quad (8.8)$$

The correlation between goethite dosage and PS contents is seen in Fig. 8.4b. The improvement in TOC removal caused by the increase in PS concentration was from 56% to 70% and from 63% to 68% for goethite dosages of 0.5 g/L and 1.5 g/L, respectively.

The effects of time and goethite content are depicted in Fig. 8.4c. The TOC removal was enhanced from 54% to 80% as the period extended from 3 to 9 hours at a goethite dosage of 1.5 g/L. On the other hand, the removal of TOC was reduced with an increment in time at goethite dosage of 0.5 g/L, going from 73% to 68.6%. With PS and goethite dosages of 400 mM and 1.5 g/L, respectively, the maximum removal of TOC (79.6%) was obtained after 9 hours.

High amounts of sodium, potassium, magnesium, calcium, chlorine, and sulfate ions were found in the actual landfill leachate, according to an IC study. Several of these ions' scavenging properties have been documented in the past. For instance, calcium interacts with hydroxyl radicals and might lower the process's effectiveness [265]. According to Van et al., adding chlorine ions to the H_2O_2/Fe^{2+} treatment caused the elimination of paracetamol to drop from 49% to 38% [266]. Halide ions like chlorine and bromine may also generate hazardous oxyanions like chlorates and bromate in addition to scavenging hydroxyl and sulfate radicals [7].

Heavy metals' Fe level was found to be 7.57 mg/L, which remains inadequate for high-strength wastewater to undergo Fenton oxidation [265]. The other examined heavy metals were all found at values lower than 1 mg/L with the exception of Zn (4.75 mg/L).

8.7. Experiments on optimization and air stripping

The photo-Fenton-like oxidation of the synthetic landfill leachate and actual landfill leachate was statistically optimized using RSM. Table 8.5 displays the outcomes of the optimization tests.

Table 8.5. Optimum experimental conditions derived from the RSM model.

Run	Landfill leachate	Experiments	TOC removal (%)			SMX degradation (%)	COD removal (%)
			Real	Expected	Δ		
1	Synthetic	477.4 mM PS, 755 mg/L Goethite under UV for 5.33 h	81.79	84.38	-2.59	100	89.12
2	Actual	419.3 mM PS, 663 mg/L Goethite under UV for 4.68 h	86.96	84.38	2.58	100	91.16

Based on the model, it was expected that under the circumstances 84.38% elimination of TOC would be accomplished, as seen in Fig. 8.5. The actual TOC elimination was 81.79%, or almost exactly what the model predicted it would be.

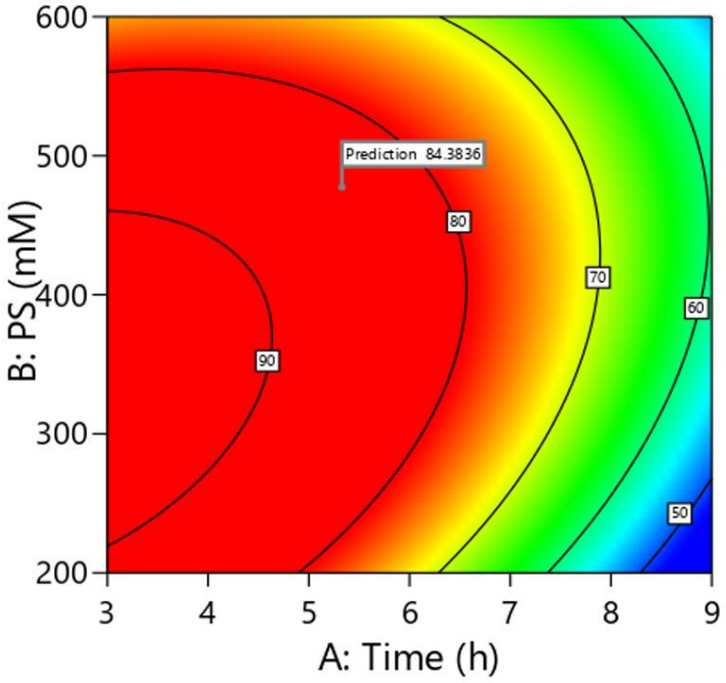

Fig. 8.5. The optimum area for the synthetic landfill leachate treatment.

The correctness of the model was then checked using the actual landfill leachate. This is a vital stage because it determines if actual leachate can be successfully treated using the outcomes and circumstances found while treating the synthetic landfill leachate. By connecting the parameter values to TOC, the PS and goethite contents were recomputed for this purpose as 419.3 mM and 663 mg/L, respectively. In the instance of the actual landfill leachate, 86.96% elimination of TOC and complete degradation of sulfamethoxazole were attained, as shown in Table 10. The choice of sulfamethoxazole as a model of emerging contaminants in this work showed that, given the ideal conditions predicted by RSM, additional antibiotics with a similar structure may also be totally eliminated.

Another crucial element in the treatment of wastewater is the COD/TOC ratio, which can reveal further details on the decomposition of contaminants. The presence of molecules with complicated structures is indicated by a significant COD to TOC ratio [97]. In contrast to aromatic alcohols like benzyl alcohol, which possess a COD/TOC ratio of 3.54 [97,267], formic acid and acetic acid have COD/TOC ratios of 1.30 and 2.67, respectively. According to Ziyang et al.'s study of actual landfill leachates from China, the COD/TOC ratios for fresh landfill leachate (2 to 4 years) ranged from 1.83 to 2.50, for landfill leachate at a transitionary period (5 to 7 years), from 2.42 to 5.92, and for old landfill leachate (8 years or above) ranged from 2.57 to 10 [268]. For landfill leachate samples with young (under 5 years), medium (between 5 and 10 years), and mature (over 10 years) ages, COD to TOC ratios of 2.3, 3.3, and 1.6, respectively, were reported [269]. Volatile fatty acids were found

in large concentrations in the medium landfill leachate but not in the mature landfill leachate [269]. Humic compounds including humic acids and fulvic acids are also present in the organic portion of landfill leachates [270].

The COD to TOC ratio of the actual landfill leachate in this investigation started off at 3.56 and then dropped to 1.96; the latter figure is typical for short-chain carboxylic acids. This change demonstrated the breakdown of complex chemicals found in the actual landfill leachate into simpler molecules. As seen in Fig. S8.7, during the photodegradation of the actual landfill leachate, pH dropped from 6 to 1.84 at the conclusion of the experiment. In general, the photochemical elimination of humic compounds is favored by the low pH [271]. For instance, Jiang et al. [271] used an Electro/UV/ZVI/PS process at pH 3 to virtually completely remove fulvic and humic acids from the landfill leachate.

The current study employed goethite and UVA irradiation to create reactive sulfate radicals. Several SR-AOPs have so far been used in the literature for the landfill leachate treatment. For instance, Yang et al. treated old landfill leachate with a TOC of 1433 mg/L using a US/PS system and obtained 77.3% TOC elimination following 147.6 min [272]. When Antony et al. treated the stabilized landfill leachate with a Al^0 mixed with PS and H_2O_2, they were able to remove 83.5% of the TOC at pH 1.5 after 20 minutes [273]. Nevertheless, a large quantity of the Al was needed, which is far more costly than Fe catalysts.

In a different study, iron containing (72%) converter sludge from the steel plant was employed to activate PS, and after 60 minutes, 48% of COD was removed at pH 2 [274]. Interestingly, after 24 hours, Kattel and Dulova only removed 30% of COD at pH 3 using ferrous iron as the only activator for PS [275]. In the current study, after an hour without irradiation, just 2% of TOC was eliminated utilizing the PS/Goethite method. Therefore, UV light must be present because it reduces ferric iron to ferrous iron and the latter is responsible for generation of sulfate radicals.

In this study, the application of UV/PS/Goethite for the actual landfill leachate treatment led to the elimination of 91.2% of COD and 87% of TOC. Fig. 8.6 illustrates the proposed process of TOC elimination by the UV/PS/Goethite.

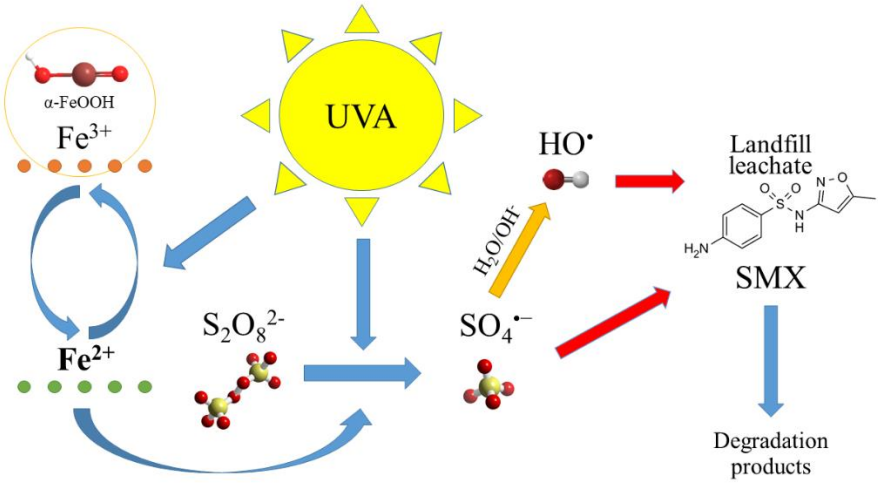

Fig. 8.6. A possible mechanism for the PS activation by goethite and UV during the remediation of landfill leachate.

Fe^{3+} may be converted to Fe^{2+} by UVA radiation, which then interacts with the persulfate ion to create sulfate radicals by direct transfer of electrons [9,231]. Furthermore, persulfate can potentially be activated by UVA. Sulfate radicals formed in aquatic environments create hydroxyl radicals at a circumneutral pH [9]. As a result, sulfate and hydroxyl radicals are used to degrade organic material as part of the landfill leachate treatment process [9,231]. Furthermore, a separate experiment was carried out under ideal circumstances excluding goethite from the process which led to a 52.7% TOC elimination from the actual landfill leachate. This shows how crucial goethite is to the landfill leachate treatment process.

It has been proven in the past that inorganic nitrogen elements like ammonium and nitrate ions are the main cytotoxic chemicals in wastewaters. Moreover, most bacteria will experience irreversible cell damage after being subjected to ammonia nitrogen levels that exceed 500 mg/L over 30 minutes [276]. The actual landfill leachate had a TN of 2300 mg/L and a concentration of ammonium nitrogen of 1644 mg/L. The substantial levels of ammonium nitrogen in this leachate from an actual landfill might also be cytotoxic. The electrochemical process, adsorption, filtering, and air stripping are generally effective methods to successfully remove any remaining ammonium nitrogen from the wastewater [257,277]. The optimum experiment with the actual landfill leachate was thus followed by air stripping at pH 11 to lower the levels of dangerous NH_4-N and volatile organic chemicals (Fig. 8.7). The selection of pH was made in light of the effective removal of ammonia nitrogen from actual landfill leachate in a prior study [277], which investigated the effects of different pH on the elimination of ammonia.

Most nitrogen species occur in ammonium form at pH levels below 8, whereas they usually exist in ammonia form at pH levels above 10, where they may be removed from solutions by air stripping.

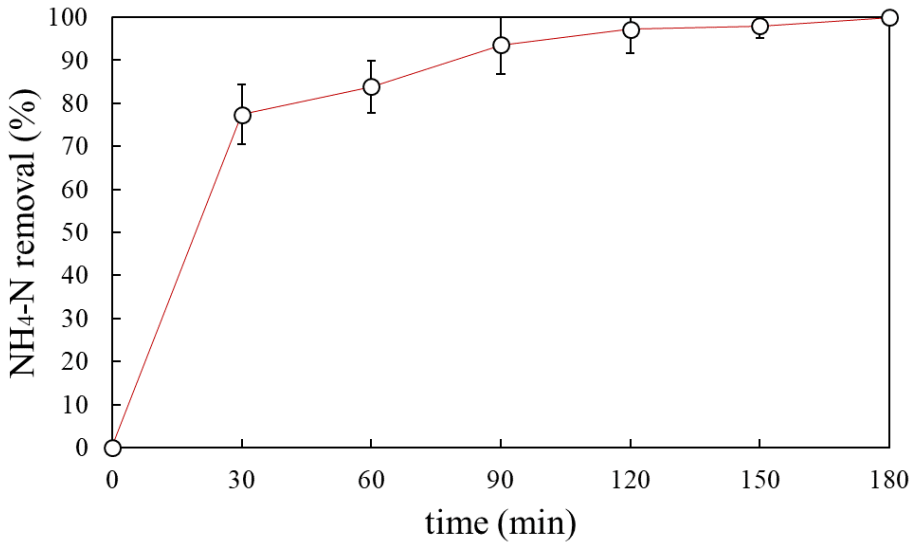

Fig. 8.7. The elimination of ammonium nitrogen from of the actual landfill leachate after the UV/PS/Goethite treatment using air stripping at pH 11 for 3 h.

Over the initial 30 minutes, 77% of NH_4-N was eliminated from the actual landfill leachate effluent after the photochemical treatment, while total elimination was obtained after three hours. In a related investigation, the actual landfill leachate had 94% NH_4-N removal after one day of air stripping at pH 12 [277]. AOPs are often ineffective at removing nitrogen species, and the majority of studies did not mention the elimination of NH_4-N. For instance, a UV/PS/Fe^{2+} system was employed for the photochemical treatment of the landfill leachate and the authors were able to remove 25.6% of NH_3-N and 80.8% of COD [265]. In contrast, Ghanbari et al. reported removing 72% of NH_4^+ and 77.9% of COD after activating PMS with $CuFe_2O_4$ and UV light [278]. It should be emphasized, too, that using Cu^{2+} is less cost-effective than using Fe^{2+} [265].

8.8. Summary of the chapter

In this study, both synthetic and actual landfill leachates underwent photochemical treatment using SR-AOPs. Dark experiments with goethite and PS only removed 2% of TOC after an hour, indicating that the introduction of UV light was necessary for significant decomposition of TOC. In order to achieve significant TOC removal, UV radiation was used in Box-Behnken design studies. ANOVA statistical study revealed that the TOC removal was significantly influenced by the time, PS content, time and PS interaction, and time and goethite concentration interaction.

Using the RSM, the optimal parameters for optimizing the TOC elimination in the instance of synthetic landfill leachate were calculated as following: 477.4 mM PS and 755 mg/L Goethite under UV for 5.33 h. Under these circumstances, the actual TOC, COD, and sulfamethoxazole reductions were 81.8%, 89.1%, and 100%, respectively. Finally, using the TOC of the actual landfill leachate, the optimal process parameters for the photochemical treatment were recomputed. With 419.3 mM PS and 663 mg/L goethite under UV for 4.68 h, the TOC and COD removals, and sulfamethoxazole degradation efficiencies for the actual landfill leachate were 87%, 91.2%, and 100%, respectively. After that, NH_4-N, which presents a significant harm to the environment, was completely eliminated using air stripping for 3 hours at pH 11. The acquired results showed that the UV/PS/Goethite treatment is a prospective method for removing the organic contaminants from the actual landfill leachate, and further study may be focused on examining its effectiveness against highly contaminated wastewater on a larger scale. The study's findings were reported in *Chemical Engineering Journal Advances* in a paper titled “UVA and goethite activated persulfate oxidation of landfill leachate”.

CHAPTER 9: CONCLUSIONS AND FUTURE WORK

The contamination of water resources with harmful organic and inorganic substances is a significant problem that requires efficient treatment methods. In recent years, there has been a growing focus on emerging pollutants, as they have been found to have detrimental effects on the environment. This chapter provides a summary of the findings from the PhD thesis and suggests potential areas for future research.

9.1. Conclusions

The biodegradability and inhibitory properties of three common commercial medications in wastewater effluents has been investigated. The study found that activated sludge treatment was effective in removing caffeine and ibuprofen, but not metronidazole. The presence of these contaminants also affected the removal of TC and TN. The study also showed that the use of advanced oxidation processes ($UV/K_2S_2O_8$) was effective in removing metronidazole from the effluents. However, more research is needed to fully understand the mechanisms of removal. Overall, the study demonstrated that AOPs can be used to treat biological treatment effluents, but the presence of emerging contaminants can hinder the removal of organic matter and nutrients.

Different treatment methods were used to treat synthetic wastewater with and without emerging contaminants. The SBR showed good removal efficiency for TOC and TN, with no significant impact from the emerging contaminants (naproxen, bisphenol A and sulfamethoxazole) at a concentration of 3 mg/L. The SBR was also able to partially remove some emerging contaminants, with bisphenol A showing the highest removal rate. Membrane filtration methods were also effective in removing emerging contaminants, with the 10 nm track-etch membrane showing the highest removal rate for bisphenol A. All membranes showed some degree of pore blockage and reduced water flux. AOPs were used after SBR and membrane filtration. The use of $UV/K_2S_2O_8$/ZVI for the membrane filtration effluents resulted in complete degradation of BPA, NPX, and SMX within 30 minutes. Overall, the combination of SBR, membrane filtration, and AOPs proved to be effective in removing both organic matter and emerging contaminants from wastewater.

The treatment of poultry slaughterhouse wastewater using different photochemical methods has been studied. The goal was to find the most effective AOPs system for removing organic carbon from the complex wastewater. UV photolysis showed minimal TOC removal, while UV/TiO_2 removed 44% of TOC after 60 minutes. Applying the H_2O_2 concentration of 98 mM in the UV/H_2O_2 system resulted in 74% TOC removal. However, increasing iron concentrations did not improve the effectiveness of the process. The $UV/K_2S_2O_8$ system

showed the highest TOC removal rate of 85% after 150 minutes, with an E_{EO} value of 226 kWh/m^3/order. The effluent quality met legal disposal limits in the US, Australia, and Europe, making it a potential solution for wastewater treatment and recycling.

Response surface methodology to optimize municipal wastewater treatment using the UV/$K_2S_2O_8$/Fe^{2+} process. The optimal parameters for complete mineralization of TOC were determined to be a time of 106 minutes, a pH of 7.7, a $K_2S_2O_8$ dosage of 30 mM, and a $K_2S_2O_8$ to Fe^{2+} ratio of 7.5. However, the RSM model did not accurately calculate the optimum parameters for TC and TN elimination. The highest TC removal (71.3%) was observed at a $K_2S_2O_8$ dosage of 30 mM and $K_2S_2O_8$ to Fe^{2+} ratio of 10 at pH 5.35 after 140 minutes. The highest TN elimination was obtained at a $K_2S_2O_8$ dosage of 10 mM and $K_2S_2O_8$ to Fe^{2+} ratio of 12.5 at pH 5.35 after 100 minutes. Using ANOVA, the crucial elements of the photochemical process were determined to be time, pH, and $K_2S_2O_8$ concentration. The study also utilized RSM to examine the effects of process factors on TOC reduction in a continuous flow UV/$K_2S_2O_8$/ZVI system. Synthetic and real municipal wastewater were used in the experiments, and a model was created based on the collected experimental data. Carbamazepine was added to both types of wastewaters to observe its fate during treatment with the UV/$K_2S_2O_8$/ZVI system. The results showed a 71% reduction in TOC and complete elimination of carbamazepine in synthetic wastewater, and a 60% reduction in TOC and complete elimination of carbamazepine in actual municipal wastewater using specific parameters.

Another study was conducted focusing on the use of photochemical treatment of both synthetic and actual landfill leachates. The addition of UV light was found to be necessary for significant decomposition of TOC, as shown in dark experiments with goethite and persulfate. Using Box-Behnken design studies and ANOVA statistical analysis, the optimal parameters for TOC removal were determined to be a persulfate content of 477.4 mM and goethite concentration of 755 mg/L under UV for 5.33 hours. This resulted in significant reductions in TOC, COD, and sulfamethoxazole levels. Similar results were obtained for actual landfill leachate, with optimal parameters of 419.3 mM persulfate and 663 mg/L goethite under UV for 4.68 hours, resulting in high removal rates for TOC, COD, and sulfamethoxazole. Additionally, air stripping at pH 11 was able to completely eliminate NH_4-N, a harmful contaminant. Overall, the study showed that the UV/PS/goethite treatment is a promising method for removing organic contaminants from landfill leachate, with potential for further examination on a larger scale.

In conclusion, the comprehensive studies carried out in this thesis provide important insights into the treatment of wastewater containing emerging pollutants, the effective approach of

using integrated membrane bioreactor and advanced oxidation processes have been proposed.

9.2. Future work

The study's outcomes present several potential avenues for future research:

- The efficiency of the membrane bioreactor could be enhanced by modifying the surface of the membrane and could be used for selective removal of the emerging pollutants. More research needs to be done with the initial material of the membrane which directly impacts the membrane performance and fouling;
- From the literature survey, it is clear that most of the research were done using model or synthetic solutions omitting the impact from the wastewater matrix. Further exploration and understanding of mechanisms in AOPs with the authentic wastewater need to be conducted. Expansion of research into diverse types of contaminants and their behavior in different treatment processes is needed;
- In the current studies, the activation of persulfate or hydrogen peroxide were conducted with iron-containing materials and UV light. Another interesting option could be using semiconductors doped with transition metals under visible or solar light which may increase the economic attractiveness of the process;
- As the emerging pollutants and their by-products pose environmental and public health risks, they should be completely mineralized to avoid this risk. The use of AOPs for the pre-treatment of the high strength wastewaters to increase their biodegradability and lower their toxicity should be considered;
- In the research, modelling the wastewater treatment process with RSM showed high accuracy in case of AOPs. The same approach could be used for biological treatment and membrane filtration processes.
- Continuous flow UV/$K_2S_2O_8$ process and compliance with legal discharge requirements should be further tested as this process showed high efficiency with the wastewater of complicated matrix in the lab scale. Dynamic RSM could be applied for continuous optimization of the process.

REFERENCES

[1] J. Schleich, T. Hillenbrand, Determinants of residential water demand in Germany, Ecol. Econ. 68 (2009) 1756–1769. https://doi.org/10.1016/j.ecolecon.2008.11.012.

[2] M. Peter-Varbanets, C. Zurbrügg, C. Swartz, W. Pronk, Decentralized systems for potable water and the potential of membrane technology, Water Res. 43 (2009) 245–265. https://doi.org/10.1016/j.watres.2008.10.030.

[3] R. Kumar, M. Qureshi, D.K. Vishwakarma, N. Al-Ansari, A. Kuriqi, A. Elbeltagi, A. Saraswat, A review on emerging water contaminants and the application of sustainable removal technologies, Case Stud. Chem. Environ. Eng. 6 (2022) 100219. https://doi.org/10.1016/j.cscee.2022.100219.

[4] J. Wang, Z. Sun, Effects of different carbon sources on 2,4,6-trichlorophenol degradation in the activated sludge process, Bioprocess Biosyst. Eng. 43 (2020) 2143–2152. https://doi.org/10.1007/s00449-020-02400-x.

[5] M.B. Ahmed, J.L. Zhou, H.H. Ngo, W. Guo, N.S. Thomaidis, J. Xu, Progress in the biological and chemical treatment technologies for emerging contaminant removal from wastewater: A critical review, J. Hazard. Mater. 323 (2017) 274–298. https://doi.org/10.1016/j.jhazmat.2016.04.045.

[6] J. Yang, M. Zhu, D.D. Dionysiou, What is the role of light in persulfate-based advanced oxidation for water treatment?, Water Res. 189 (2021). https://doi.org/10.1016/j.watres.2020.116627.

[7] J. Lee, U. Von Gunten, J.H. Kim, Persulfate-Based Advanced Oxidation: Critical Assessment of Opportunities and Roadblocks, Environ. Sci. Technol. 54 (2020) 3064–3081. https://doi.org/10.1021/acs.est.9b07082.

[8] S. Guerra-Rodríguez, E. Rodríguez, D.N. Singh, J. Rodríguez-Chueca, Assessment of sulfate radical-based advanced oxidation processes for water and wastewater treatment: A review, Water (Switzerland). 10 (2018). https://doi.org/10.3390/w10121828.

[9] B. Kaur, L. Kuntus, P. Tikker, E. Kattel, M. Trapido, N. Dulova, Photo-induced oxidation of ceftriaxone by persulfate in the presence of iron oxides, Sci. Total Environ. 676 (2019) 165–175. https://doi.org/10.1016/j.scitotenv.2019.04.277.

[10] K. Zhi, Z. Li, P. Ma, Y. Tan, Y. Zhou, W. Zhang, J. Zhang, A review of activation persulfate by iron-based catalysts for degrading wastewater, Appl. Sci. 11 (2021). https://doi.org/10.3390/app112311314.

[11] K. Wetchakun, N. Wetchakun, S. Sakulsermsuk, An overview of solar/visible light-driven heterogeneous photocatalysis for water purification: TiO2- and ZnO-based photocatalysts used in suspension photoreactors, J. Ind. Eng. Chem. 71 (2019) 19–49. https://doi.org/10.1016/j.jiec.2018.11.025.

[12] G. Odling, N. Robertson, Bridging the gap between laboratory and application in photocatalytic water purification, Catal. Sci. Technol. 9 (2019) 533–545. https://doi.org/10.1039/c8cy02438c.

[13] A. Tetorou, A. Makhatova, S.G. Poulopoulos, Photochemical mineralization of Ibuprofen medicinal product by means of UV, hydrogen peroxide, titanium dioxide and Iron, Water Sci. Technol. (2020). https://doi.org/10.2166/wst.2020.041.

[14] F.H. Hussein, Comparison between solar and artificial photocatalytic decolorization of textile industrial wastewater, Int. J. Photoenergy. 2012 (2012).

https://doi.org/10.1155/2012/793648.

[15] E.M. Siedlecka, Application of Bismuth-Based Photocatalysts in Environmental Protection, 2020. https://doi.org/10.1007/978-3-030-12619-3_4.

[16] A.T. Besha, A.Y. Gebreyohannes, R.A. Tufa, D.N. Bekele, E. Curcio, L. Giorno, Removal of emerging micropollutants by activated sludge process and membrane bioreactors and the effects of micropollutants on membrane fouling: A review, J. Environ. Chem. Eng. 5 (2017) 2395–2414. https://doi.org/10.1016/j.jece.2017.04.027.

[17] O.T. Iorhemen, R.A. Hamza, J.H. Tay, Membrane Bioreactor (MBR) Technology for Wastewater Treatment and Reclamation: Membrane Fouling, Membranes (Basel). 6 (2016). https://doi.org/10.3390/MEMBRANES6020033.

[18] G. Laera, D. Cassano, A. Lopez, A. Pinto, A. Pollice, G. Ricco, G. Mascolo, Removal of organics and degradation products from industrial wastewater by a membrane bioreactor integrated with ozone or UV/H 2O 2 treatment, Environ. Sci. Technol. 46 (2012) 1010–1018. https://doi.org/10.1021/es202707w.

[19] A.B. Rostam, M. Taghizadeh, Advanced oxidation processes integrated by membrane reactors and bioreactors for various wastewater treatments: A critical review, J. Environ. Chem. Eng. 8 (2020) 104566. https://doi.org/10.1016/J.JECE.2020.104566.

[20] A. Kozlovskiy, M. Zdorovets, E. Arkhangelsky, Track-etch membranes: The Kazakh experience, Desalin. Water Treat. 76 (2017) 143–147. https://doi.org/10.5004/dwt.2017.20786.

[21] M. Fidaleo, R. Lavecchia, E. Petrucci, A. Zuorro, Application of a novel definitive screening design to decolorization of an azo dye on boron-doped diamond electrodes, Int. J. Environ. Sci. Technol. 13 (2016) 835–842. https://doi.org/10.1007/s13762-016-0933-3.

[22] R. Davarnejad, S. Nasiri, Slaughterhouse wastewater treatment using an advanced oxidation process: Optimization study, Environ. Pollut. 223 (2017) 1–10. https://doi.org/10.1016/j.envpol.2016.11.008.

[23] D.P. Häder, Ecotoxicological monitoring of wastewater, Bioassays Adv. Methods Appl. (2018) 369–386. https://doi.org/10.1016/B978-0-12-811861-0.00018-8.

[24] E.R. Jones, M.T.H. Van Vliet, M. Qadir, M.F.P. Bierkens, Country-level and gridded estimates of wastewater production, collection, treatment and reuse, Earth Syst. Sci. Data. 13 (2021) 237–254. https://doi.org/10.5194/essd-13-237-2021.

[25] 2021 UN-Water, Summary Progress Update 2021: SDG 6-water and sanitation for all, Geneva, Switzerland., 2021.

[26] Indicator | SDG 6 Data, (n.d.).

[27] T. Sato, M. Qadir, S. Yamamoto, T. Endo, A. Zahoor, Global, regional, and country level need for data on wastewater generation, treatment, and use, Agric. Water Manag. 130 (2013) 1–13. https://doi.org/10.1016/j.agwat.2013.08.007.

[28] D. Andraka, K. Ospanov, M. Myrzakhmetov, Current state of communal sewage treatment in the republic of Kazakhstan, J. Ecol. Eng. 16 (2015) 101–109. https://doi.org/10.12911/22998993/60463.

[29] H.K. Shon, S. Vigneswaran, S.A. Snyder, Effluent organic matter (EfOM) in

wastewater: Constituents, effects, and treatment, Crit. Rev. Environ. Sci. Technol. 36 (2006) 327–374. https://doi.org/10.1080/10643380600580011.

[30] N.R.C. Committee on the Use of Treated Municipal Wastewater Effluents and Sludge in the Production of Crops for Human Consumption, Use of Reclaimed Water and Sludge in Food Crop Production - Committee on the Use of Treated Municipal Wastewater Effluents and Sludge in the Production of Crops for Human Consumption, Commission on Geosciences, Environment and Resources, Division on Earth, NATIONAL ACADEMY PRESS, Washington, D.C., 1996.

[31] C. Stamm, K. Räsänen, F.J. Burdon, F. Altermatt, J. Jokela, A. Joss, M. Ackermann, R.I.L. Eggen, Unravelling the Impacts of Micropollutants in Aquatic Ecosystems: Interdisciplinary Studies at the Interface of Large-Scale Ecology, Adv. Ecol. Res. 55 (2016) 183–223. https://doi.org/10.1016/bs.aecr.2016.07.002.

[32] Y. Yun, Z. Li, Y.H. Chen, M. Saino, S. Cheng, L. Zheng, Elimination of nitrate in secondary effluent of wastewater treatment plants by Fe0 and pd-cu/diatomite, J. Water Reuse Desalin. 8 (2018) 29–37. https://doi.org/10.2166/wrd.2016.122.

[33] N.H. Tran, V.T. Nguyen, T. Urase, H.H. Ngo, Role of nitrification in the biodegradation of selected artificial sweetening agents in biological wastewater treatment process, Bioresour. Technol. 161 (2014) 40–46. https://doi.org/10.1016/j.biortech.2014.02.116.

[34] D.M. Golea, P. Jarvis, B. Jefferson, G. Moore, S. Sutherland, S.A. Parsons, S.J. Judd, Influence of granular activated carbon media properties on natural organic matter and disinfection by-product precursor removal from drinking water, Water Res. 174 (2020). https://doi.org/10.1016/j.watres.2020.115613.

[35] N.A.A. Qasem, R.H. Mohammed, D.U. Lawal, Removal of heavy metal ions from wastewater: a comprehensive and critical review, Npj Clean Water. 4 (2021). https://doi.org/10.1038/s41545-021-00127-0.

[36] S.C. Ameta, Introduction, Adv. Oxid. Process. Wastewater Treat. Emerg. Green Chem. Technol. (2018) 1–12. https://doi.org/10.1016/B978-0-12-810499-6.00001-2.

[37] N. Tadkaew, F.I. Hai, J.A. McDonald, S.J. Khan, L.D. Nghiem, Removal of trace organics by MBR treatment: The role of molecular properties, Water Res. 45 (2011) 2439–2451. https://doi.org/10.1016/j.watres.2011.01.023.

[38] A. Gogoi, P. Mazumder, V.K. Tyagi, G.G. Tushara Chaminda, A.K. An, M. Kumar, Occurrence and fate of emerging contaminants in water environment: A review, Groundw. Sustain. Dev. 6 (2018) 169–180. https://doi.org/10.1016/j.gsd.2017.12.009.

[39] D.J. Lapworth, N. Baran, M.E. Stuart, R.S. Ward, Emerging organic contaminants in groundwater: A review of sources, fate and occurrence, Environ. Pollut. 163 (2012) 287–303. https://doi.org/10.1016/j.envpol.2011.12.034.

[40] D. Fatta-Kassinos, S. Meric, A. Nikolaou, Pharmaceutical residues in environmental waters and wastewater: Current state of knowledge and future research, Anal. Bioanal. Chem. 399 (2011) 251–275. https://doi.org/10.1007/s00216-010-4300-9.

[41] Q. Sun, Y. Li, M. Li, M. Ashfaq, M. Lv, H. Wang, A. Hu, C.P. Yu, PPCPs in Jiulong River estuary (China): Spatiotemporal distributions, fate, and their use as chemical markers of wastewater, Chemosphere. 150 (2016) 596–604. https://doi.org/10.1016/j.chemosphere.2016.02.036.

[42] J.J. Jiang, C.L. Lee, P. Brimblecombe, L. Vydrova, M. Der Fang, Source contributions and mass loadings for chemicals of emerging concern: Chemometric application of pharmaco-signature in different aquatic systems, Environ. Pollut. 208 (2016) 79–86. https://doi.org/10.1016/j.envpol.2015.06.039.

[43] S.W. Nam, B. Il Jo, Y. Yoon, K.D. Zoh, Occurrence and removal of selected micropollutants in a water treatment plant, Chemosphere. 95 (2014) 156–165. https://doi.org/10.1016/j.chemosphere.2013.08.055.

[44] S. Tewari, R. Jindal, Y.L. Kho, S. Eo, K. Choi, Major pharmaceutical residues in wastewater treatment plants and receiving waters in Bangkok, Thailand, and associated ecological risks, Chemosphere. 91 (2013) 697–704. https://doi.org/10.1016/j.chemosphere.2012.12.042.

[45] C.I. Kosma, D.A. Lambropoulou, T.A. Albanis, Investigation of PPCPs in wastewater treatment plants in Greece: Occurrence, removal and environmental risk assessment, Sci. Total Environ. 466–467 (2014) 421–438. https://doi.org/10.1016/j.scitotenv.2013.07.044.

[46] J.P.R. Sorensen, D.J. Lapworth, D.C.W. Nkhuwa, M.E. Stuart, D.C. Gooddy, R.A. Bell, M. Chirwa, J. Kabika, M. Liemisa, M. Chibesa, S. Pedley, Emerging contaminants in urban groundwater sources in Africa, Water Res. 72 (2015) 51–63. https://doi.org/10.1016/j.watres.2014.08.002.

[47] E.B. Estrada-Arriaga, J.E. Cortés-Muñoz, A. González-Herrera, C.G. Calderón-Mólgora, M. de Lourdes Rivera-Huerta, E. Ramírez-Camperos, L. Montellano-Palacios, S.L. Gelover-Santiago, S. Pérez-Castrejón, L. Cardoso-Vigueros, A. Martín-Domínguez, L. García-Sánchez, Assessment of full-scale biological nutrient removal systems upgraded with physico-chemical processes for the removal of emerging pollutants present in wastewaters from Mexico, Sci. Total Environ. 571 (2016) 1172–1182. https://doi.org/10.1016/j.scitotenv.2016.07.118.

[48] M. Petrović, B. Škrbić, J. Živančev, L. Ferrando-Climent, D. Barcelo, Determination of 81 pharmaceutical drugs by high performance liquid chromatography coupled to mass spectrometry with hybrid triple quadrupole-linear ion trap in different types of water in Serbia, Sci. Total Environ. 468–469 (2014) 415–428. https://doi.org/10.1016/j.scitotenv.2013.08.079.

[49] S. Zhang, Q. Zhang, S. Darisaw, O. Ehie, G. Wang, Simultaneous quantification of polycyclic aromatic hydrocarbons (PAHs), polychlorinated biphenyls (PCBs), and pharmaceuticals and personal care products (PPCPs) in Mississippi river water, in New Orleans, Louisiana, USA, Chemosphere. 66 (2007) 1057–1069. https://doi.org/10.1016/j.chemosphere.2006.06.067.

[50] J.W. Kim, H.S. Jang, J.G. Kim, H. Ishibashi, M. Hirano, K. Nasu, N. Ichikawa, Y. Takao, R. Shinohara, K. Arizono, Occurrence of Pharmaceutical and Personal Care Products (PPCPs) in Surface Water from Mankyung River, South Korea, J. Heal. Sci. 55 (2009) 249–258. https://doi.org/10.1248/jhs.55.249.

[51] T.H. Fang, F.H. Nan, T.S. Chin, H.M. Feng, The occurrence and distribution of pharmaceutical compounds in the effluents of a major sewage treatment plant in Northern Taiwan and the receiving coastal waters, Mar. Pollut. Bull. 64 (2012) 1435–1444. https://doi.org/10.1016/j.marpolbul.2012.04.008.

[52] N. Gottschall, E. Topp, C. Metcalfe, M. Edwards, M. Payne, S. Kleywegt, P. Russell, D.R. Lapen, Pharmaceutical and personal care products in groundwater, subsurface drainage, soil, and wheat grain, following a high single application of

municipal biosolids to a field, Chemosphere. 87 (2012) 194–203. https://doi.org/10.1016/j.chemosphere.2011.12.018.

[53] M. Wagil, J. Maszkowska, A. Białk-Bielińska, M. Caban, P. Stepnowski, J. Kumirska, Determination of metronidazole residues in water, sediment and fish tissue samples, Chemosphere. 119 (2015) S28–S34. https://doi.org/10.1016/j.chemosphere.2013.12.061.

[54] M.J. Gómez, M. Petrović, A.R. Fernández-Alba, D. Barceló, Determination of pharmaceuticals of various therapeutic classes by solid-phase extraction and liquid chromatography-tandem mass spectrometry analysis in hospital effluent wastewaters, J. Chromatogr. A. 1114 (2006) 224–233. https://doi.org/10.1016/j.chroma.2006.02.038.

[55] R. Lindberg, P.Å. Jarnheimer, B. Olsen, M. Johansson, M. Tysklind, Determination of antibiotic substances in hospital sewage water using solid phase extraction and liquid chromatography/mass spectrometry and group analogue internal standards, Chemosphere. 57 (2004) 1479–1488. https://doi.org/10.1016/j.chemosphere.2004.09.015.

[56] B. Kasprzyk-Hordern, R.M. Dinsdale, A.J. Guwy, Multi-residue method for the determination of basic/neutral pharmaceuticals and illicit drugs in surface water by solid-phase extraction and ultra performance liquid chromatography-positive electrospray ionisation tandem mass spectrometry, J. Chromatogr. A. 1161 (2007) 132–145. https://doi.org/10.1016/j.chroma.2007.05.074.

[57] Y. Cabeza, L. Candela, D. Ronen, G. Teijon, Monitoring the occurrence of emerging contaminants in treated wastewater and groundwater between 2008 and 2010. The Baix Llobregat (Barcelona, Spain), J. Hazard. Mater. 239–240 (2012) 32–39. https://doi.org/10.1016/j.jhazmat.2012.07.032.

[58] L. Patrolecco, J. Rauseo, N. Ademollo, P. Grenni, M. Cardoni, C. Levantesi, M.L. Luprano, A.B. Caracciolo, Persistence of the antibiotic sulfamethoxazole in river water alone or in the co-presence of ciprofloxacin, Sci. Total Environ. 640–641 (2018) 1438–1446. https://doi.org/10.1016/j.scitotenv.2018.06.025.

[59] A. Shimizu, H. Takada, T. Koike, A. Takeshita, M. Saha, Rinawati, N. Nakada, A. Murata, T. Suzuki, S. Suzuki, N.H. Chiem, B.C. Tuyen, P.H. Viet, M.A. Siringan, C. Kwan, M.P. Zakaria, A. Reungsang, Ubiquitous occurrence of sulfonamides in tropical Asian waters, Sci. Total Environ. 452–453 (2013) 108–115. https://doi.org/10.1016/j.scitotenv.2013.02.027.

[60] M.J. Benotti, R.A. Trenholm, B.J. Vanderford, J.C. Holady, B.D. Stanford, S.A. Snyder, Pharmaceuticals and endocrine disrupting compounds in U.S. drinking water, Environ. Sci. Technol. 43 (2009) 597–603. https://doi.org/10.1021/es801845a.

[61] R. Loos, G. Locoro, S. Comero, S. Contini, D. Schwesig, F. Werres, P. Balsaa, O. Gans, S. Weiss, L. Blaha, M. Bolchi, B.M. Gawlik, Pan-European survey on the occurrence of selected polar organic persistent pollutants in ground water, Water Res. 44 (2010) 4115–4126. https://doi.org/10.1016/j.watres.2010.05.032.

[62] D.P. Mohapatra, S.K. Brar, R.D. Tyagi, R.Y. Surampalli, Occurrence of bisphenol A in wastewater and wastewater sludge of CUQ treatment plant, J. Xenobiotics. 1 (2011) 3. https://doi.org/10.4081/xeno.2011.e3.

[63] D. Balabanič, A.K. Klemenčič, Presence of phthalates, bisphenol a, and

nonylphenol in paper mill wastewaters in slovenia and efficiency of aerobic and combined aerobic-anaerobic biological wastewater treatment plants for their removal, Fresenius Environ. Bull. 20 (2011) 86–92.

[64] X.-L. Shao, J. Ma, G. Wen, Investigation of endocrine disrupting chemicals in a drinking water work located in Songhua River basin, Huan jing ke xue= Huanjing kexue. 29 (2008) 2723–2728.

[65] G. Shanmugam, S. Sampath, K.K. Selvaraj, D.G.J. Larsson, B.R. Ramaswamy, Non-steroidal anti-inflammatory drugs in Indian rivers, Environ. Sci. Pollut. Res. 21 (2014) 921–931. https://doi.org/10.1007/s11356-013-1957-6.

[66] A.E.B. Kermia, D. Fouial-Djebbar, M. Trari, Occurrence, fate and removal efficiencies of pharmaceuticals in wastewater treatment plants (WWTPs) discharging in the coastal environment of Algiers, Comptes Rendus Chim. 19 (2016) 963–970. https://doi.org/10.1016/j.crci.2016.05.005.

[67] J.M. Brozinski, M. Lahti, A. Meierjohann, A. Oikari, L. Kronberg, The anti-inflammatory drugs diclofenac, naproxen and ibuprofen are found in the bile of wild fish caught downstream of a wastewater treatment plant, Environ. Sci. Technol. 47 (2013) 342–348. https://doi.org/10.1021/es303013j.

[68] F. Gagné, C. Blaise, C. André, Occurrence of pharmaceutical products in a municipal effluent and toxicity to rainbow trout (Oncorhynchus mykiss) hepatocytes, Ecotoxicol. Environ. Saf. 64 (2006) 329–336. https://doi.org/10.1016/j.ecoenv.2005.04.004.

[69] H.C. Chen, P.L. Wang, W.H. Ding, Using liquid chromatography-ion trap mass spectrometry to determine pharmaceutical residues in Taiwanese rivers and wastewaters, Chemosphere. 72 (2008) 863–869. https://doi.org/10.1016/j.chemosphere.2008.04.005.

[70] R. López-Serna, A. Jurado, E. Vázquez-Suñé, J. Carrera, M. Petrović, D. Barceló, Occurrence of 95 pharmaceuticals and transformation products in urban groundwaters underlying the metropolis of Barcelona, Spain, Environ. Pollut. 174 (2013) 305–315. https://doi.org/10.1016/j.envpol.2012.11.022.

[71] H. V. Phan, F.I. Hai, J. Kang, H.K. Dam, R. Zhang, W.E. Price, A. Broeckmann, L.D. Nghiem, Simultaneous nitrification/denitrification and trace organic contaminant (TrOC) removal by an anoxic-aerobic membrane bioreactor (MBR), Bioresour. Technol. 165 (2014) 96–104. https://doi.org/10.1016/j.biortech.2014.03.094.

[72] I.C. Vasilachi, D.M. Asiminicesei, D.I. Fertu, M. Gavrilescu, Occurrence and fate of emerging pollutants in water environment and options for their removal, Water (Switzerland). 13 (2021) 1–34. https://doi.org/10.3390/w13020181.

[73] C. Valhondo, J. Carrera, Water as a finite resource: From historical accomplishments to emerging challenges and artificial recharge, Sustain. Water Wastewater Process. (2019) 1–17. https://doi.org/10.1016/B978-0-12-816170-8.00001-6.

[74] S. Li, B. He, J. Wang, J. Liu, X. Hu, Risks of caffeine residues in the environment: Necessity for a targeted ecopharmacovigilance program, Chemosphere. 243 (2020). https://doi.org/10.1016/j.chemosphere.2019.125343.

[75] S. Chopra, D. Kumar, Ibuprofen as an emerging organic contaminant in environment, distribution and remediation, Heliyon. 6 (2020) e04087.

https://doi.org/10.1016/j.heliyon.2020.e04087.

[76] P.F. Lanzky, B. Halling-Sørensen, The toxic effect of the antibiotic metronidazole on aquatic organisms, Chemosphere. 35 (1997) 2553–2561. https://doi.org/10.1016/S0045-6535(97)00324-X.

[77] S. Magalhães, C. Brêtas, J. Brêtas, G. Pianetti, M. Franco, F. Barbosa, Toxic concentrations of metronidazole to Microcystis protocystis, Brazilian J. Biol. 74 (2014) S120–S124. https://doi.org/10.1590/1519-6984.03513.

[78] D. Xu, Y. Xie, J. Li, Toxic effects and molecular mechanisms of sulfamethoxazole on Scenedesmus obliquus, Ecotoxicol. Environ. Saf. 232 (2022) 113258. https://doi.org/10.1016/j.ecoenv.2022.113258.

[79] A. V Krishnan, P. Stathis, S.F. Permuth, L. Tokes, D. Feldman, Bisphenol-A: an estrogenic substance is released from polycarbonate flasks during autoclaving, Endocrinology. 132 (1993) 2279–2286. https://doi.org/10.1081/MC-100107861.

[80] D. Wojcieszyńska, U. Guzik, Naproxen in the environment: its occurrence, toxicity to nontarget organisms and biodegradation, Appl. Microbiol. Biotechnol. 104 (2020) 1849–1857.

[81] A. Kohl, N. Golan, Y. Cinnamon, O. Genin, B. Chefetz, D. Sela-Donenfeld, A proof of concept study demonstrating that environmental levels of carbamazepine impair early stages of chick embryonic development, Environ. Int. 129 (2019) 583–594. https://doi.org/10.1016/j.envint.2019.03.064.

[82] J.W. Nichols, B. Du, J.P. Berninger, K.A. Connors, C.K. Chambliss, R.J. Erickson, A.D. Hoffman, B.W. Brooks, Observed and modeled effects of pH on bioconcentration of diphenhydramine, a weakly basic pharmaceutical, in fathead minnows, Environ. Toxicol. Chem. 34 (2015) 1425–1435. https://doi.org/10.1002/etc.2948.

[83] N.H. Tran, T. Urase, H.H. Ngo, J. Hu, S.L. Ong, Insight into metabolic and cometabolic activities of autotrophic and heterotrophic microorganisms in the biodegradation of emerging trace organic contaminants, Bioresour. Technol. 146 (2013) 721–731. https://doi.org/10.1016/j.biortech.2013.07.083.

[84] M.B. Ahmed, J.L. Zhou, H.H. Ngo, W. Guo, N.S. Thomaidis, J. Xu, Progress in the biological and chemical treatment technologies for emerging contaminant removal from wastewater: A critical review, J. Hazard. Mater. 323 (2017) 274–298. https://doi.org/10.1016/j.jhazmat.2016.04.045.

[85] D. Sreekanth, D. Sivaramakrishna, V. Himabindu, Y. Anjaneyulu, Thermophilic treatment of bulk drug pharmaceutical industrial wastewaters by using hybrid up flow anaerobic sludge blanket reactor, Bioresour. Technol. 100 (2009) 2534–2539. https://doi.org/10.1016/j.biortech.2008.11.028.

[86] C. Elmerich, Nitrification and denitrification in the activated sludge process, 2002. https://doi.org/10.1016/s0923-2508(02)01315-3.

[87] G.K. Nesseris, A.S. Stasinakis, Investigation of municipal and olive mill wastewater co-treatment in activated sludge-powdered activated carbon (AS-PAC) systems, J. Chem. Technol. Biotechnol. 87 (2012) 540–545. https://doi.org/10.1002/jctb.2745.

[88] R.L. Irvine, T.P. Fox, R.O. Richter, Investigation of fill and batch periods of sequencing batch biological reactors, Water Res. 11 (1977) 713–717. https://doi.org/10.1016/0043-1354(77)90112-9.

[89] A. Dutta, S. Sarkar, Sequencing Batch Reactor for Wastewater Treatment: Recent Advances, Curr. Pollut. Reports. 1 (2015) 177–190. https://doi.org/10.1007/s40726-015-0016-y.

[90] D. Doskaliyev, S.G. Poulopoulos, A. Yeshmuratov, F. Aldyngurova, A.A. Zorpas, V.J. Inglezakis, Effects of 2-chlorophenol and 2,4,6-trichlorophenol on an activated sludge sequencing batch reactor, Desalin. Water Treat. 133 (2018) 283–291. https://doi.org/10.5004/dwt.2018.23065.

[91] V.M. Monsalvo, J. Lopez, M. Munoz, Z.M. de Pedro, J.A. Casas, A.F. Mohedano, J.J. Rodriguez, Application of Fenton-like oxidation as pre-treatment for carbamazepine biodegradation, Chem. Eng. J. 264 (2015) 856–862. https://doi.org/10.1016/j.cej.2014.11.141.

[92] H.L. Osachoff, M. Mohammadali, R.C. Skirrow, E.R. Hall, L.L.Y. Brown, G.C. van Aggelen, C.J. Kennedy, C.C. Helbing, Evaluating the treatment of a synthetic wastewater containing a pharmaceutical and personal care product chemical cocktail: Compound removal efficiency and effects on juvenile rainbow trout, Water Res. 62 (2014) 271–280. https://doi.org/10.1016/j.watres.2014.05.057.

[93] M.J. Shreve, R.A. Brennan, Trace organic contaminant removal in six full-scale integrated fixed-film activated sludge (IFAS) systems treating municipal wastewater, Water Res. 151 (2019) 318–331. https://doi.org/10.1016/j.watres.2018.12.042.

[94] J. Park, C. Kim, Y. Hong, W. Lee, H. Chung, D.H. Jeong, H. Kim, Distribution and removal of pharmaceuticals in liquid and solid phases in the unit processes of sewage treatment plants, Int. J. Environ. Res. Public Health. 17 (2020). https://doi.org/10.3390/ijerph17030687.

[95] N.K. Stamatis, I.K. Konstantinou, Occurrence and removal of emerging pharmaceutical, personal care compounds and caffeine tracer in municipal sewage treatment plant in Western Greece, J. Environ. Sci. Heal. - Part B Pestic. Food Contam. Agric. Wastes. 48 (2013) 800–813. https://doi.org/10.1080/03601234.2013.781359.

[96] C. Quintelas, D.P. Mesquita, A.M. Torres, I. Costa, E.C. Ferreira, Degradation of widespread pharmaceuticals by activated sludge: Kinetic study, toxicity assessment, and comparison with adsorption processes, J. Water Process Eng. 33 (2020) 101061. https://doi.org/10.1016/j.jwpe.2019.101061.

[97] V.A. Jiménez-Silva, F. Santoyo-Tepole, N. Ruiz-Ordaz, J. Galíndez-Mayer, Study of the ibuprofen impact on wastewater treatment mini-plants with bioaugmented sludge, Process Saf. Environ. Prot. 123 (2019) 140–149. https://doi.org/10.1016/j.psep.2018.08.006.

[98] A. Kruglova, P. Ahlgren, N. Korhonen, P. Rantanen, A. Mikola, R. Vahala, Biodegradation of ibuprofen, diclofenac and carbamazepine in nitrifying activated sludge under 12°C temperature conditions, Sci. Total Environ. 499 (2014) 394–401. https://doi.org/10.1016/j.scitotenv.2014.08.069.

[99] P. Verlicchi, A. Galletti, M. Petrovic, D. Barceló, M. Al Aukidy, E. Zambello, Removal of selected pharmaceuticals from domestic wastewater in an activated sludge system followed by a horizontal subsurface flow bed - Analysis of their respective contributions, Sci. Total Environ. 454–455 (2013) 411–425. https://doi.org/10.1016/j.scitotenv.2013.03.044.

[100] A. Aboudalle, H. Djelal, F. Fourcade, L. Domergue, A.A. Assadi, T. Lendormi, S. Taha, A. Amrane, Metronidazole removal by means of a combined system coupling an electro-Fenton process and a conventional biological treatment: By-products monitoring and performance enhancement, J. Hazard. Mater. 359 (2018) 85–95. https://doi.org/10.1016/j.jhazmat.2018.07.006.

[101] I. Saidi, I. Soutrel, D. Floner, F. Fourcade, N. Bellakhal, A. Amrane, F. Geneste, Indirect electroreduction as pretreatment to enhance biodegradability of metronidazole, J. Hazard. Mater. 278 (2014) 172–179. https://doi.org/10.1016/j.jhazmat.2014.06.003.

[102] O. Velasco-Garduño, G. González-Blanco, M. del C. Fajardo-Ortiz, R. Beristain-Cardoso, Influence of metronidazole on activated sludge activity, Environ. Technol. (United Kingdom). 42 (2021) 2815–2822. https://doi.org/10.1080/09593330.2020.1714746.

[103] M. Clara, B. Strenn, O. Gans, E. Martinez, N. Kreuzinger, H. Kroiss, Removal of selected pharmaceuticals, fragrances and endocrine disrupting compounds in a membrane bioreactor and conventional wastewater treatment plants, Water Res. 39 (2005) 4797–4807. https://doi.org/10.1016/j.watres.2005.09.015.

[104] P. Drillia, S.N. Dokianakis, M.S. Fountoulakis, M. Kornaros, K. Stamatelatou, G. Lyberatos, On the occasional biodegradation of pharmaceuticals in the activated sludge process: The example of the antibiotic sulfamethoxazole, J. Hazard. Mater. 122 (2005) 259–265. https://doi.org/10.1016/j.jhazmat.2005.03.009.

[105] J. Radjenović, M. Petrović, D. Barceló, Fate and distribution of pharmaceuticals in wastewater and sewage sludge of the conventional activated sludge (CAS) and advanced membrane bioreactor (MBR) treatment, Water Res. 43 (2009) 831–841. https://doi.org/10.1016/j.watres.2008.11.043.

[106] J. Radjenovic, M. Petrovic, D. Barceló, Analysis of pharmaceuticals in wastewater and removal using a membrane bioreactor, Anal. Bioanal. Chem. 387 (2007) 1365–1377. https://doi.org/10.1007/s00216-006-0883-6.

[107] S. Suarez, J.M. Lema, F. Omil, Removal of Pharmaceutical and Personal Care Products (PPCPs) under nitrifying and denitrifying conditions, Water Res. 44 (2010) 3214–3224. https://doi.org/10.1016/j.watres.2010.02.040.

[108] E. Ferrer-Polonio, C.B. Alvim, J. Fernández-Navarro, R. Mompó-Curell, J.A. Mendoza-Roca, A. Bes-Piá, J.L. Alonso-Molina, I. Amorós-Muñoz, Influence of bisphenol A occurrence in wastewaters on biomass characteristics and activated sludge process performance, Sci. Total Environ. 778 (2021) 146355. https://doi.org/10.1016/J.SCITOTENV.2021.146355.

[109] J. Shao, K. Tian, F. Meng, S. Li, H. Li, Y. Yu, Q. Qiu, M. Chang, Effects of Bisphenol A Stress on Activated Sludge in Sequential Batch Reactors and Functional Recovery, Appl. Sci. 12 (2022) 8026.

[110] F. Spataro, N. Ademollo, T. Pescatore, J. Rauseo, L. Patrolecco, Antibiotic residues and endocrine disrupting compounds in municipal wastewater treatment plants in Rome, Italy, Microchem. J. 148 (2019) 634–642. https://doi.org/10.1016/j.microc.2019.05.053.

[111] P. Guerra, M. Kim, S. Teslic, M. Alaee, S.A. Smyth, Bisphenol-A removal in various wastewater treatment processes: Operational conditions, mass balance, and optimization, J. Environ. Manage. 152 (2015) 192–200.

https://doi.org/10.1016/j.jenvman.2015.01.044.

[112] Y. Bon, K. Lai, Y. Fai, F. Tat, K. Lau, W. Cheong, M. Hung, Fate of bisphenol A, perfluorooctanoic acid and perfluorooctanesulfonate in two different types of sewage treatment works in Hong Kong, Chemosphere. 190 (2018) 358–367. https://doi.org/10.1016/j.chemosphere.2017.10.001.

[113] M. Qurie, M. Khamis, F. Malek, S. Nir, S.A. Bufo, J. Abbadi, L. Scrano, R. Karaman, Stability and removal of naproxen and its metabolite by advanced membrane wastewater treatment plant and micelle-clay complex, Clean - Soil, Air, Water. 42 (2014) 594–600. https://doi.org/10.1002/clen.201300179.

[114] X. Du, Y. Shi, V. Jegatheesan, I. Ul Haq, A review on the mechanism, impacts and control methods of membrane fouling in MBR system, 2020. https://doi.org/10.3390/membranes10020024.

[115] J. Radjenovic, M. Matosic, I. Mijatovic, M. Petrovic, D. Barceló, Membrane bioreactor as an advanced wastewater treatment technology, Elsevier Inc., 2021. https://doi.org/10.1016/B978-0-323-85583-9.00002-8.

[116] M.F. Tay, C. Liu, E.R. Cornelissen, B. Wu, T.H. Chong, The feasibility of nanofiltration membrane bioreactor (NF-MBR)+reverse osmosis (RO) process for water reclamation: Comparison with ultrafiltration membrane bioreactor (UF-MBR)+RO process, Water Res. 129 (2018) 180–189. https://doi.org/10.1016/j.watres.2017.11.013.

[117] K. Kimura, S. Okazaki, T. Ohashi, Y. Watanabe, Importance of the co-presence of silica and organic matter in membrane fouling for RO filtering MBR effluent, J. Memb. Sci. 501 (2016) 60–67. https://doi.org/10.1016/j.memsci.2015.12.016.

[118] P. Kumar, M.K. Mandal, S. Pal, H. Chaudhuri, K.K. Dubey, Membrane bioreactor for the treatment of emerging pharmaceutical compounds in a circular bioeconomy, Elsevier Inc., 2022. https://doi.org/10.1016/b978-0-323-88511-9.00008-2.

[119] T. Urase, C. Kagawa, T. Kikuta, Factors affecting removal of pharmaceutical substances and estrogens in membrane separation bioreactors, Desalination. 178 (2005) 107–113. https://doi.org/10.1016/j.desal.2004.11.031.

[120] S.K. Maeng, B.G. Choi, K.T. Lee, K.G. Song, Influences of solid retention time, nitrification and microbial activity on the attenuation of pharmaceuticals and estrogens in membrane bioreactors, Water Res. 47 (2013) 3151–3162. https://doi.org/10.1016/j.watres.2013.03.014.

[121] J. Ma, R. Dai, M. Chen, S.J. Khan, Z. Wang, Applications of membrane bioreactors for water reclamation: Micropollutant removal, mechanisms and perspectives, Bioresour. Technol. 269 (2018) 532–543. https://doi.org/10.1016/j.biortech.2018.08.121.

[122] S. Suárez, R. Reif, J.M. Lema, F. Omil, Mass balance of pharmaceutical and personal care products in a pilot-scale single-sludge system: Influence of T, SRT and recirculation ratio, Chemosphere. 89 (2012) 164–171. https://doi.org/10.1016/j.chemosphere.2012.05.094.

[123] J.L. Tambosi, R.F. de Sena, M. Favier, W. Gebhardt, H.J. José, H.F. Schröder, R. de Fatima Peralta Muniz Moreira, Removal of pharmaceutical compounds in membrane bioreactors (MBR) applying submerged membranes, Desalination. 261 (2010) 148–156. https://doi.org/10.1016/j.desal.2010.05.014.

[124] H. V. Phan, F.I. Hai, J.A. McDonald, S.J. Khan, J.P. van de Merwe, F.D.L. Leusch, R. Zhang, W.E. Price, A. Broeckmann, L.D. Nghiem, Impact of hazardous events on the removal of nutrients and trace organic contaminants by an anoxic-aerobic membrane bioreactor receiving real wastewater, Bioresour. Technol. 192 (2015) 192–201. https://doi.org/10.1016/j.biortech.2015.05.059.

[125] P.R. Richle, Removal of Estrogens in Municipal Wastewater Treatment under Aerobic and Anaerobic Conditions : Consequences for Plant Optimization, (2004) 3047–3055.

[126] M. Chtourou, M. Mallek, M. Dalmau, J. Mamo, E. Santos-Clotas, A. Ben Salah, K. Walha, V. Salvadó, H. Monclús, Triclosan, carbamazepine and caffeine removal by activated sludge system focusing on membrane bioreactor, Process Saf. Environ. Prot. 118 (2018) 1–9. https://doi.org/10.1016/j.psep.2018.06.019.

[127] F.I. Hai, K. Tessmer, L.N. Nguyen, J. Kang, W.E. Price, L.D. Nghiem1, Removal of micropollutants by membrane bioreactor under temperature variation, J. Memb. Sci. (2011) 144–151.

[128] P. Cartagena, M. El Kaddouri, V. Cases, A. Trapote, D. Prats, Reduction of emerging micropollutants, organic matter, nutrients and salinity from real wastewater by combined MBR-NF/RO treatment, Sep. Purif. Technol. 110 (2013) 132–143. https://doi.org/10.1016/j.seppur.2013.03.024.

[129] V.M. Monsalvo, J.A. McDonald, S.J. Khan, P. Le-Clech, Removal of trace organics by anaerobic membrane bioreactors, Water Res. 49 (2014) 103–112. https://doi.org/10.1016/j.watres.2013.11.026.

[130] M. Bernhard, J. Müller, T.P. Knepper, Biodegradation of persistent polar pollutants in wastewater: Comparison of an optimised lab-scale membrane bioreactor and activated sludge treatment, Water Res. 40 (2006) 3419–3428. https://doi.org/10.1016/j.watres.2006.07.011.

[131] D. Dolar, M. Gros, S. Rodriguez-Mozaz, J. Moreno, J. Comas, I. Rodriguez-Roda, D. Barceló, Removal of emerging contaminants from municipal wastewater with an integrated membrane system, MBR-RO, J. Hazard. Mater. 239–240 (2012) 64–69. https://doi.org/10.1016/j.jhazmat.2012.03.029.

[132] K. Gurung, M.C. Ncibi, J.M. Fontmorin, Incorporating Submerged MBR in Conventional Activated Sludge Process for Municipal Wastewater Treatment: A Feasibility and Performance Assessment, J. Membr. Sci. Technol. 6 (2016). https://doi.org/10.4172/2155-9589.1000158.

[133] L.N. Nguyen, F.I. Hai, J. Kang, L.D. Nghiem, W.E. Price, W. Guo, H.H. Ngo, K.L. Tung, Comparison between sequential and simultaneous application of activated carbon with membrane bioreactor for trace organic contaminant removal, Bioresour. Technol. 130 (2013) 412–417. https://doi.org/10.1016/j.biortech.2012.11.131.

[134] C.H. Wei, C. Sanchez-Huerta, T.O. Leiknes, G. Amy, H. Zhou, X. Hu, Q. Fang, H. Rong, Removal and biotransformation pathway of antibiotic sulfamethoxazole from municipal wastewater treatment by anaerobic membrane bioreactor, J. Hazard. Mater. 380 (2019) 120894. https://doi.org/10.1016/j.jhazmat.2019.120894.

[135] J. Lee, B.C. Lee, J.S. Ra, J. Cho, I.S. Kim, N.I. Chang, H.K. Kim, S.D. Kim, Comparison of the removal efficiency of endocrine disrupting compounds in pilot scale sewage treatment processes, Chemosphere. 71 (2008) 1582–1592. https://doi.org/10.1016/j.chemosphere.2007.11.021.

[136] N. Tadkaew, M. Sivakumar, S.J. Khan, J.A. McDonald, L.D. Nghiem, Effect of mixed liquor pH on the removal of trace organic contaminants in a membrane bioreactor, Bioresour. Technol. 101 (2010) 1494–1500. https://doi.org/10.1016/j.biortech.2009.09.082.

[137] N.H. Tran, K.Y.H. Gin, Occurrence and removal of pharmaceuticals, hormones, personal care products, and endocrine disrupters in a full-scale water reclamation plant, Sci. Total Environ. 599–600 (2017) 1503–1516. https://doi.org/10.1016/j.scitotenv.2017.05.097.

[138] J. Sipma, B. Osuna, N. Collado, H. Monclús, G. Ferrero, J. Comas, I. Rodriguez-Roda, Comparison of removal of pharmaceuticals in MBR and activated sludge systems, Desalination. 250 (2010) 653–659. https://doi.org/10.1016/j.desal.2009.06.073.

[139] D.B. Miklos, C. Remy, M. Jekel, K.G. Linden, J.E. Drewes, U. Hübner, Evaluation of advanced oxidation processes for water and wastewater treatment – A critical review, Water Res. 139 (2018) 118–131. https://doi.org/10.1016/j.watres.2018.03.042.

[140] P.V. Nidheesh, C. Couras, A. V Karim, H. Nadais, P. Veetil, C. Couras, A. V Karim, H. Nadais, A review of integrated advanced oxidation processes and biological processes for organic pollutant removal, Chem. Eng. Commun. 0 (2021) 1–43. https://doi.org/10.1080/00986445.2020.1864626.

[141] R. Xiao, L. Gao, Z. Wei, R. Spinney, S. Luo, D. Wang, D.D. Dionysiou, J. Tang, W. Yang, Mechanistic insight into degradation of endocrine disrupting chemical by hydroxyl radical : An experimental and theoretical approach *, Environ. Pollut. 231 (2017) 1446–1452. https://doi.org/10.1016/j.envpol.2017.09.006.

[142] K. Rusevova Crincoli, S.G. Huling, Contrasting hydrogen peroxide- and persulfate-driven oxidation systems: Impact of radical scavenging on treatment efficiency and cost, Chem. Eng. J. 404 (2021). https://doi.org/10.1016/J.CEJ.2020.126404.

[143] H. Zhou, D.W. Smith, Advanced technologies in water and wastewater treatment, Can. J. Civ. Eng. 28 (2001) 49–66. https://doi.org/10.1139/l00-091.

[144] S. Giannakis, K.A. Lin, F. Ghanbari, A review of the recent advances on the treatment of industrial wastewaters by Sulfate Radical-based Advanced Oxidation Processes (SR-AOPs), Chem. Eng. J. 406 (2021) 127083. https://doi.org/10.1016/j.cej.2020.127083.

[145] P. Tikker, N. Dulova, I. Kornev, S. Preis, Effects of persulfate and hydrogen peroxide on oxidation of oxalate by pulsed corona discharge, Chem. Eng. J. 411 (2021) 128586. https://doi.org/10.1016/j.cej.2021.128586.

[146] X. Xia, F. Zhu, J. Li, H. Yang, L. Wei, Q. Li, J. Jiang, G. Zhang, Q. Zhao, A Review Study on Sulfate-Radical-Based Advanced Oxidation Processes for Domestic/Industrial Wastewater Treatment: Degradation, Efficiency, and Mechanism, Front. Chem. 8 (2020). https://doi.org/10.3389/fchem.2020.592056.

[147] P. Mako, G. Boczkaj, Treatment of bitumen post oxidative ef fl uents by sulfate radicals based advanced oxidation processes (S-AOPs) under alkaline pH conditions, 195 (2018) 374–384. https://doi.org/10.1016/j.jclepro.2018.05.207.

[148] I.A. Ike, K.G. Linden, J.D. Orbell, M. Duke, Critical review of the science and sustainability of persulphate advanced oxidation processes, Chem. Eng. J. 338 (2018) 651–669. https://doi.org/10.1016/j.cej.2018.01.034.

[149] M. Watson, J. Agbaba, Environmental Science Water Research & Technology Degradation of a chloroacetanilide herbicide in natural waters using UV activated hydrogen peroxide , persulfate and peroxymonosulfate, (2020). https://doi.org/10.1039/d0ew00358a.

[150] C. Amor, J.R. Fernandes, M.S. Lucas, J.A. Peres, Environmental Technology & Innovation Hydroxyl and sulfate radical advanced oxidation processes : Application to an agro-industrial wastewater, Environ. Technol. Innov. 21 (2021) 101183. https://doi.org/10.1016/j.eti.2020.101183.

[151] T. Olmez-hanci, I. Arslan-alaton, Comparison of sulfate and hydroxyl radical based advanced oxidation of phenol, Chem. Eng. J. 224 (2013) 10–16. https://doi.org/10.1016/j.cej.2012.11.007.

[152] H. V Lutze, K. Grübel, V.V.T. Padil, Č. Miroslav, D.D. Dionysiou, Chemistry of persulfates in water and wastewater treatment : A review, 330 (2017) 44–62. https://doi.org/10.1016/j.cej.2017.07.132.

[153] K. Fedorov, M. Plata-gryl, J. Ali, G. Boczkaj, Ultrasound-assisted heterogeneous activation of persulfate and peroxymonosulfate by asphaltenes for the degradation of BTEX in water, J. Hazard. Mater. 397 (2020) 122804. https://doi.org/10.1016/j.jhazmat.2020.122804.

[154] Q. Zhong, Q. Lin, W. He, H. Fu, Z. Huang, Y. Wang, Study on the nonradical pathways of nitrogen-doped biochar activating persulfate for tetracycline degradation, Sep. Purif. Technol. 276 (2021) 119354. https://doi.org/10.1016/j.seppur.2021.119354.

[155] K. Fedorov, X. Sun, G. Boczkaj, Combination of hydrodynamic cavitation and SR-AOPs for simultaneous degradation of BTEX in water, Chem. Eng. J. 417 (2021) 128081. https://doi.org/10.1016/j.cej.2020.128081.

[156] Y. Ji, Y. Shi, Y. Yang, P. Yang, L. Wang, J. Lu, J. Li, L. Zhou, C. Ferronato, J. Chovelon, Rethinking sulfate radical-based oxidation of nitrophenols : Formation of toxic polynitrophenols , nitrated biphenyls and diphenyl ethers, J. Hazard. Mater. 361 (2019) 152–161. https://doi.org/10.1016/j.jhazmat.2018.08.083.

[157] L. Gao, Q. Mao, S. Luo, L. Cao, X. Xie, Y. Yang, Experimental and theoretical insights into kinetics and mechanisms of hydroxyl and sulfate radicals-mediated degradation of sulfamethoxazole : Similarities and differences *, Environ. Pollut. 259 (2020) 113795. https://doi.org/10.1016/j.envpol.2019.113795.

[158] E. Brillas, S. Garcia-Segura, Benchmarking recent advances and innovative technology approaches of Fenton, photo-Fenton, electro-Fenton, and related processes: A review on the relevance of phenol as model molecule, Sep. Purif. Technol. 237 (2020) 116337. https://doi.org/10.1016/j.seppur.2019.116337.

[159] R. Ameta, A.K. Chohadia, A. Jain, P.B. Punjabi, Fenton and Photo-Fenton Processes, Adv. Oxid. Process. Wastewater Treat. Emerg. Green Chem. Technol. (2018) 49–87. https://doi.org/10.1016/B978-0-12-810499-6.00003-6.

[160] R.H. Waldemer, P.G. Tratnyek, R.L. Johnson, J.T. Nurmi, Oxidation of chlorinated ethenes by heat-activated persulfate: Kinetics and products, Environ. Sci. Technol. 41 (2007) 1010–1015. https://doi.org/10.1021/es062237m.

[161] A. De Luca, R.F. Dantas, S. Esplugas, Assessment of iron chelates efficiency forphoto-Fenton at neutral pH, Water Res. 61 (2014) 232–242. https://doi.org/10.1016/j.watres.2014.05.033.

[162] G. Pliego, P. Garcia-Muñoz, J.A. Zazo, J.A. Casas, J.J. Rodriguez, Improving the Fenton process by visible LED irradiation, Environ. Sci. Pollut. Res. 23 (2016) 23449–23455. https://doi.org/10.1007/s11356-016-7543-y.

[163] J.A. Ortega-Méndez, J.A. Herrera-Melián, J. Araña, M.R. Espino-Estévez, J.M. Doña-Rodríguez, Performance and Economic Assessment of the Treatment of Phenol with TiO2 Photocatalysis, Photo-Fenton, Biological Aerated Filter, and Wetland Reactors, Chem. Eng. Technol. 40 (2017) 1165–1175. https://doi.org/10.1002/ceat.201600159.

[164] G. Prasannamedha, P.S. Kumar, A review on contamination and removal of sulfamethoxazole from aqueous solution using cleaner techniques: Present and future perspective, J. Clean. Prod. 250 (2020). https://doi.org/10.1016/j.jclepro.2019.119553.

[165] Q. Li, H. Kong, R. Jia, J. Shao, Y. He, Enhanced catalytic degradation of amoxicillin with TiO2-Fe3O4 composites: Via a submerged magnetic separation membrane photocatalytic reactor (SMSMPR), RSC Adv. 9 (2019) 12538–12546. https://doi.org/10.1039/c9ra00158a.

[166] G. Divyapriya, I.M. Nambi, J. Senthilnathan, Nanocatalysts in fenton based advanced oxidation process for water and wastewater treatment, J. Bionanoscience. 10 (2016) 356–368. https://doi.org/10.1166/jbns.2016.1387.

[167] J. An, L. Zhu, Y. Zhang, H. Tang, Efficient visible light photo-Fenton-like degradation of organic pollutants using in situ surface-modified BiFeO3 as a catalyst, J. Environ. Sci. (China). 25 (2013) 1213–1225. https://doi.org/10.1016/S1001-0742(12)60172-7.

[168] ISO11733, ISO 11733:2004 Water quality — Determination of the elimination and biodegradability of organic compounds in an aqueous medium — Activated sludge simulation test, (2004). https://www.iso.org/standard/34416.html.

[169] R.K. Rowe, J.F. VanGulck, S.C. Millward, Biologically induced clogging of a granular medium permeated with synthetic leachate, J. Environ. Eng. Sci. 1 (2002) 135–156. https://doi.org/10.1139/S02-008.

[170] A. Ioannidi, O.S. Arvaniti, M.-C. Nika, R. Aalizadeh, N.S. Thomaidis, D. Mantzavinos, Z. Frontistis, Removal of drug losartan in environmental aquatic matrices by heat-activated persulfate: Kinetics, transformation products and synergistic effects, Chemosphere. 287 (2022) 131952. https://doi.org/10.1016/j.chemosphere.2021.131952.

[171] Y.N. Kanafin, Y. Kakimov, A. Adamov, A. Makhatova, A. Yeshmuratov, S.G. Poulopoulos, V.J. Inglezakis, E. Arkhangelsky, The effect of caffeine, metronidazole and ibuprofen on continuous flow activated sludge process, J. Chem. Technol. Biotechnol. 96 (2021) 1370–1380. https://doi.org/https://doi.org/10.1002/jctb.6658.

[172] Y.N. Kanafin, P. Abdirova, E. Arkhangelsky, D.D. Dionysiou, S.G. Poulopoulos, UVA and goethite activated persulfate oxidation of landfill leachate, Chem. Eng. J. Adv. 14 (2023) 100452. https://doi.org/10.1016/j.ceja.2023.100452.

[173] Y.N. Kanafin, P. Abdirova, D. Kanafina, E. Arkhangelsky, G.Z. Kyzas, S.G. Poulopoulos, UV and Zero-Valent Iron (ZVI) Activated Continuous Flow Persulfate Oxidation of Municipal Wastewater, Catalysts. 13 (2022) 25. https://doi.org/10.3390/catal13010025.

[174] Y.N. Kanafin, A. Satayeva, P. Abdirova, V.J. Inglezakis, E. Arkhangelsky, S.G. Poulopoulos, Membrane bioreactor and advanced oxidation processes for combined treatment of synthetic wastewater containing naproxen, bisphenol A, and sulfamethoxazole, J. Water Process Eng. 55 (2023) 104250. https://doi.org/10.1016/j.jwpe.2023.104250.

[175] R. Venkataraghavan, R. Thiruchelvi, D. Sharmila, Statistical optimization of textile dye effluent adsorption by Gracilaria edulis using Plackett-Burman design and response surface methodology, Heliyon. 6 (2020) e05219. https://doi.org/10.1016/j.heliyon.2020.e05219.

[176] T.Q.Q. Viet, V.H. Khoi, N. Thi Huong Giang, H. Thi Van Anh, N.M. Dat, M.T. Phong, N.H. Hieu, Statistical screening and optimization of photocatalytic degradation of methylene blue by ZnO–TiO2/rGO nanocomposite, Colloids Surfaces A Physicochem. Eng. Asp. 629 (2021) 127464. https://doi.org/10.1016/j.colsurfa.2021.127464.

[177] Q. Sui, X. Cao, S. Lu, W. Zhao, Z. Qiu, G. Yu, Occurrence, sources and fate of pharmaceuticals and personal care products in the groundwater: A review, Emerg. Contam. 1 (2015) 14–24. https://doi.org/10.1016/j.emcon.2015.07.001.

[178] R. Chen, H. Jiang, Y.Y. Li, Caffeine degradation by methanogenesis: Efficiency in anaerobic membrane bioreactor and analysis of kinetic behavior, Chem. Eng. J. 334 (2018) 444–452. https://doi.org/10.1016/j.cej.2017.10.052.

[179] P. Mazzafera, Degradaç ão de cafeína por microrganismos e o emprego da palha e polpa de café descafeinados na alimentaç ão animal, Sci. Agric. 59 (2002) 815–821. https://doi.org/10.1590/S0103-90162002000400030.

[180] S. Nanjundaiah, S. Mutturi, P. Bhatt, Modeling of caffeine degradation kinetics during cultivation of Fusarium solani using sucrose as co-substrate, Biochem. Eng. J. 125 (2017) 73–80. https://doi.org/10.1016/j.bej.2017.05.018.

[181] B.R. Mohapatra, N. Harris, R. Nordin, A. Mazumder, Purification and characterization of a novel caffeine oxidase from Alcaligenes species, J. Biotechnol. 125 (2006) 319–327. https://doi.org/10.1016/j.jbiotec.2006.03.018.

[182] A. Aboudalle, F. Fourcade, A.A. Assadi, L. Domergue, H. Djelal, T. Lendormi, S. Taha, A. Amrane, Reactive oxygen and iron species monitoring to investigate the electro-Fenton performances. Impact of the electrochemical process on the biodegradability of metronidazole and its by-products, Chemosphere. 199 (2018) 486–494. https://doi.org/10.1016/j.chemosphere.2018.02.075.

[183] B. Halling-Sørensen, Inhibition of aerobic growth and nitrification of bacteria in sewage sludge by antibacterial agents, Arch. Environ. Contam. Toxicol. 40 (2001) 451–460. https://doi.org/10.1007/s002440010197.

[184] S. Han, K. Choi, J. Kim, K. Ji, S. Kim, B. Ahn, J. Yun, K. Choi, J.S. Khim, X. Zhang, J.P. Giesy, Endocrine disruption and consequences of chronic exposure to ibuprofen in Japanese medaka (Oryzias latipes) and freshwater cladocerans Daphnia magna and Moina macrocopa, Aquat. Toxicol. 98 (2010) 256–264. https://doi.org/10.1016/J.AQUATOX.2010.02.013.

[185] H. Shemer, Y.K. Kunukcu, K.G. Linden, Degradation of the pharmaceutical Metronidazole via UV, Fenton and photo-Fenton processes, Chemosphere. 63 (2006) 269–276. https://doi.org/10.1016/j.chemosphere.2005.07.029.

[186] S.A. Abdullah, N.M. Majdi, S. Fatin, R. Shikh, N. Abdullah, A. Yuzir, Research

Journal of Pharmaceutical , Biological and Chemical Sciences Sequencing Batch Reactor for Treatment of Palm Oil Mill Effluent . September - October, Res. J. Pharm. Biol. Chem. Sci. 5 (2014) 1242–1249.

[187] M. Nsenga Kumwimba, F. Meng, Roles of ammonia-oxidizing bacteria in improving metabolism and cometabolism of trace organic chemicals in biological wastewater treatment processes: A review, Sci. Total Environ. 659 (2019) 419–441. https://doi.org/10.1016/J.SCITOTENV.2018.12.236.

[188] H. Sargsyan, L. Gabrielyan, A. Trchounian, Concentration-dependent effects of metronidazole, inhibiting nitrogenase, on hydrogen photoproduction and proton-translocating ATPase activity of Rhodobacter sphaeroides, Int. J. Hydrogen Energy. 39 (2014) 100–106. https://doi.org/10.1016/j.ijhydene.2013.10.049.

[189] Y. Jia, L. Yin, S.K. Khanal, H. Zhang, A.S. Oberoi, H. Lu, Biotransformation of ibuprofen in biological sludge systems: Investigation of performance and mechanisms, Water Res. 170 (2020) 115303. https://doi.org/10.1016/j.watres.2019.115303.

[190] J.R. Lawrence, G.D.W. Swerhone, L.I. Wassenaar, T.R. Neu, Effects of selected pharmaceuticals on riverine biofilm communities, Can. J. Microbiol. 51 (2005) 655–669. https://doi.org/10.1139/w05-047.

[191] M. Majewsky, T. Gallé, V. Yargeau, K. Fischer, Active heterotrophic biomass and sludge retention time (SRT) as determining factors for biodegradation kinetics of pharmaceuticals in activated sludge, Bioresour. Technol. 102 (2011) 7415–7421. https://doi.org/10.1016/j.biortech.2011.05.032.

[192] K. Brown, A.J. Ghoshdastidar, J. Hanmore, J. Frazee, A.Z. Tong, Membrane bioreactor technology: A novel approach to the treatment of compost leachate, Waste Manag. 33 (2013) 2188–2194. https://doi.org/10.1016/j.wasman.2013.04.006.

[193] S. Hena, L. Gutierrez, J.P. Croué, Removal of metronidazole from aqueous media by C. vulgaris, J. Hazard. Mater. 384 (2019). https://doi.org/10.1016/j.jhazmat.2019.121400.

[194] M. Davids, D. Gudra, I. Radovica-Spalvina, D. Fridmanis, V. Bartkevics, O. Muter, The effects of ibuprofen on activated sludge: Shift in bacterial community structure and resistance to ciprofloxacin, J. Hazard. Mater. 340 (2017) 291–299. https://doi.org/10.1016/j.jhazmat.2017.06.065.

[195] Wastewater Technology Fact Sheet Sequencing Batch Reactors, (1999).

[196] K. Kołecka, M. Gajewska, S. Cytawa, P. Stepnowski, M. Caban, Is sequential batch reactor an efficient technology to protect recipient against non-steroidal anti-inflammatory drugs and paracetamol in treated wastewater?, Bioresour. Technol. 318 (2020). https://doi.org/10.1016/J.BIORTECH.2020.124068.

[197] T.A. Larsen, J. Lienert, A. Joss, H. Siegrist, How to avoid pharmaceuticals in the aquatic environment, J. Biotechnol. 113 (2004) 295–304. https://doi.org/10.1016/j.jbiotec.2004.03.033.

[198] M. Sajjad, K.S. Kim, A study on TOC and nutrients removal in SBR and CFSTR systems in relation to sludge EPS during granulation process, Desalin. Water Treat. 55 (2015) 1683–1689. https://doi.org/10.1080/19443994.2014.943062.

[199] H.J. Knackmuss, Basic knowlegde and perpectives of bioelimination of xenobiotic compounds, J. Biotechnol. 51 (1996) 287–295. https://doi.org/10.1016/S0168-

1656(96)01608-2.

[200] P. Guerra, M. Kim, S. Teslic, M. Alaee, S.A. Smyth, Bisphenol-A removal in various wastewater treatment processes : Operational conditions, mass balance, and optimization, J. Environ. Manage. 152 (2015) 192–200. https://doi.org/10.1016/j.jenvman.2015.01.044.

[201] X. Chen, J. Zhao, L. Bao, L. Wang, The investigation of different pollutants and operation processes on sludge toxicity in sequencing batch bioreactors, Environ. Technol. 3330 (2016). https://doi.org/10.1080/09593330.2016.1140813.

[202] Y. Tang, X. Li, Z. Xu, Q. Guo, C. Hong, Y. Bing, Removal of naproxen and bezafibrate by activated sludge under aerobic conditions : Kinetics and effect of substrates, (n.d.). https://doi.org/10.1002/bab.1168.

[203] C. Geng, Fate of 14 C-acetyl sulfamethoxazole during the activated sludge process, (2019).

[204] N. Collado, G. Buttiglieri, E. Marti, L. Ferrando-Climent, S. Rodriguez-Mozaz, D. Barceló, J. Comas, I. Rodriguez-Roda, Effects on activated sludge bacterial community exposed to sulfamethoxazole, Chemosphere. 93 (2013) 99–106. https://doi.org/10.1016/j.chemosphere.2013.04.094.

[205] D.M. González-Pérez, J.I. Pérez, M.A. Gómez, Behaviour of the main nonsteroidal anti-inflammatory drugs in a membrane bioreactor treating urban wastewater at high hydraulic- and sludge-retention time, J. Hazard. Mater. 336 (2017) 128–138. https://doi.org/10.1016/J.JHAZMAT.2017.04.059.

[206] B. Seyhi, P. Drogui, G. Buelna, J.F. Blais, Biodegradation of Bisphenol-A in aerobic membrane bioreactor sludge, Water Sci. Technol. 68 (2013) 1926–1931. https://doi.org/10.2166/WST.2013.442.

[207] F.I. Hai, X. Li, W.E. Price, L.D. Nghiem, Removal of carbamazepine and sulfamethoxazole by MBR under anoxic and aerobic conditions, Bioresour. Technol. 102 (2011) 10386–10390. https://doi.org/10.1016/j.biortech.2011.09.019.

[208] S. Kim, K.H. Chu, Y.A.J. Al-Hamadani, C.M. Park, M. Jang, D.H. Kim, M. Yu, J. Heo, Y. Yoon, Removal of contaminants of emerging concern by membranes in water and wastewater: A review, Chem. Eng. J. 335 (2018) 896–914. https://doi.org/10.1016/j.cej.2017.11.044.

[209] Z. Hu, X. Si, Z. Zhang, X. Wen, Enhanced EDCs removal by membrane fouling during the UF process, Desalination. 336 (2014) 18–23. https://doi.org/10.1016/j.desal.2013.12.027.

[210] H. Yu, S. Shangguan, C. Xie, H. Yang, C. Wei, H. Rong, F. Qu, Chemical Cleaning and Membrane Aging in MBR for Textile Wastewater Treatment, Membranes (Basel). 12 (2022). https://doi.org/10.3390/membranes12070704.

[211] D. Sun, H. Zheng, W. Xue, Oxidation of phenol by persulfate activated with UV-light and Ag+, Adv. Mater. Res. 610–613 (2013) 1806–1809. https://doi.org/10.4028/www.scientific.net/AMR.610-613.1806.

[212] B. Wang, F. Wu, P. Li, N. Deng, UV-light induced photodegradation of bisphenol a in water: Kinetics and influencing factors, React. Kinet. Catal. Lett. 92 (2007) 3–9. https://doi.org/10.1007/s11144-007-5045-0.

[213] A. Cai, J. Deng, X. Ling, C. Ye, H. Sun, Y. Deng, S. Zhou, X. Li, Degradation of bisphenol A by UV/persulfate process in the presence of bromide: Role of reactive

bromine, Water Res. 215 (2022) 118288. https://doi.org/10.1016/j.watres.2022.118288.

[214] Y.Q. Gao, N.Y. Gao, W.H. Chu, Q.L. Yang, D.Q. Yin, Kinetics and mechanistic investigation into the degradation of naproxen by a UV/chlorine process, RSC Adv. 7 (2017) 33627–33634. https://doi.org/10.1039/c7ra04540a.

[215] E. Aydin, Photolysis of Naproxen under UV Light: Effect of Natural Organic Matter and Nitrate to Transformation Product Formation, Clean - Soil, Air, Water. 43 (2015) 59–66. https://doi.org/10.1002/clen.201300601.

[216] E. Borowska, E. Felis, K. Miksch, Degradation of sulfamethoxazole using UV and UV/H2O2 processes, J. Adv. Oxid. Technol. 18 (2015) 69–77. https://doi.org/10.1515/jaots-2015-0109.

[217] G. Gopalakrishnan, R.B. Jeyakumar, A. Somanathan, Challenges and Emerging Trends in Advanced Oxidation Technologies and Integration of Advanced Oxidation Processes with Biological Processes for Wastewater Treatment, Sustain. 15 (2023). https://doi.org/10.3390/su15054235.

[218] P. Fang, Z.J. Tang, X.B. Chen, J.H. Huang, Z.X. Tang, C.P. Cen, Removal of High-Concentration Sulfate Ions from the Sodium Alkali FGD Wastewater Using Ettringite Precipitation Method: Factor Assessment, Feasibility, and Prospect, J. Chem. 2018 (2018). https://doi.org/10.1155/2018/1265168.

[219] N.R. Mirza, R. Huang, E. Du, M. Peng, Z. Pan, H. Ding, G. Shan, L. Ling, Z. Xie, A review of the textile wastewater treatment technologies with special focus on advanced oxidation processes (Aops), membrane separation and integrated aop-membrane processes, Desalin. Water Treat. 206 (2020) 83–107. https://doi.org/10.5004/dwt.2020.26363.

[220] V. Del Nery, I.R. de Nardi, M.H.R.Z. Damianovic, E. Pozzi, A.K.B. Amorim, M. Zaiat, Long-term operating performance of a poultry slaughterhouse wastewater treatment plant, Resour. Conserv. Recycl. 50 (2007) 102–114. https://doi.org/10.1016/j.resconrec.2006.06.001.

[221] K. Eryuruk, U. Tezcan Un, U. Bakır Ogutveren, Electrochemical treatment of wastewaters from poultry slaughtering and processing by using iron electrodes, J. Clean. Prod. 172 (2018) 1089–1095. https://doi.org/10.1016/j.jclepro.2017.10.254.

[222] F. Meng, S. Zhang, Y. Oh, Z. Zhou, H.S. Shin, S.R. Chae, Fouling in membrane bioreactors: An updated review, Water Res. 114 (2017) 151–180. https://doi.org/10.1016/j.watres.2017.02.006.

[223] A.A. Zarei, P. Tavassoli, E. Bazrafshan, Evaluation of UV/S2O8 process efficiency for removal of metronidazole (MNZ) from aqueous solutions, Water Sci. Technol. 2017 (2018) 126–133. https://doi.org/10.2166/wst.2018.096.

[224] E.K. Silbergeld, Drinking Water and the Developing Brain., Cerebrum. 2016 (2016) 1–15. http://www.ncbi.nlm.nih.gov/pubmed/28058090%0Ahttp://www.pubmedcentral.nih.gov/articlerender.fcgi?artid=PMC5198753.

[225] K. Thirugnanasambandham, S. Kandasamy, V. Sivakumar, R.K. kumar, R. Mohanavelu, Modeling of by-product recovery and performance evaluation of Electro-Fenton treatment technique to treat poultry wastewater, J. Taiwan Inst. Chem. Eng. 46 (2015) 89–97. https://doi.org/10.1016/j.jtice.2014.09.004.

[226] C.F. Bustillo-Lecompte, S. Ghafoori, M. Mehrvar, Photochemical degradation of an actual slaughterhouse wastewater by continuous UV/H2O2 photoreactor with recycle, J. Environ. Chem. Eng. 4 (2016) 719–732. https://doi.org/10.1016/j.jece.2015.12.009.

[227] C. Bustillo-Lecompte, M. Mehrvar, Slaughterhouse Wastewater: Treatment, Management and Resource Recovery, Physico-Chemical Wastewater Treat. Resour. Recover. (2017). https://doi.org/10.5772/65499.

[228] C.F. Bustillo-Lecompte, M. Mehrvar, Slaughterhouse wastewater characteristics, treatment, and management in the meat processing industry: A review on trends and advances, J. Environ. Manage. 161 (2015) 287–302. https://doi.org/10.1016/j.jenvman.2015.07.008.

[229] Y.H. Cai, X.J. Yang, A.I. Schäfer, Removal of naturally occurring strontium by nanofiltration/reverse osmosis from groundwater, Membranes (Basel). 10 (2020) 1–23. https://doi.org/10.3390/membranes10110321.

[230] J. Vidal, C. Huiliñir, R. Salazar, Removal of organic matter contained in slaughterhouse wastewater using a combination of anaerobic digestion and solar photoelectro-Fenton processes, Electrochim. Acta. 210 (2016) 163–170. https://doi.org/10.1016/j.electacta.2016.05.064.

[231] L. Clarizia, D. Russo, I. Di Somma, R. Marotta, R. Andreozzi, Homogeneous photo-Fenton processes at near neutral pH: A review, Appl. Catal. B Environ. 209 (2017) 358–371. https://doi.org/10.1016/j.apcatb.2017.03.011.

[232] G.R.B. Marriott N. G., Schilling M. W., Sanitizers, in: Princ. Food. Sanit. Food Sci. Text Ser., Springer International Publishing AG, Cham, Switzerland, 2018: pp. 175–198. https://doi.org/10.1007/978-3-319-67166-6.

[233] K. Dutta, M.Y. Lee, W.W.P. Lai, C.H. Lee, A.Y.C. Lin, C.F. Lin, J.G. Lin, Removal of pharmaceuticals and organic matter from municipal wastewater using two-stage anaerobic fluidized membrane bioreactor, Bioresour. Technol. 165 (2014) 42–49. https://doi.org/10.1016/j.biortech.2014.03.054.

[234] X. Liu, Y. Liu, S. Lu, Z. Wang, Y. Wang, G. Zhang, X. Guo, W. Guo, T. Zhang, B. Xi, Degradation difference of ofloxacin and levofloxacin by UV/H2O2 and UV/PS (persulfate): Efficiency, factors and mechanism, Chem. Eng. J. 385 (2020) 123987. https://doi.org/10.1016/j.cej.2019.123987.

[235] X. Xin, S. Sun, A. Zhou, M. Wang, Y. Song, Q. Zhao, R. Jia, Sulfadimethoxine photodegradation in UV-C/H2O2 system: Reaction kinetics, degradation pathways, and toxicity, J. Water Process Eng. 36 (2020) 101293. https://doi.org/10.1016/j.jwpe.2020.101293.

[236] M. Li, M. Sun, H. Dong, J. Zhang, Y. Su, Z. Qiang, Enhancement of micropollutant degradation in UV/H2O2 process via iron-containing coagulants, Water Res. 172 (2020) 115497. https://doi.org/10.1016/j.watres.2020.115497.

[237] J.J. Pignatello, E. Oliveros, A. MacKay, Advanced oxidation processes for organic contaminant destruction based on the fenton reaction and related chemistry, Crit. Rev. Environ. Sci. Technol. 36 (2006) 1–84. https://doi.org/10.1080/10643380500326564.

[238] A. Makhatova, G. Ulykbanova, S. Sadyk, K. Sarsenbay, T.S. Atabaev, V.J. Inglezakis, S.G. Poulopoulos, Degradation and mineralization of 4-tert-butylphenol in water using Fe-doped TiO2 catalysts, Sci. Rep. 9 (2019) 1–15.

https://doi.org/10.1038/s41598-019-55775-7.

[239] X.Q. Chen, J.Y. Yang, J.S. Zhang, Preparation and photocatalytic properties of Fe-doped TiO2 nanoparticles, J. Cent. South Univ. Technol. (English Ed. 11 (2004) 161–165. https://doi.org/10.1007/s11771-004-0033-2.

[240] K. Bukhari, N. Ahmad, I.A. Sheikh, T.M. Akram, Effects of different parameters on photocatalytic oxidation of slaughterhouse wastewater using TiO 2 and silver-doped TiO 2 nanoparticles, Polish J. Environ. Stud. 28 (2019) 1591–1600. https://doi.org/10.15244/pjoes/90635.

[241] I. Velo-Gala, J.J. López-Peñalver, M. Sánchez-Polo, J. Rivera-Utrilla, Comparative study of oxidative degradation of sodium diatrizoate in aqueous solution by H2O2/Fe2+, H2O2/Fe3+, Fe (VI) and UV, H2O2/UV, K2S2O8/UV, Chem. Eng. J. 241 (2014) 504–512. https://doi.org/10.1016/j.cej.2013.10.036.

[242] A. Acosta-Rangel, M. Sánchez-Polo, A.M.S. Polo, J. Rivera-Utrilla, M.S. Berber-Mendoza, Sulfonamides degradation assisted by UV, UV/H2O2 and UV/K2S2O8: Efficiency, mechanism and byproducts cytotoxicity, J. Environ. Manage. 225 (2018) 224–231. https://doi.org/10.1016/j.jenvman.2018.06.097.

[243] C.F. Bustillo-Lecompte, M. Mehrvar, Treatment of an actual slaughterhouse wastewater by integration of biological and advanced oxidation processes: Modeling, optimization, and cost-effectiveness analysis, J. Environ. Manage. 182 (2016) 651–666. https://doi.org/10.1016/j.jenvman.2016.07.044.

[244] J. Páramo-Vargas, S.G. Granados, M.I. Maldonado-Rubio, J.M. Peralta-Hernández, Up to 95 % reduction of chemical oxygen demand of slaughterhouse effluents using Fenton and photo-Fenton oxidation, Environ. Chem. Lett. 14 (2016) 149–154. https://doi.org/10.1007/s10311-015-0534-2.

[245] K.V. Naderi, C.F. Bustillo-Lecompte, M. Mehrvar, M.J. Abdekhodaie, Combined UV-C/H2O2-VUV processes for the treatment of an actual slaughterhouse wastewater, J. Environ. Sci. Heal. - Part B Pestic. Food Contam. Agric. Wastes. 52 (2017) 314–325. https://doi.org/10.1080/03601234.2017.1281650.

[246] D. Ozturk, A.E. Yilmaz, Treatment of slaughterhouse wastewater with the electrochemical oxidation process: Role of operating parameters on treatment efficiency and energy consumption, J. Water Process Eng. 31 (2019) 100834. https://doi.org/10.1016/j.jwpe.2019.100834.

[247] C. Tan, D. Fu, N. Gao, Q. Qin, Y. Xu, H. Xiang, Kinetic degradation of chloramphenicol in water by UV/persulfate system, J. Photochem. Photobiol. A Chem. 332 (2017) 406–412. https://doi.org/10.1016/j.jphotochem.2016.09.021.

[248] Y. Xiao, L. Zhang, W. Zhang, K.Y. Lim, R.D. Webster, T.T. Lim, Comparative evaluation of iodoacids removal by UV/persulfate and UV/H 2 O 2 processes, Water Res. 102 (2016) 629–639. https://doi.org/10.1016/j.watres.2016.07.004.

[249] T. Ölmez-Hancı, İ. Arslan-Alaton, C. İmren, Performance of the Persulfate/UV-C Process for the Treatment of Dimethyl Phthalate from Aquatic Environments, Int. J. Environ. Geoinformatics. 5 (2016) 189–196. https://doi.org/10.30897/ijegeo.

[250] C.C. Lin, M.S. Wu, Degradation of ciprofloxacin by UV/S2O82- process in a large photoreactor, J. Photochem. Photobiol. A Chem. 285 (2014) 1–6. https://doi.org/10.1016/j.jphotochem.2014.04.002.

[251] D. Salari, A. Niaei, S. Aber, M.H. Rasoulifard, The photooxidative destruction of

C.I. Basic Yellow 2 using UV/S2O82- process in a rectangular continuous photoreactor, J. Hazard. Mater. 166 (2009) 61–66. https://doi.org/10.1016/j.jhazmat.2008.11.039.

[252] H. se Ou, J. Liu, J. shao Ye, L. lin Wang, N. yun Gao, J. Ke, Degradation of tris(2-chloroethyl) phosphate by ultraviolet-persulfate: Kinetics, pathway and intermediate impact on proteome of Escherichia coli, Chem. Eng. J. 308 (2017) 386–395. https://doi.org/10.1016/j.cej.2016.09.076.

[253] Y. qiong Gao, N. yun Gao, Y. Deng, D. qiang Yin, Y. sen Zhang, Degradation of florfenicol in water by UV/Na2S2O8 process, Environ. Sci. Pollut. Res. 22 (2015) 8693–8701. https://doi.org/10.1007/s11356-014-4054-6.

[254] C. Tan, X. Jian, L. Su, X. Lu, J. Huang, J. Deng, W. Chu, Kinetic removal of acetaminophen and phenacetin during LED-UV365 photolysis of persulfate system: Reactive oxygen species generation, Chemosphere. 269 (2021). https://doi.org/10.1016/j.chemosphere.2020.129337.

[255] Y. Deng, R. Zhao, Advanced Oxidation Processes (AOPs) in Wastewater Treatment, Curr. Pollut. Reports. 1 (2015) 167–176. https://doi.org/10.1007/s40726-015-0015-z.

[256] M.N. Pervez, W. He, T. Zarra, V. Naddeo, Y. Zhao, New sustainable approach for the production of Fe3O4/Graphene oxide-activated persulfate system for dye removal in real wastewater, Water (Switzerland). 12 (2020). https://doi.org/10.3390/w12030733.

[257] S. Renou, J.G. Givaudan, S. Poulain, F. Dirassouyan, P. Moulin, Landfill leachate treatment: Review and opportunity, J. Hazard. Mater. 150 (2008) 468–493. https://doi.org/10.1016/j.jhazmat.2007.09.077.

[258] H. Zhang, Y. Li, X. Wu, Y. Zhang, D. Zhang, Application of response surface methodology to the treatment landfill leachate in a three-dimensional electrochemical reactor, Waste Manag. 30 (2010) 2096–2102. https://doi.org/10.1016/j.wasman.2010.04.029.

[259] A.R. Ishak, F.S. Hamid, S. Mohamad, K.S. Tay, Stabilized landfill leachate treatment by coagulation-flocculation coupled with UV-based sulfate radical oxidation process, Waste Manag. 76 (2018) 575–581. https://doi.org/10.1016/j.wasman.2018.02.047.

[260] R. Li, S. Hong, X. Li, B. Zhang, H. Tian, Y. Huang, Optimization of photocatalytic degradation of Cefradine using a “green” goethite/H2O2 system, J. Ind. Eng. Chem. 78 (2019) 90–96. https://doi.org/10.1016/j.jiec.2019.06.035.

[261] S.S. Chung, J.S. Zheng, S.R. Burket, B.W. Brooks, Select antibiotics in leachate from closed and active landfills exceed thresholds for antibiotic resistance development, Environ. Int. 115 (2018) 89–96. https://doi.org/10.1016/j.envint.2018.03.014.

[262] J. Ding, L. Shen, R. Yan, S. Lu, Y. Zhang, X. Zhang, H. Zhang, Heterogeneously activation of H2O2 and persulfate with goethite for bisphenol A degradation: A mechanistic study, Chemosphere. 261 (2020) 127715. https://doi.org/10.1016/j.chemosphere.2020.127715.

[263] S. Hadi, E. Taheri, M.M. Amin, A. Fatehizadeh, T.M. Aminabhavi, Synergistic degradation of 4-chlorophenol by persulfate and oxalic acid mixture with heterogeneous Fenton like system for wastewater treatment: Adaptive neuro-fuzzy

inference systems modeling, J. Environ. Manage. 268 (2020). https://doi.org/10.1016/j.jenvman.2020.110678.

[264] R. Li, J. Kong, H. Liu, P. Chen, G. Liu, F. Li, W. Lv, A sulfate radical based ferrous-peroxydisulfate oxidative system for indomethacin degradation in aqueous solutions, RSC Adv. 7 (2017) 22802–22809. https://doi.org/10.1039/c7ra03364h.

[265] S.Y. Masouleh, M. Mozaffarian, B. Dabir, S.F. Ramezani, COD and ammonia removal from landfill leachate by UV/PMS/Fe2+ process: ANN/RSM modeling and optimization, Process Saf. Environ. Prot. 159 (2022) 716–726. https://doi.org/10.1016/j.psep.2022.01.031.

[266] H.T. Van, L.H. Nguyen, T.K. Hoang, T.T. Nguyen, T.N.H. Tran, T.B.H. Nguyen, X.H. Vu, M.T. Pham, T.P. Tran, T.T. Pham, H.D. Nguyen, H.P. Chao, C.C. Lin, X.C. Nguyen, Heterogeneous Fenton oxidation of paracetamol in aqueous solution using iron slag as a catalyst: Degradation mechanisms and kinetics: Iron slag-based heterogeneous Fenton degradation of paracetamol, Environ. Technol. Innov. 18 (2020) 100670. https://doi.org/10.1016/j.eti.2020.100670.

[267] X. Hua, X. Song, M. Yuan, D. Donga, The factors affecting relationship between COD and TOC of typical papermaking wastewater, Adv. Intell. Soft Comput. 105 (2011) 239–244. https://doi.org/10.1007/978-3-642-23756-0_39.

[268] L. Ziyang, Z. Youcai, Y. Tao, S. Yu, C. Huili, Z. Nanwen, H. Renhua, Natural attenuation and characterization of contaminants composition in landfill leachate under different disposing ages, Sci. Total Environ. 407 (2009) 3385–3391. https://doi.org/10.1016/j.scitotenv.2009.01.028.

[269] K.H. Kang, H.S. Shin, H. Park, Characterization of humic substances present in landfill leachates with different landfill ages and its implications, Water Res. 36 (2002) 4023–4032. https://doi.org/10.1016/S0043-1354(02)00114-8.

[270] A. Makhatova, B. Mazhit, Y. Sarbassov, K. Meiramkulova, V.J. Inglezakis, S.G. Poulopoulos, Effective photochemical treatment of a municipal solid waste landfill leachate, PLoS One. 15 (2020) 1–22. https://doi.org/10.1371/journal.pone.0239433.

[271] B. Jiang, J. Wang, L. Chen, Y. Sun, X. Wang, J. Ruan, Experimental Study on the Treatment of Landfill Leachate by Electro-Assisted ZVI/UV Synergistic Activated Persulfate System, Catalysts. 12 (2022). https://doi.org/10.3390/catal12070768.

[272] Q. Yang, Y. Zhong, H. Zhong, X. Li, W. Du, X. Li, R. Chen, G. Zeng, A novel pretreatment process of mature landfill leachate with ultrasonic activated persulfate: Optimization using integrated Taguchi method and response surface methodology, Process Saf. Environ. Prot. 98 (2015) 268–275. https://doi.org/10.1016/j.psep.2015.08.009.

[273] J. Antony, S. V. Niveditha, R. Gandhimathi, S.T. Ramesh, P. V. Nidheesh, Stabilized landfill leachate treatment by zero valent aluminium-acid system combined with hydrogen peroxide and persulfate based advanced oxidation process, Waste Manag. 106 (2020) 1–11. https://doi.org/10.1016/j.wasman.2020.03.005.

[274] A.M. Soubh, M. Baghdadi, M.A. Abdoli, B. Aminzadeh, Activation of persulfate using an industrial iron-rich sludge as an efficient nanocatalyst for landfill leachate treatment, Catalysts. 8 (2018). https://doi.org/10.3390/catal8050218.

[275] E. Kattel, N. Dulova, Ferrous ion-activated persulphate process for landfill leachate treatment: removal of organic load, phenolic micropollutants and nitrogen, Environ. Technol. (United Kingdom). 38 (2017) 1223–1231.

https://doi.org/10.1080/09593330.2016.1221472.

[276] M. Ridhwan, M. Hafiz, D. Othman, R. Abu, M. Hafiz, A.F. Ismail, A. Mustafa, M.A. Rahman, J. Jaafar, Current trends and future prospects of ammonia removal in wastewater : A comprehensive review on adsorptive membrane development, Sep. Purif. Technol. 213 (2019) 114–132. https://doi.org/10.1016/j.seppur.2018.12.030.

[277] V.J. Inglezakis, A. Amzebek, B. Kuspangaliyeva, Y. Sarbassov, G. Balbayeva, A. Yerkinova, S.G. Poulopoulos, Treatment of municipal solid waste landfill leachate by use of combined biological, physical and photochemical processes, Desalin. Water Treat. 112 (2018) 218–231. https://doi.org/10.5004/dwt.2018.22252.

[278] F. Ghanbari, J. Wu, M. Khatebasreh, D. Ding, K.Y.A. Lin, Efficient treatment for landfill leachate through sequential electrocoagulation, electrooxidation and PMS/UV/CuFe2O4 process, Sep. Purif. Technol. 242 (2020). https://doi.org/10.1016/j.seppur.2020.116828.

APPENDICES

Table S6.1. The description of FTIR spectra of the poultry wastewater.

Wavelength (cm^{-1})	Vibration	Functional group or component
3343	O–H stretching	Bonded and non-bonded hydroxyl groups and water
	≡C-H stretching	Alkyne group
2337	C-N	Cyanides (nitriles), cyanates, isocyanates, thiocyanates, and diazo compounds
1636	C=C stretching	Alkene and aromatic ring
	C=O stretching	Carboxylate and amide I
	O-H bending	Absorbed water
	N-H bending	Amines
497	C-Br	Bromide
	C-I	Chloride

Table S6.2. Comparison of different AOPs applied for slaughterhouse wastewater treatment

#	Type of wastewater	Technology	Experimental conditions	Removal rate, %	Ref.
a	Slaughterhouse wastewater [TOC = 50 mg/L]	$UV_{254\ nm}/H_2O_2$ continuous photoreactor with recycle	Flow rate = 75 ml/min, H_2O_2 = 500 mg/L, pH 7	TOC (99.89%)	[243]
b	Slaughterhouse wastewater [TOC = 23.9 mg/L]	$UV_{254\ nm}/H_2O_2$ continuous photoreactor with recycle	Flow rate = 15.2 ml/min, H_2O_2 = 861.5 mg/L, pH 6.9	TOC (81%)	[226]
c	Slaughterhouse wastewater after anaerobic digestion [COD = 1159 mg/L]	Solar photo-Fenton	H_2O_2 = 200 mg/L, Fe^{2+} = 55.8 mg/L, pH 3	COD (92%)	[244]
d	Slaughterhouse wastewater [TOC = 213 mg/L]	UV-C/H_2O_2/Vacuum UV process	H_2O_2 = 450 mg/L, irradiation time = 9 min, treatment time 2.4 h, pH 6.0-7.1	TOC (45.7%)	[245]
e	Poultry slaughterhouse wastewater [COD = 2932 mg/L]	Electro-Fenton process	Iron electrodes, pH 4.38,current density 74.1 mA/cm^2, molar ratio (H_2O_2/Fe^{2+}) 3.7, H_2O_2 to wastewater ratio 1.6 mL/L, treatment time 55.6 min	COD (92.37%)	[22]
f	Slaughterhouse wastewater [TOC = 4429 – 10250 mg/L, Total COD = 17626 – 23268 mg/L]	Electrochemical oxidation	Ti/Pt anode, interelectrode gap 3 mm, 0.025M NaCl, current density 4.73 mA/cm^2, treatment time 4 h, pH 7	TOC (88%), COD (92.2%)	[246]
g	Poultry slaughterhouse wastewater [TC = 115.6 mg/L, TOC = 68.66 mg/L]	$UV_{254\ nm}$ /$K_2S_2O_8$	$K_2S_2O_8$ = 15 mM	TOC (85%)	Current work
h	Poultry slaughterhouse wastewater [TC = 115.6 mg/L, TOC = 68.66 mg/L]	$UV_{254\ nm}$ / H_2O_2	H_2O_2 = 98 mM, Fe^{2+} = 20 mg/L, pH 3.3	TOC (82.5%)	Current work

Table S6.3. Comparison of energy per order (E_{EO}) values of persulfate based AOPs.

Type of wastewater	Method	Energy per order, kWh/m^3/order	Ref.
0.03 mM chloramphenicol solution	$UV_{254\ nm}/Na_2S_2O_8$ [1 mM]	16.76	[247]
1.5 μM ICH_2CO_2H (iodinated disinfection by-product) solution	$UV_{254\ nm}/Na_2S_2O_8$ [60 μM]	0.39	[248]
0.515 mM dimethylphthalate solution	$UV_{253.7\ nm}/K_2S_2O_8$ [30 mM]	1.79	[249]
10 mg/L ciprofloxacin solution	$UV_{254\ nm}/Na_2S_2O_8$ [3.84 g/L]	0.653	[250]
1.5 μM florfenicol solution	$UV_{254\ nm}/Na_2S_2O_8$ [2 mM]	415.58	[253]
10 μM of phenacetin and acetaminophen, 10 mM sodium dihydrogen phosphate dihydrate solution	LED-$UV_{365\ nm}$/ $Na_2S_2O_8$ [2 mM]	0.589	[254]
40 mg/L metronidazole solution	$UV/Na_2S_2O_8$ [1 g/L]	3.49	[223]
Decolorization of 20 mg/L C.I. Basic Yellow 2 solution	$UV_{254\ nm}/K_2S_2O_8$ [5 mM]	4.23	[251]
3.5 μM tris(2- chloroethyl) phosphate solution	$UV_{254\ nm}/Na_2S_2O_8$ [175 μM]	0.0290	[252]
Poultry SWW [TC = 115.6 mg/L, TOC = 68.66 mg/L]	$UV_{254\ nm}$ /$K_2S_2O_8$ [15 mM]	226	Current work
Poultry SWW [TC = 115.6 mg/L, TOC = 68.66 mg/L]	$UV_{254\ nm}$ /$K_2S_2O_8$ [15 mM] /Fe^{2+} [20 mg/L]	325	Current work

Table S7.1. The municipal wastewater treatment experiments with confidence intervals.

Run	Experimental variables				Actual responses		95% Confidence intervals	
	Time	pH	$K_2S_2O_8$, mM	$K_2S_2O_8$ / Fe^{2+}	TC	TOC	TC	TOC
1	60	5.35	30	10	56.35	45.79	(45.09; 64.45)	(39.28; 60.55)
2	100	3	30	10	50.8	27.98	(38.50; 57.86)	(22.14; 43.42)
3	140	5.35	20	7.5	60.69	58.06	(47.87; 67.22)	(50.90; 72.17)
4	100	3	10	10	68.35	53.03	(55.83; 75.18)	(46.19; 67.47)
5	140	3	20	10	58.5	46.89	(54.85; 74.20)	(41.61; 62.89)
6	140	5.35	30	10	71.31	73.9	(53.89; 73.25)	(59.03; 80.30)
7	100	5.35	20	10	50.96	55.74	(40.21; 54.84)	(47.83; 63.91)
8	100	7.7	10	10	39.86	76.27	(27.62; 46.98)	(61.95; 83.22)
9	100	5.35	20	10	47.17	59.64	(40.21; 54.84)	(47.83; 63.91)
10	60	5.35	20	7.5	68.24	46.06	(54.62; 73.98)	(38.94; 60.21)
11	60	3	20	10	65.61	24.68	(56.60; 75.95)	(11.00; 32.27)
12	60	5.35	10	10	57.39	56.96	(53.61; 72.97)	(49.77; 71.04)
13	140	5.35	20	12.5	61.69	63.61	(50.78; 70.13)	(50.57; 71.84)
14	100	7.7	20	12.5	46.36	72.34	(37.31; 56.67)	(64.37; 85.64)
15	100	3	20	7.5	60.63	37.45	(48.48; 67.84)	(23.36; 44.64)
16	140	7.7	20	10	49.32	67.99	(45.99; 65.35)	(60.07; 81.34)
17	100	3	20	12.5	57.51	55.8	(49.07; 68.43)	(37.70; 58.97)
18	100	5.35	20	10	44.44	52.23	(40.21; 54.84)	(47.83; 63.91)
19	100	7.7	20	7.5	55.07	79.09	(42.31; 61.67)	(75.13; 96.41)
20	60	5.35	20	12.5	59.01	55.83	(47.30; 66.66)	(42.83; 64.11)
21	100	5.35	10	7.5	46.11	60.96	(39.12; 58.48)	(46.05; 67.32)
22	100	5.35	30	12.5	44.19	53.94	(38.84; 58.19)	(47.25; 68.52)
23	60	7.7	20	10	56.21	87.31	(47.52; 66.88)	(70.98; 92.26)
24	100	7.7	30	10	60.79	98.15	(48.78; 68.14)	(84.83; 106.1)
25	100	5.35	10	12.5	54.74	66.9	(42.13; 61.49)	(61.88; 83.16)
26	100	5.35	30	7.5	45.98	76.1	(46.25; 65.61)	(59.51; 80.79)
27	140	5.35	10	10	51.47	65.26	(41.53; 60.89)	(49.71; 70.99)

Table 7.2. Confidence interval (CI) of TC model coefficients (coded).

Term	Coef	SE Coef	95% CI Low	95% CI High	P-Value
Constant	45.6	12.6	18.2	73.1	0.003
X_1	-2.31	6.29	-16.02	11.39	0.72
X_2	-0.57	6.29	-14.27	13.14	0.929
X_3	1.21	6.29	-12.5	14.91	0.851
X_4	10.46	6.29	-3.25	24.16	0.122
X_1*X_1	-12.27	9.44	-32.83	8.28	0.218
X_2*X_2	-13.58	9.44	-34.14	6.97	0.176
X_3*X_3	-9.4	9.44	-29.96	11.15	0.339
X_4*X_4	4.6	9.44	-15.95	25.16	0.634
X_1*X_2	3.6	10.9	-20.1	27.3	0.747
X_1*X_3	-7.4	10.9	-31.1	16.4	0.511
X_1*X_4	-1.2	10.9	-24.9	22.5	0.915
X_2*X_3	8.6	10.9	-15.1	32.4	0.443
X_2*X_4	-6.7	10.9	-30.5	17	0.549
X_3*X_4	-7.2	10.9	-30.9	16.5	0.521

Table 7.3. Confidence interval (CI) of TOC model coefficients (coded).

Term	Coef	SE Coef	95% CI Low	95% CI High	P-Value
Constant	55.87	3.69	47.83	63.91	0
X_1	4.92	1.85	0.9	8.94	0.02
X_2	19.61	1.85	15.59	23.63	0
X_3	-0.29	1.85	-4.31	3.73	0.876
X_4	0.89	1.85	-3.13	4.91	0.638
X_1*X_1	-1.82	2.77	-7.85	4.21	0.522
X_2*X_2	2.51	2.77	-3.52	8.54	0.383
X_3*X_3	6.04	2.77	0.01	12.07	0.05
X_4*X_4	2.4	2.77	-3.63	8.43	0.403
X_1*X_2	-10.38	3.2	-17.35	-3.42	0.007
X_1*X_3	4.95	3.2	-2.01	11.92	0.147
X_1*X_4	-1.05	3.2	-8.02	5.91	0.747
X_2*X_3	11.73	3.2	4.77	18.7	0.003
X_2*X_4	-6.28	3.2	-13.24	0.69	0.073
X_3*X_4	-7.02	3.2	-13.99	-0.06	0.048

Table S7.4. Intermediates of the photo-Fenton like oxidation of the municipal wastewater.

Run	OC, mg L^{-1}				
	Initial	**Formic acid**	**Acetic acid**	**Mineralized (CO_2)**	**Remaining intermediates**
1	20.30	0.00	0.42	9.30	10.58
2	20.62	0.02	0.61	5.77	14.22
3	21.84	0.09	0.00	12.68	9.07
4	21.78	0.21	0.00	11.55	10.02
5	20.11	0.23	0.92	9.43	9.53
6	21.15	0.21	0.80	15.63	4.51
7	20.40	0.28	0.65	11.37	8.10
8	21.53	0.06	0.00	16.42	5.05
9	21.38	0.25	0.55	12.75	7.82
10	18.78	0.25	0.48	8.65	9.40
11	21.09	0.25	0.71	5.21	14.92
12	19.10	0.22	0.46	10.88	7.54
13	20.28	0.23	0.01	12.90	7.14
14	20.28	0.12	0.00	14.67	5.49
15	19.04	0.28	0.73	7.13	10.90
16	19.04	0.12	0.00	12.95	5.97
17	21.04	0.26	0.77	11.74	8.28
18	21.04	0.23	0.00	10.99	9.82
19	19.13	0.00	0.00	15.13	4.00
20	19.13	0.00	0.00	10.68	8.45
21	18.62	0.25	0.00	11.35	7.02
22	20.04	0.00	1.74	10.81	7.49
23	20.02	0.00	2.66	17.48	0.00
24	18.88	0.15	0.00	18.53	0.19
25	18.88	0.00	0.00	12.63	6.25
26	20.77	0.00	0.00	15.81	4.96
27	18.45	0.12	0.00	12.04	6.29
TC opt.	18.90	0.06	0.26	8.58	10.00
TOC opt.	18.58	0.00	0.00	18.58	0.00
TN opt.	21.00	0.00	0.00	10.44	10.56

Table S8.1. The results of nitrogen porosimetry analysis of goethite.

Parameters	Value unit
BET Surface Area	11.4 m^2/g
BJH Surface Area	7.6 m^2/g
BJH Pore Volume	0.044 cm^3/g
BJH Pore Radius Dv (r)	15.3 Å
DR Micropore Volume	0.005 cm^3/g

Table S8.2. The results of the screening experiments with PBD with 95% confidence intervals.

Run	Experimental variables				Removals, %		95% confidence intervals	
	PS (mM)	Time (h)	Goethite (g/L)	UV light	TOC	SMX	TOC	SMX
1	450	3	0.5	Off	0.36	100	(-10.33; 21.97)	(79.24; 104.27)
2	450	3	0.5	On	63.1	100	(26.97; 59.27)	(89.08; 114.11)
3	150	3	2.5	On	43.73	100	(25.72; 58.02)	(85.64; 110.67)
4	150	1	0.5	On	32.39	100	(16.81; 49.11)	(92.21; 117.24)
5	150	1	2.5	Off	1.95	89.67	(-20.75; 11.55)	(76.05; 101.07)
6	450	1	0.5	On	20.5	100	(17.80; 50.10)	(89.33; 114.36)
7	150	3	0.5	Off	0	100	(-11.32; 20.98)	(82.12; 107.15)
8	450	1	2.5	On	33.21	100	(17.54; 49.84)	(83.01; 108.03)
9	150	1	0.5	Off	0	89.45	(-20.49; 11.81)	(82.37; 107.40)
10	150	3	2.5	On	34.52	100	(25.72; 58.02)	(85.64; 110.67)
11	450	1	2.5	Off	0	92.1	(-19.76; 12.54)	(73.17; 98.19)
12	450	3	2.5	Off	1.36	69.73	(-10.59; 21.71)	(72.92; 97.94)

Table S8.3. Confidence intervals (CI) of TOC screening model coefficients (coded).

Term	Coef	SE Coef	95% CI Low	95% CI High	P-Value
Constant	19.26	3.05	12.04	26.48	0
X_1	0.5	3.05	-6.73	7.72	0.876
X_2	4.58	3.05	-2.64	11.81	0.177
X_3	-0.13	3.05	-7.35	7.09	0.967
X_4	18.65	3.05	11.43	25.87	0

Table S8.4. The results of the synthetic landfill leachate treatment experiments with 95% confidence intervals.

Run	Experimental variables			Removals, %		95% confidence intervals	
	PS (mM)	Time (h)	Goethite (g/L)	TOC	SMX	TOC	SMX
1	200	3	1	50.39	100	(45.32; 58.07)	(95.01; 101.65)
2	400	9	0.5	68.6	100	(61.58; 74.33)	(95.85; 102.49)
3	200	6	1.5	56.41	100	(48.08; 60.83)	(97.51; 104.15)
4	200	6	0.5	62.78	100	(55.56; 68.31)	(97.51; 104.15)
5	600	6	1.5	70.64	100	(65.11; 77.86)	(95.85; 102.49)
6	200	9	1	47.69	100	(42.81; 55.56)	(96.68; 103.32)
7	400	3	1.5	53.99	100	(48.26; 61.01)	(97.51; 104.15)
8	600	9	1	75.87	93.33	(68.19; 80.94)	(91.68; 98.32)
9	600	6	0.5	67.85	100	(63.43; 76.18)	(95.85; 102.49)
10	400	3	0.5	72.97	100	(66.13; 78.88)	(97.51; 104.15)
11	400	9	1.5	79.57	100	(73.66; 86.41)	(95.85; 102.49)
12	400	6	1	78.39	100	(71.54; 80.04)	(97.79; 102.21)
13	600	3	1	52.7	100	(44.83; 57.58)	(96.68; 103.32)
14	400	6	1	71.97	100	(71.54; 80.04)	(97.79; 102.21)
15	400	6	1	77.01	100	(71.54; 80.04)	(97.79; 102.21)

Table S8.5. Confidence intervals of TOC model coefficients (coded).

Term	Coef	SE Coef	95% CI Low	95% CI High	P-Value
Constant	75.79	1.65	71.54	80.04	0
X_1	6.22	1.01	3.62	8.83	0.002
X_2	5.21	1.01	2.61	7.81	0.004
X_3	-1.45	1.01	-4.05	1.15	0.212
X_1*X_1	-11.74	1.49	-15.58	-7.91	0.001
X_2*X_2	-7.38	1.49	-11.21	-3.55	0.004
X_3*X_3	0.37	1.49	-3.46	4.21	0.811
X_1*X_2	6.47	1.43	2.79	10.15	0.006
X_1*X_3	2.29	1.43	-1.39	5.97	0.171
X_2*X_3	7.49	1.43	3.81	11.17	0.003

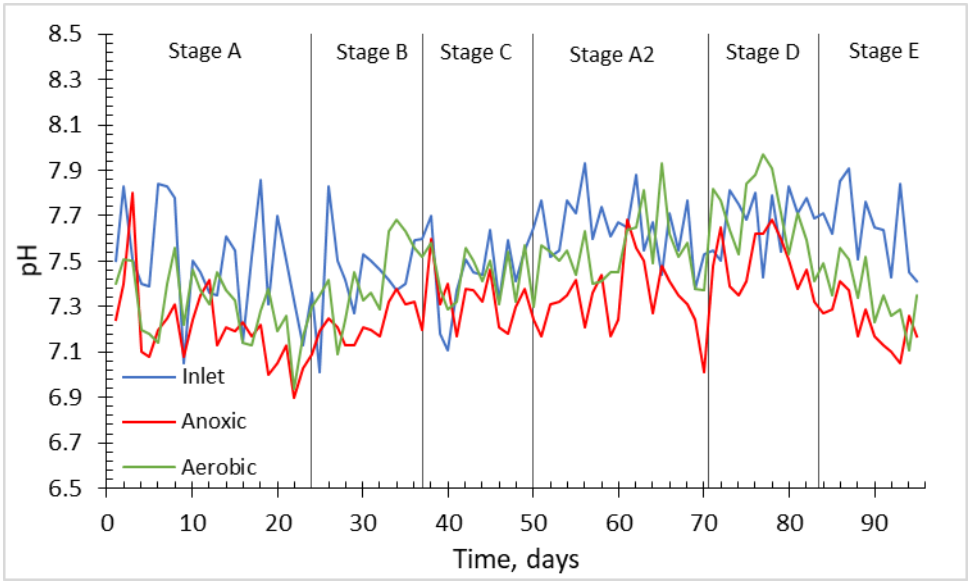

Fig. S4.1. pH of activated sludge process over time.

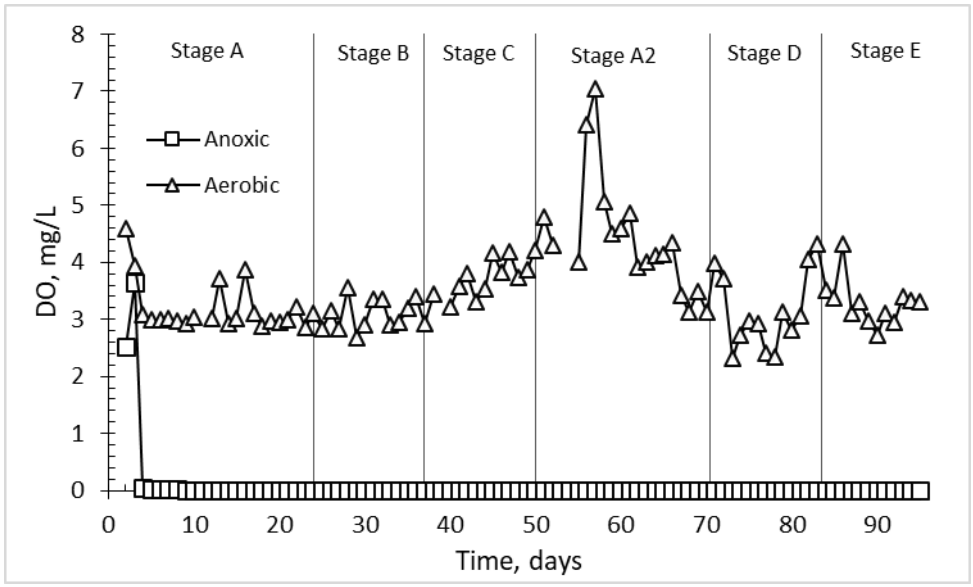

Fig. S4.2. DO of activated sludge process over time.

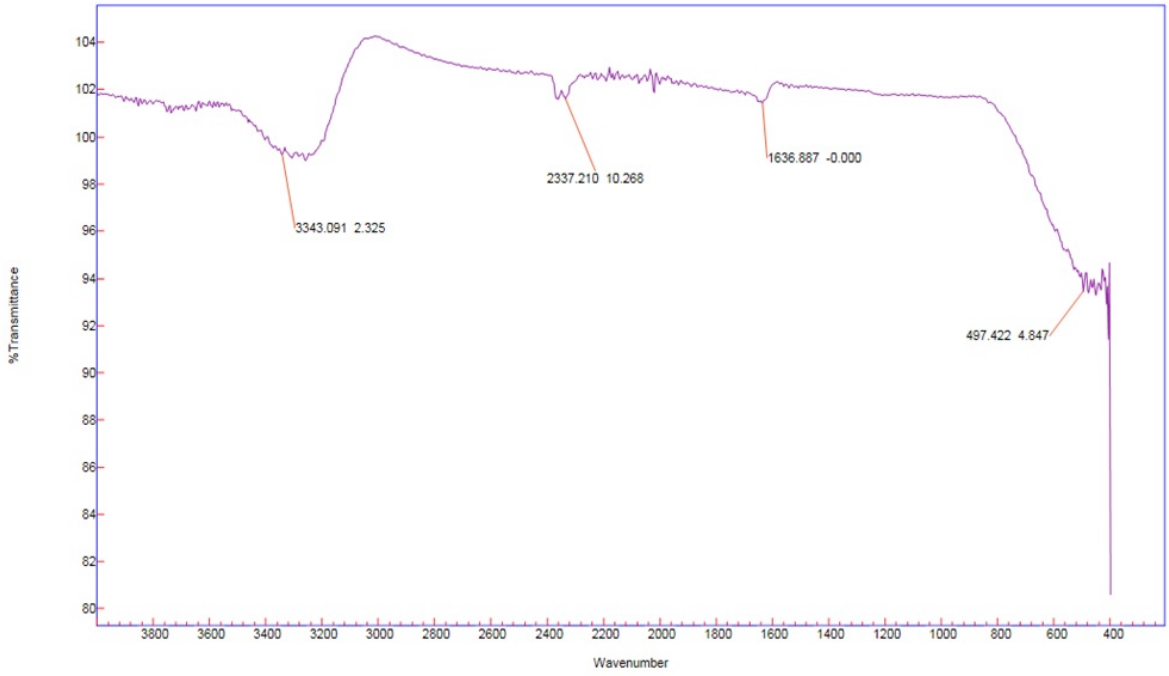

Fig. S6.1. FTIR analysis of the poultry wastewater.

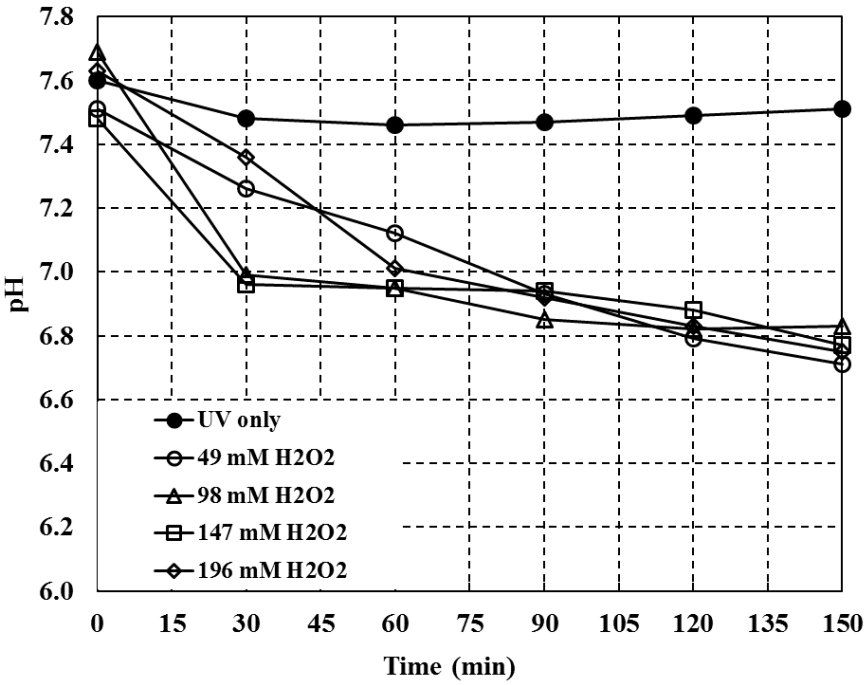

Fig. S6.2. The evolution of pH with time in the UV/H_2O_2 process.

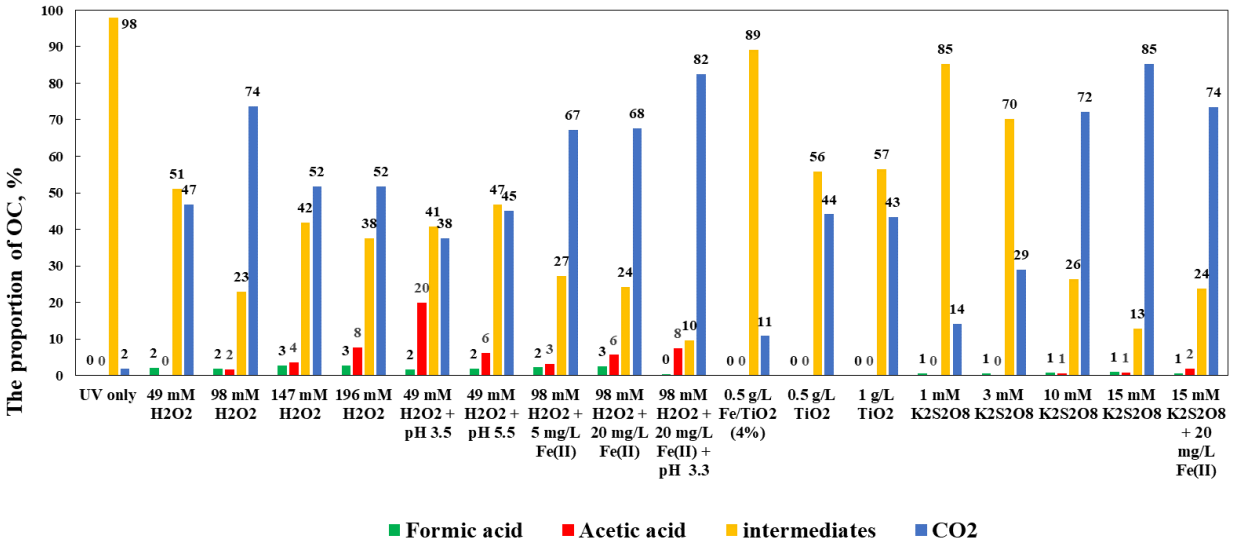

Fig. S6.3. The proportions OC originating from formic acid, acetic acid, intermediates and CO_2 for each process.

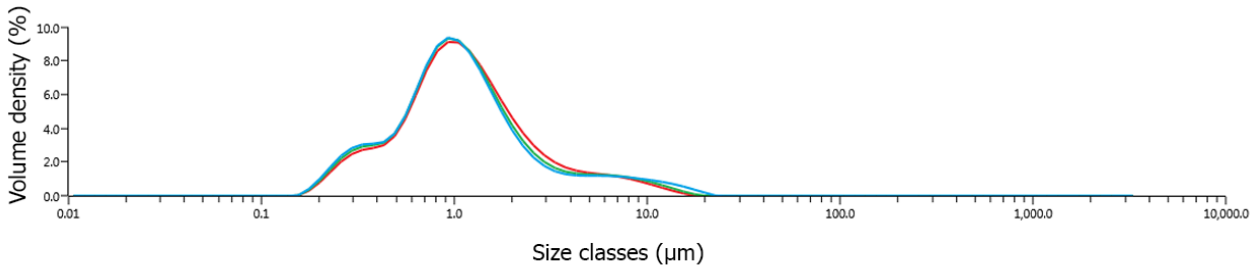

Fig. S8.1. Particle size distribution of goethite.

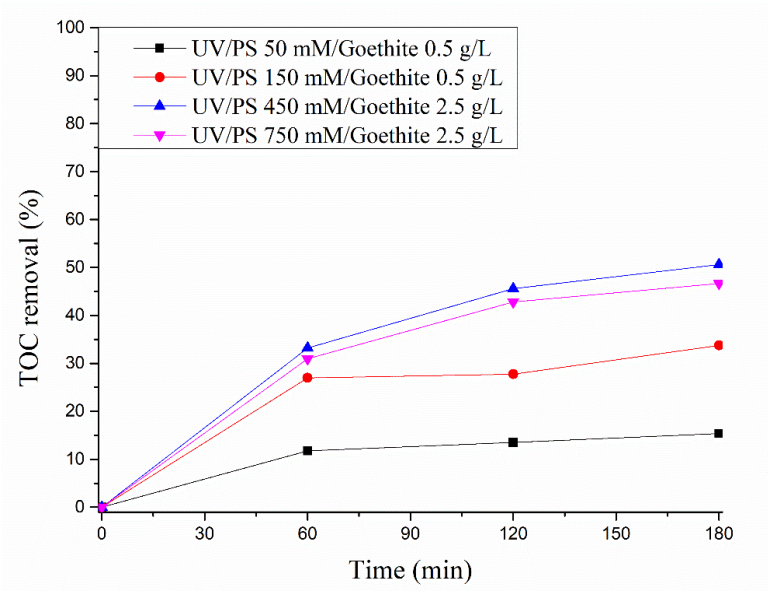

Fig. S8.2. Preliminary experiments with the SLL using UV/PS/Goethite process

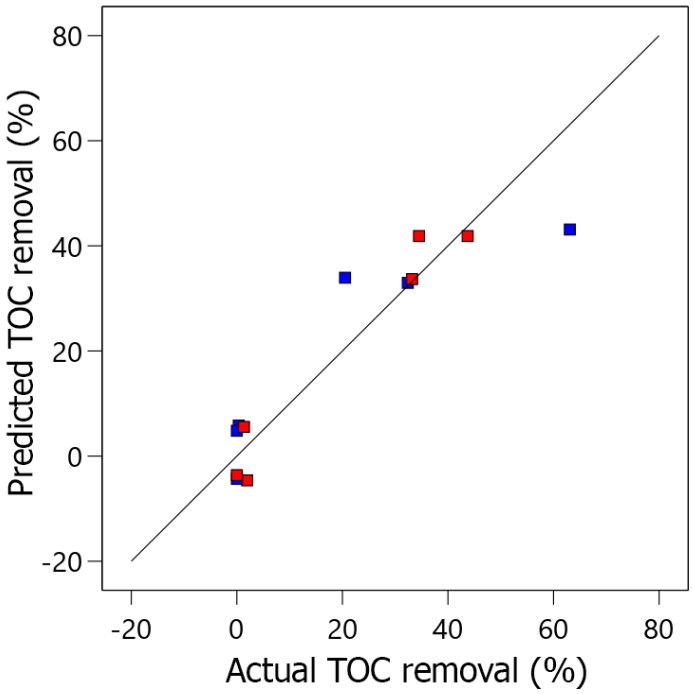

Fig. S8.3. PBD predicted vs. actual values for TOC removal.

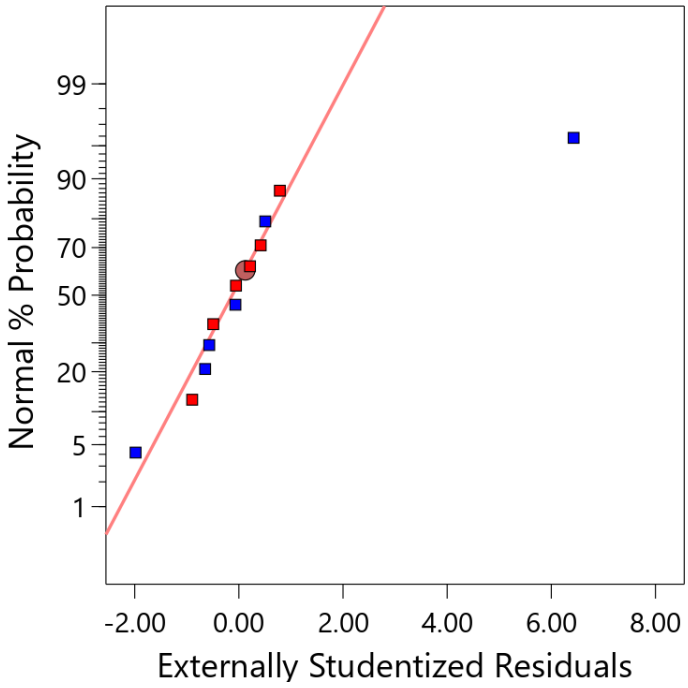

Fig. S8.4. Normal probability vs. externally studentized residuals values for TOC removal.

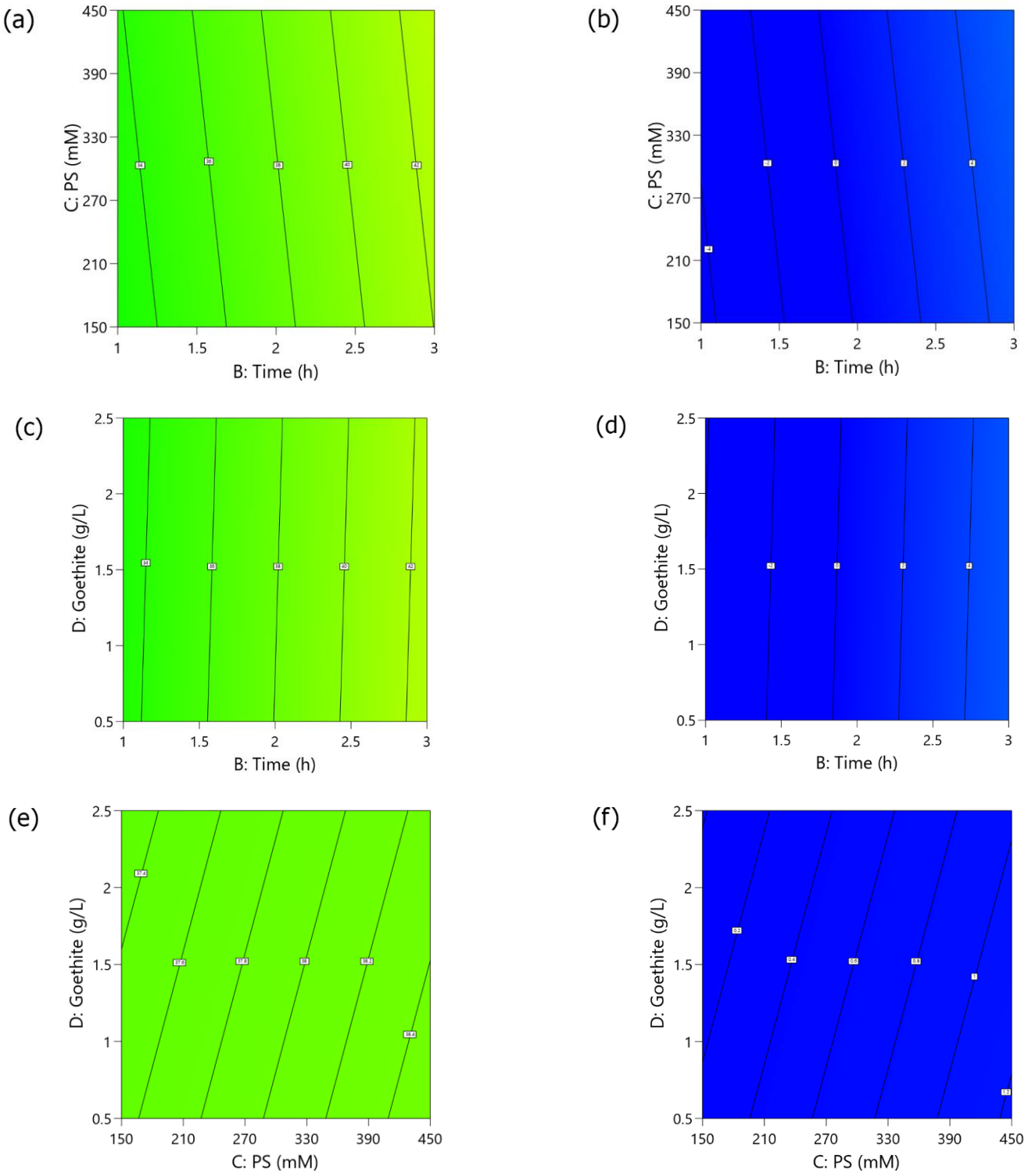

Fig. S8.5. Contour plots at the center-points for TOC removal: (a) UVA on, reaction time (min) and PS (mM), (b) UVA off, reaction time (min) and PS (mM), (c) UVA on, reaction time and goethite (g/L), (d) UVA off, reaction time and goethite (g/L), (e) UVA on, PS (mM) and goethite (g/L), (f) UVA off, PS (mM) and goethite (g/L).

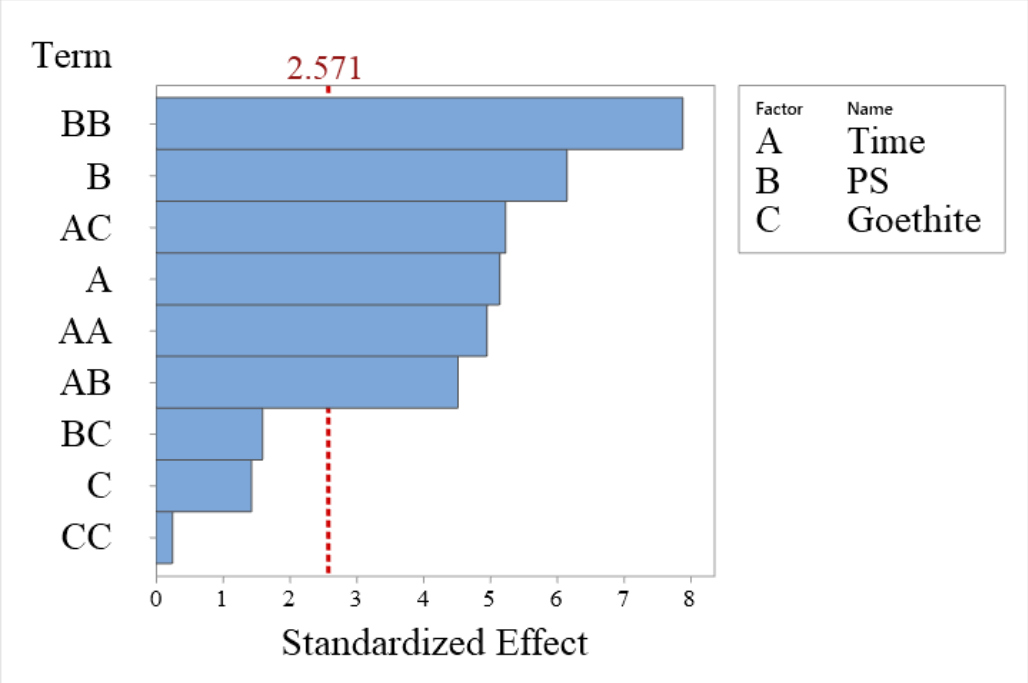

Fig. S8.6. Pareto plot for Box-Behnken design

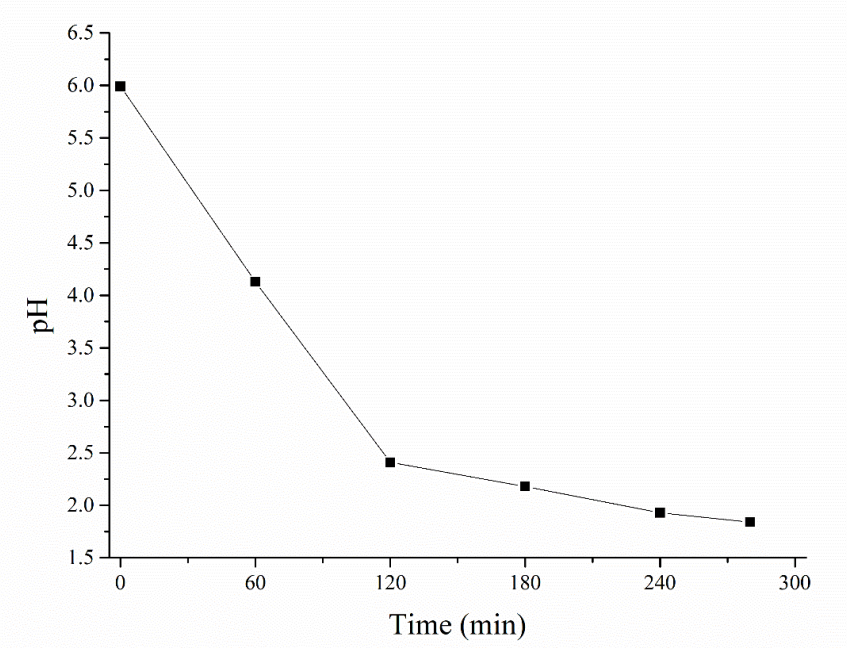

Fig. S8.7. pH profile of the photochemical treatment of RLL with UVA/PS/Goethite process under optimum conditions.